

## **Modeling of ultrashort optical pulses in nonlinear fibers**

Shalva Amiranashvili

submitted: Januar 28, 2022

Weierstrass Institute  
Mohrenstr. 39  
10117 Berlin  
Germany  
E-Mail: [shalva.amiranashvili@wias-berlin.de](mailto:shalva.amiranashvili@wias-berlin.de)

No. 2918  
Berlin 2022



---

*2020 Mathematics Subject Classification.* 78-02, 78A40, 78A60, 78M22, 35Q60.

*Key words and phrases.* Nonlinear fibers, ultrashort pulses, pulse propagation, Hamiltonian mechanics for waves, nonlinear Schrödinger equation, generalized nonlinear Schrödinger equation, rational approximation, Padé approximant, short-pulse equation, soliton, wave scattering, soliton perturbation theory, pulse manipulation, split-step methods.

Edited by  
Weierstraß-Institut für Angewandte Analysis und Stochastik (WIAS)  
Leibniz-Institut im Forschungsverbund Berlin e. V.  
Mohrenstraße 39  
10117 Berlin  
Germany

Fax: +49 30 20372-303  
E-Mail: [preprint@wias-berlin.de](mailto:preprint@wias-berlin.de)  
World Wide Web: <http://www.wias-berlin.de/>

# Modeling of ultrashort optical pulses in nonlinear fibers

Shalva Amiranashvili

## Abstract

This work deals with theoretical aspects of pulse propagation. The core focus is on extreme, few-cycle pulses in optical fibers, pulses that are strongly affected by both dispersion and nonlinearity. Using Hamiltonian methods, we discuss how the meaning of pulse envelope changes, as pulses become shorter and shorter, and why an envelope equation can still be used. We also discuss how the standard set of dispersion coefficients yields useful rational approximations for the chromatic dispersion in optical fibers.

Three more specific problems are addressed thereafter. First, we present an alternative framework for ultrashort pulses in which non-envelope propagation models are used. The approach yields the limiting, shortest solitons and reveals their universal features. Second, we describe how one can manipulate an ultrashort pulse, i.e., to change its amplitude and duration in a predictable manner. Quantitative theory of the manipulation is presented based on perturbation theory for solitons and analogy between classical fiber optics and quantum mechanics. Last but not least, we consider a recently found alternative to the standard split-step approach for numerical solutions of the pulse propagation equations.

# Contents

<b>Contents</b>	<b>2</b>
<b>List of Figures</b>	<b>4</b>
<b>List of Tables</b>	<b>4</b>
<b>Introduction</b>	<b>5</b>
<b>1 Background</b>	<b>7</b>
1.1 Short optical pulses . . . . .	7
1.2 Complex amplitude . . . . .	8
1.3 Analytic signal . . . . .	9
1.4 Beyond the envelope . . . . .	11
1.5 Laplace transform and causality . . . . .	12
1.6 Space evolution problem . . . . .	13
<b>2 Methods</b>	<b>15</b>
2.1 Hamiltonian framework . . . . .	15
2.2 Complex mechanics . . . . .	17
2.3 Hamiltonian description of waves . . . . .	18
2.4 Examples . . . . .	19
2.5 Hamiltonian framework for space evolution . . . . .	21
<b>3 Envelope equations</b>	<b>24</b>
3.1 Adiabatic approach . . . . .	24
3.2 An exemplary application . . . . .	27
3.3 What may be wrong with GNLSE? . . . . .	30
3.4 Polynomial approximations . . . . .	32
3.5 Padé approximants . . . . .	35
<b>4 Short pulse equations</b>	<b>37</b>
4.1 Key concepts . . . . .	37
4.2 Real SPEs . . . . .	38
4.3 Complex SPEs . . . . .	40
4.4 Peaked solitons . . . . .	41
4.5 Universality . . . . .	43
<b>5 Manipulation of light by light</b>	<b>45</b>
5.1 Relativistic mirrors . . . . .	45
5.2 Solitons as mirrors . . . . .	47
5.3 An empirical approach to scattering . . . . .	49
5.4 Relation to quantum mechanics . . . . .	49

---

5.5	Soliton perturbation theory . . . . .	51
5.6	Raman scattering . . . . .	52
5.7	Why to reduce the model? . . . . .	54
<b>6</b>	<b>Parallel splitting methods</b>	<b>56</b>
6.1	Split step methods . . . . .	56
6.2	Companions . . . . .	57
6.3	Main result . . . . .	58
6.4	Proof . . . . .	60
6.5	Outlook . . . . .	61
<b>7</b>	<b>Conclusions</b>	<b>62</b>
<b>8</b>	<b>Appendices</b>	<b>64</b>
8.1	Acronyms . . . . .	64
8.2	Notations . . . . .	65
	<b>Bibliography</b>	<b>66</b>

# List of Figures

0.1	Scale separation . . . . .	5
1.1	Pulses and their envelopes . . . . .	9
1.2	If the envelope fails . . . . .	11
3.1	Evolution of $\cosh^{-1}$ pulses . . . . .	27
3.2	Nearly fundamental solitons . . . . .	30
3.3	Huge expansions are not good expansions . . . . .	32
3.4	Dielectric function in the complex plane . . . . .	32
3.5	Approximations beyond the convergence radius . . . . .	34
4.1	Approximations for SPEs . . . . .	39
4.2	Potential wells and cusps . . . . .	43
4.3	The shortest soliton . . . . .	44
5.1	Moving mirrors in vacuum . . . . .	45
5.2	Mirrors in a dispersive medium . . . . .	46
5.3	Soliton as a mirror . . . . .	46
5.4	Scattering at a soliton . . . . .	47
5.5	An example of the forward reflection . . . . .	48
5.6	All optical switching . . . . .	48
5.7	SC generation . . . . .	49
5.8	Exemplary dispersion law . . . . .	50
5.9	Soliton perturbation theory . . . . .	53
5.10	Self-frequency shift . . . . .	53
5.11	Caustic structure . . . . .	54

# List of Tables

3.1	Examples of the Padé approximants . . . . .	35
4.1	Dispersion approximations for SPEs . . . . .	40
8.1	List of acronyms . . . . .	64
8.2	List of notations . . . . .	65

# Introduction

Mathematical modelling of physical systems greatly benefits from separation of scales and availability of small parameters. Notably, in some situations these parameters should be *small but not too small*. A short optical pulse, for instance, represents a small, particle-like piece of light. However, such a “particle” usually contains enough field oscillations to be still considered as a wave. It is then safe to talk about its envelope, phase, and frequency. Pulse evolution can be treated as a relatively slow variation of its amplitude and carrier frequency, which is translated into a slow variation of its complex envelope. But what should scientists do about ultrashort, few-cycle pulses with a too small duration? As schematically shown in Fig. 0.1, such pulses seem to have no envelope at all. Even if one employs a so-called *analytic signal* or *Hilbert transform* to define a complex amplitude for a single-cycle pulse, what is the physical meaning of such quantity?

- ❗ This work attempts to shed some light on fundamental questions related to pulses that, being too short, violate separation of scales and cannot be considered as a modulated wave.

There are many practical reasons to study few-cycle pulses. The most evident one is that optical pulses are used to track physical processes and ultrashort pulses make it possible to investigate ultrafast processes, e.g., to track chemical reactions on molecular level. Most (if not all) traditional applications of short optical pulses, such as spectroscopy or optical communication, also benefit from the decrease of pulse duration. Starting from the invention of a first laser source, scientists were extremely successful in producing shorter and shorter pulses. Nowadays more or less *single-cycle pulses* in the optical spectral range are available.

This rapid development resulted in new exciting applications. For instance, optical pulses have been used to reproduce key properties of systems that are beyond reach of experimentalists. In this way, an optical analogue of black holes was found, as well as the optical realization of spontaneously appearing, extremely high killer-waves in an ocean.

On the other hand, there is a need to revisit the classical concepts and models of wave theory and to adapt them to ultrashort pulses. Among other reasons, simply because such pulses are still waves and not particles. Here are some typical problems:

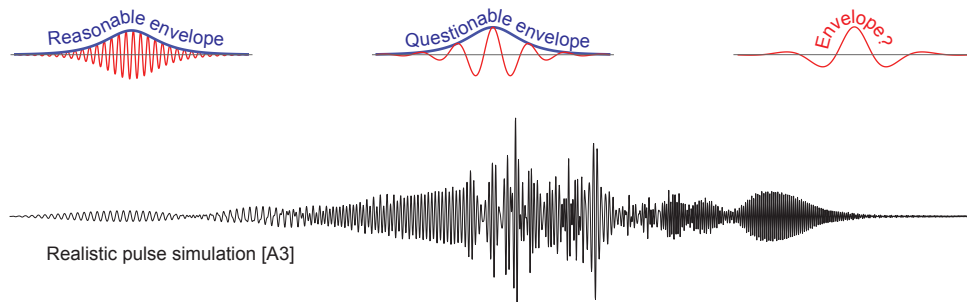


**Figure 0.1:** Top: even if we somehow define an envelope for a pulse on the right, what is the meaning if such quantity? Bottom: some segments of an initially smooth pulse with a longer duration seem to to have no envelope.

- ❶ Can one describe an ultra-short pulse by its envelope? If so, how and why this new envelope is related to the standard (slowly varying) one and to the analytic signal, which is used in signal processing?
- ❷ Leaving aside the complex-valued pulse envelope, is there any alternative approach to nonlinear optical pulses? Ideally, such an approach should be independent of pulse duration and yet provide a familiar envelope-like propagation equation.
- ❸ How it happens that a standard envelope equation, which is based on scales-separation, requires only a minimal modification, to apply to ultrashort pulses with no scale separation at all? What are benefits and pitfalls of a generalized envelope equation?
- ❹ Given an extreme pulse, which is too short for any kind of envelope, is a straightforward numerical solution of the full Maxwell system plus material equations the only way out? Or are there new model equations allowing for simplified description?
- ❺ Does the limiting pulse duration exist? Is it possible to have a stable pulse that contains, e.g., half an oscillation? If not, what is the mathematical reason that prevents short optical pulses from being too short?
- ❻ Are there any new possibilities to manipulate an ultrashort pulse, e.g., to make it even shorter? A standard point of view is that all-optical pulse manipulation is problematic due to the weakness of optical nonlinearities. Is it still so for a high-amplitude ultrashort pulse?

These problems are, as far as it was possible, respectively addressed in what follows.



# Chapter 1

## Background

This introductory Chapter deals with the interplay of a general theory of waves and short optical pulses. To begin with, we will look for a suitable definition of the pulse envelope. The definition, first simple, turns out to be insufficient and is gradually becoming more and more complex. It will be finally related to Hamiltonian variables and to classical analogue of the creation and annihilation operators in Chapter 2. Another topic of this Chapter is causality. Later on in Chapter 3 we will see how a violation of the causality principle imposes a limit on validity of a generalized envelope equation. Last but not least, we will discuss why a wave propagation equation in a guided system, such as an optical fiber, is usually solved along a suitable space variable, which to some extent replaces time.

### 1.1 Short optical pulses

The idea of ultrafast phenomena has been greatly changed over time and so to speak “shortened”. For an obvious reason, there is no strict definition of an ultrashort pulse other than a trivial remark that it should be as short as possible. History of short optical pulses arguably began in 1960, when the ruby laser came into operation. 10 ps pulses comprising  $\approx 4000$  of field cycles became available from 1965. They may be considered as first ultrashort pulses. Of course, these pulses can still be treated as modulated waves with a well-defined envelope.

Many laser systems and compression schemes were developed since then (for a historical perspective see, e.g., Fig. 2-1 in [1]). In 1987 the minimal pulse duration reached 6 fs [1, 2]. This full width at half maximum (**FWHM**) approximately corresponds to two field cycles of the carrier wave.

Nowadays, nearly single-cycle pulses are routinely available in optical labs [3, 4, 5, 6]. Moreover, extreme ultraviolet pulses with a duration of several hundreds attoseconds have been produced [7, 8, 9, 10]. A “modern” ultrashort pulse is then approximately  $10^5$  times shorter than the original one and, actually, is no longer a wave. On the other hand, in terms of the “carrier wave” these pulses still contain  $\approx 1.5$  of field cycles, which suggests existence of a limiting duration.

In what follows we will address several fundamental problems related to modelling of such few-cycle pulses *with the optical fibers in mind*. In order to do so, all “technical” aspects will be treated as simple as possible. Namely:

- We assume that all pulses belong to a transparency window and are not affected by dissipation. The transverse structure of the electric field is ignored in favor of *one-dimensional propagation equations*. Fiber nonlinearity is taken in its simplest (Kerr) form. Examples of a systematic reduction of a general pulse propagation problem to an effective one-dimensional equation can be found in [11, 12, 13, 14].

As ultrashort pulses of interest have wide spectra and high intensity, they will be affected by both fiber dispersion and nonlinearity. Furthermore, one should distinguish between the robust long-living solitary pulses, which propagate without changes over large distances, and short-living, extreme field states, e.g., a compressed linear

pulse or a nonlinear breather. The latter represents a periodically compressed and decompressed field state, subject to nonlinear interactions [15].

For instance, a properly chirped linear pulse can be quickly compressed due to fiber dispersion. It instantly provides an extremely short duration and high peak intensity, and is then decompressed. Such pulses are important in the context of power delivery and fast imaging. Breathers are different and yet these self-organized nonlinear objects share the same qualitative behavior: a compressed ultra-short field state suddenly appears and disappears [16, 17, 18, 19].

The short-living extreme field states are opposed by *ultrashort solitons*, which are in the focus of this work. An ideal soliton retains its shape all way along a nonlinear fiber. Such pulses are of interest for, e.g., optical communications [20]. There are reasons to believe that the shortest soliton contains approximately one-and-half cycles of the carrier frequency such that its limiting duration is comparable with that of the short-living field states [21].

It is clear that theory of few-cycle pulses can benefit from a properly reduced propagation equation. The latter should avoid the use of the slowly varying pulse envelope and yet be simpler than a full set of Maxwell and material equations. Two classes of such models will be discussed in Chapters 3 and 4. One class corresponds to generalized envelope equations, the other includes non-envelope models for the electric field that were specifically derived for short pulses.

We then turn to the pulse manipulation problem and to optical switching. Construction of an all-optical network is an important practical goal and requires an all-optical switch: a weak pulse should be capable to modify a strong one. In addition to optical communications, all-optical devices may be useful for, e.g., quantum computers [22]. However, their construction is an extremely difficult problem [23, 24].

Conceptually, a switching beam should act upon a nonlinear optical material to modify the interaction between the material and the main beam. In practice, the switching pulse and the main pulse tend to pass through one another without noticeable changes, because optical nonlinearities are simply too weak. One workaround is to employ materials with the resonant (i.e., very strong) light-matter interactions, such as rubidium vapor [25, 26] or organic materials [27]. Another option is to look for exceptional situations where even a weak interaction with the switching beam leads to a considerable change of the main pulse. One such possibility is discussed in Chapter 5.

Last but not least, as a rule, the problems related to the behaviour of short pulses require a numerical solution. Comprehensive description of all relevant techniques is far beyond the scope of the numerical Chapter 6. Instead we discuss a recently suggested modification of the standard split-step approach. The new scheme was built to take advantage of a multi-core computer systems with shared memory. Here, computation of the next system state is divided in several almost independent sub-problems that can be calculated on different computer cores with minimum communications between them.

## 1.2 Complex amplitude

As discussed in many textbooks devoted to oscillations and waves (see, e.g., [28, 29]), it happens to be extremely useful to have a complex-valued extension of a real-valued physical quantity. In the first place, this applies to quantities that appear as solutions of linear differential equations with constant real coefficients, e.g., to simple electric circuits or linearly-coupled oscillators. All real-valued solutions of such equations are naturally embedded in a larger set of the complex-valued solutions, which are much easier to calculate. This approach goes back to Heaviside, mathematicians call it *complexification* [30].

In the simplest case of a pure harmonic oscillation, the fundamental periodic function  $A \cos(\omega_0 t + \phi)$  is replaced by the Ansatz  $\mathcal{A} e^{i\omega_0 t}$  with the complex amplitude  $\mathcal{A} = A e^{i\phi}$ . The Ansatz is substituted into the linear differential equation at hand. One obtains an algebraic relation for the frequency  $\omega_0$ , the latter may happen to be real or complex. Either way, the original physical quantity is  $\text{Re}(\mathcal{A} e^{i\omega_0 t})$ . At this level, we have just a useful technique to find special solutions of the linear ordinary differential equations. It does not make sense to ask

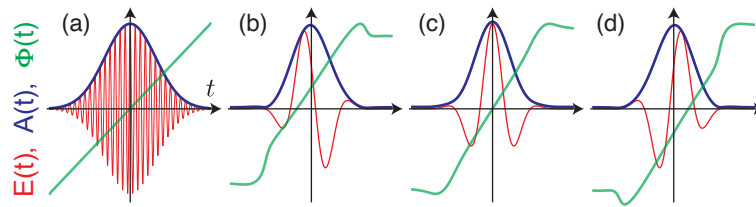


**Figure 1.1:** (a) For a smooth multi-cycle pulse (red) both its amplitude (blue) and full phase (green) are well-defined. The full phase  $\Phi(t)$ , being an almost linear function, is approximated by  $\omega_0 t + \phi$ , which gives access to the carrier frequency  $\omega_0$ . On the other hand, neither amplitude nor phase are directly accessible for the few-cycle pulses shown in (b-d). Here, an accurate definition of the complex envelope requires use of the analytic signal.

about the meaning of, e.g., complex current in an electric circuit or complex velocity of an oscillating electron.

- ❗ The standard complex amplitude is just a convenient mathematical “box” for the true real amplitude and real phase.

Another well-known fact is that the complex representation can be employed to describe a nearly-harmonic (modulated) real field, say  $E(t)$ . One follows the successive oscillations to retrieve their amplitude  $A(t)$  and full phase  $\Phi(t)$ . An example of a suitable pulse is shown in Fig. 1.1(a). Its carrier frequency  $\omega_0$  is yielded by the best linear fit  $\Phi(t) = \omega_0 t + \phi(t)$ , where an appropriate norm of the difference  $\|\Phi(t) - \omega_0 t\|$  should be minimized. This leaves us with a quasi-harmonic representation  $E(t) = A(t) \cos[\omega_0 t + \phi(t)]$ , introduced by Van der Pol in his now classical work [31].

As above, the real amplitude and phase can be combined in a single complex box-variable  $\mathcal{A}(t) = A(t)e^{i\phi(t)}$ , where  $E(t) = \text{Re}[\mathcal{A}(t)e^{i\omega_0 t}]$ . Such a definition of the complex amplitude  $\mathcal{A}(t)$  is non-unique and involves approximations [32]. It applies as long as  $\mathcal{A}(t)$  does not change much over the time scale introduced by  $e^{i\omega_0 t}$ . In return, the complex amplitude provides an extremely useful framework for description of weakly modulated linear and nonlinear oscillations [33].

- ❗ Van der Pol’s approximation goes far beyond the mere complexification. And yet, it cannot be applied to few-cycle pulses.

For instance, there is no evident way to describe the pulses shown in Fig. 1.1(b–d) by a real amplitude  $A(t)$  and phase  $\Phi(t)$ , i.e., no evident way to construct the complex amplitude. This is where an analytic signal comes into play.

### 1.3 Analytic signal

Given a real pulse field  $E(t)$ , there are infinitely many complex fields  $\mathcal{E}(t)$  such that  $E(t) = \text{Re}[\mathcal{E}(t)]$ , see a discussion in [32]. If we do not have a linear ODE for  $E(t)$  at our disposal and cannot require that  $\mathcal{E}(t)$  solves the same equation, what is the best known choice? Following the seminal work of Gabor [34], one sets that  $\mathcal{E}(t)$  shall comprise all positive-frequency components of  $E(t)$ . The complex conjugated field  $\mathcal{E}^*(t)$  comprises all negative frequencies.

- An elementary oscillation is usually written as  $\text{Re}[\mathcal{A}e^{i\omega t}]$ , whereas a common notation for an elementary wave is  $\text{Re}[\mathcal{A}e^{i(\mathbf{k}\mathbf{r} - \omega t)}]$ . In what follows, we switch to the second option. A positive-frequency oscillation is set to be  $\mathcal{A}e^{-i\omega t}$  with  $\omega > 0$ . That is, the complex amplitude from the previous section will be silently replaced by its conjugate.

This agreement also explains our choices in the definition of the Fourier transform  $E(t) \mapsto \tilde{E}(\omega)$ , where

$$\tilde{E}(\omega) = \int_{-\infty}^{\infty} E(t)e^{i\omega t} dt \quad \text{and} \quad E(t) = \int_{-\infty}^{\infty} \tilde{E}(\omega)e^{-i\omega t} \frac{d\omega}{2\pi}. \quad (1.1)$$

To define a complex signal, we take the inverse Fourier transform

$$E(t) = \left( \int_{-\infty}^0 + \int_0^{\infty} \right) \tilde{E}(\omega)e^{-i\omega t} \frac{d\omega}{2\pi} = \int_0^{\infty} \tilde{E}(\omega)e^{-i\omega t} \frac{d\omega}{2\pi} + \text{c.c.},$$

and picks the positive-frequency components by setting

$$\mathcal{E}(t) = \int_0^{\infty} \tilde{E}(\omega)e^{-i\omega t} \frac{d\omega}{\pi} \Rightarrow E(t) = \text{Re}[\mathcal{E}(t)]. \quad (1.2)$$

The complex field  $\mathcal{E}(t)$  is referred to as the analytic signal [28].

The above definition of  $\mathcal{E}(t)$  might be accompanied by a statement that only positive frequencies make sense. It is worth noting that

- ❗ For a real, e.g. cosine, electric field proportional to  $e^{-i\omega t} + e^{i\omega t}$ , there is no reason to believe that  $e^{-i\omega t}$  does make sense and  $e^{i\omega t}$  does not.

The positive-frequency component of a classical field is a matter of agreement. The choice in Eq. (1.2) is motivated by quantum mechanics, where the wave function of a free particle is proportional to  $e^{i(\mathbf{k}\mathbf{r} - \omega t)}$  and particle's energy  $\hbar\omega$  is positive for  $\omega > 0$ .

Comparing the relation  $E(t) = \text{Re}[\mathcal{A}(t)e^{-i\omega_0 t}]$  with  $E(t) = \text{Re}[\mathcal{E}(t)]$ , we arrive to a seemingly trivial connection

$$\mathcal{E}(t) = \mathcal{A}(t)e^{-i\omega_0 t}, \quad (1.3)$$

between the analytic signal and the complex pulse envelope. To illustrate Eq. (1.3), consider a modulated wave of the form [32]

$$E(t) = a(t) \cos(\omega_0 t) + b(t) \sin(\omega_0 t),$$

where by construction spectrum of both  $a(t)$  and  $b(t)$  belongs to  $[-\omega_0, \omega_0]$ . We then have

$$E(t) = \underbrace{\frac{1}{2}(a - ib)e^{i\omega_0 t}}_{\text{all freq.} \in [-2\omega_0, 0]} + \underbrace{\frac{1}{2}(a + ib)e^{-i\omega_0 t}}_{\text{all freq.} \in [0, 2\omega_0]},$$

such that by definition

$$\mathcal{E}(t) = (a + ib)e^{-i\omega_0 t} \Rightarrow \mathcal{A}(t) = a(t) + ib(t),$$

as expected for the envelope. The latter does not have to be slow, spectrum of  $\mathcal{A}(t)$  should only belong to  $[-\omega_0, \omega_0]$ .

We are in a good position to stress that:

- ❗ The complex envelope (if accessible) and the analytic signal (always accessible) are related by Eq. (1.3). And yet, calculation of the analytic signal requires neither approximations nor the carrier frequency.

An expansion of physical quantities near the carrier frequency has been used to derive a simplified propagation equation for the pulse envelope, see [35, 36, 37, 38, 39, 40] and discussion in Chapter 3. However, a proper propagation equation for an ultrashort pulse can be derived directly for its analytic signal, without referring to the carrier frequency [41]. A principle difference between this approach and the standard one is that the familiar nonlinear terms in the propagation equation, like  $|\mathcal{E}|^2 \mathcal{E}$ , must be replaced by their positive-frequency parts. This modification leads to new physical effects, e.g., new radiation lines, see [42, 43]. Another principle consequence of the seemingly trivial Eq. (1.3) is that:

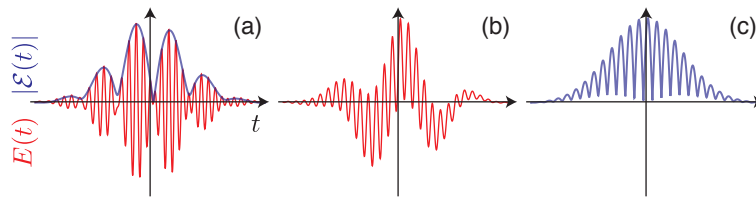


**Figure 1.2:** The field  $E(t)$  (red) and its analytic signal  $|\mathcal{E}(t)|$  (blue) for superposition of two Gaussian pulses (see [45]). (a) the pulses have similar frequencies and the analytic signal is shaped to the beat oscillations. (b-c) the pulses have considerably different frequencies. The field (b) and the envelope (c) look very different, the envelope is neither smooth nor slow.

- ❗ The spectrum of the envelope  $\mathcal{A}(t)$  of a pulse with the carrier frequency  $\omega_0$ , must belong to the interval  $[-\omega_0, \omega_0]$ . If pulse spectrum becomes too broad, even the most general envelope equation must be replaced by the equation for the analytic signal.

In the first place, this applies to situations where the initial pulse spectrum naturally broadens over several octaves [44].

## 1.4 Beyond the envelope

First, let's check if the extended envelope from Eq. (1.2) is of use for pulses like in Fig. 0.1(top). Figure 1.1(b-d) shows that an isolated few-cycle pulse is indeed wrapped by its analytic signal. We next consider a more irregular field, e.g., a superposition of two Gaussian pulses. As long as their carrier frequencies are close to each other, we get a perfect envelope for the beat oscillations, see Fig. 1.2(a). If the pulses are centered at different frequencies, as in Fig. 1.2(b), the analytical signal experiences rapid oscillations and does not look like an envelope, Fig. 1.2(c). The more so for an optical field with a complicated broad spectrum like in Fig. 0.1(bottom).

- ❓ Neither the local phase nor the local amplitude are well-defined for a superposition of pulses with different frequencies. What is then the meaning of the analytic signal?

A formal way to understand the imaginary part of the complex electric field relies on Hilbert transform. It is well known that:

- 📖 Given a complex function  $f(\zeta)$  with  $\zeta = x + iy$  that is analytic in the half-plane  $y \geq 0$  in which  $|f(\zeta)| \rightarrow 0$  for  $|\zeta| \rightarrow \infty$ , we have

$$f(x) = \frac{1}{\pi i} \text{p.v.} \int_{-\infty}^{\infty} \frac{f(x') dx'}{x' - x}, \quad (1.4)$$

where p.v. refers to the principle value of the integral. If, instead, the same applies to the half-plane  $y \leq 0$ , we have

$$f(x) = -\frac{1}{\pi i} \text{p.v.} \int_{-\infty}^{\infty} \frac{f(x') dx'}{x' - x}. \quad (1.5)$$

See any standard textbook on complex analysis, e.g., [46].


Equation (1.4) is usually combined with a frequency-dependent permeability to derive the Kramers-Kronig relations [47],  $\zeta$  is then replaced by a complex frequency. Analyticity in the upper half-plane follows from the causality principle, as discussed in the next Section. Another option is to apply Eq. (1.5) to the analytic signal (1.2). Just for a moment,  $\zeta$  is a “complex time”. Note, that any weighted sum of the exponents  $e^{-i\omega t}$  with  $\omega > 0$  has the required properties for  $\text{Im}(t) \leq 0$ . Equations (1.2) and (1.5) yield the relation

$$\mathcal{E}(t) = -\frac{1}{\pi i} \text{p.v.} \int_{-\infty}^{\infty} \frac{\mathcal{E}(t') dt'}{t' - t},$$

such that

$$\mathcal{E}(t) = E(t) + \frac{i}{\pi} \text{p.v.} \int_{-\infty}^{\infty} \frac{E(t') dt'}{t' - t}, \quad (1.6)$$

where  $t \in \mathbb{R}$ . We conclude that:

 The imaginary part of  $\mathcal{E}(t)$  is just a convolution between  $E(t)$  and  $-1/(\pi t)$ , i.e., (minus) Hilbert transform of the electric field.

Equation (1.6) provides a frequency independent definition of the analytic signal and gives insight into the meaning of  $\text{Im}[\mathcal{E}(t)]$ . Still, a more physical interpretation of  $\text{Im}[\mathcal{E}(t)]$  would be most welcome. As we will see in the next Chapter, which follows [45, 48], this can be done assuming that  $E(t)$  is governed by a Hamiltonian equation.

## 1.5 Laplace transform and causality

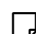
Wave equations by construction should admit special solutions of the form  $e^{i(\mathbf{k}\mathbf{r}-\omega t)}$  [29]. Given that the wave-solution is defined in the whole space, the above Ansatz requires a real  $\mathbf{k}$ . Temporal behaviour is different. If some external sources gradually bring the system out of equilibrium and system's reaction is of interest, we expect  $e^{-i\omega t} \rightarrow 0$  for  $t \rightarrow -\infty$ . If the external sources are switched off and the system evolves towards its equilibrium, we expect  $e^{-i\omega t} \rightarrow 0$  for  $t \rightarrow +\infty$ . In both setups the frequency  $\omega$  is complex.

On the other hand, the Fourier transform (1.1) is defined for  $\omega \in \mathbb{R}$  and cannot be extended to  $\omega \in \mathbb{C}$ . Indeed, given a complex frequency, the integral  $\int_{-\infty}^{\infty} E(t)e^{i\omega t} dt$  diverges for a generic  $E(t)$ , because  $e^{i\omega t} \rightarrow \infty$  either for  $t \rightarrow -\infty$  or for  $t \rightarrow \infty$ .

To introduce spectral components for complex frequencies, we define the quantity

$$\hat{E}(\omega) = \int_0^{\infty} E(t)e^{i\omega t} dt. \quad (1.7)$$

For a causal  $E(t)$ , which by definition strictly vanishes for  $t < 0$ , we have  $\hat{E}(\omega) = \tilde{E}(\omega)$ . Alternatively, field's behaviour for negative times may be considered as "known" or "not of interest",  $\hat{E}(\omega)$  and  $\tilde{E}(\omega)$  are then different. Note, that even growing (unstable) signals yield  $\hat{E}(\omega)$ , if  $\text{Im}(\omega)$  is large enough.

 Equation (1.7) is just a trivial reformulation of the Laplace transform, the latter maps  $p \in \mathbb{C}$  into  $\int_0^{\infty} E(t)e^{-pt} dt$ . We use the reformulation to replace an abstract variable  $p$  by frequency.

Given a bounded  $E(t)$ , the image  $\hat{E}(\omega)$  is an analytic function at least for  $\text{Im}(\omega) > 0$ . If we deal with an instability and  $E(t)$  increases as  $e^{\mu t}$ , Eq. (1.7) provides an analytic function for  $\text{Im}(\omega) > \mu$ . The field for  $t > 0$  is reconstructed from  $\hat{E}(\omega)$  using the so-called *Bromwich integral*

$$E(t) = \int_{\mathbb{R}+i\sigma} \hat{E}(\omega)e^{-i\omega t} \frac{d\omega}{2\pi}. \quad (1.8)$$

Here the real-frequency axis is shifted by  $i\sigma$  in such a way that  $\hat{E}(\omega)$  is an analytic function for  $\text{Im} \omega \geq \sigma$ . For instance, an arbitrarily small  $\sigma > 0$  suffices for a bounded signal. However,  $\hat{E}(\omega)$  may have singularities for real frequencies and in general it is not possible to take  $\sigma = 0$ .

Given a causal  $E(t)$ , Eq. (1.8) is valid for all times, otherwise the values of  $E(t)$  for  $t < 0$  are not covered and have no influence on Eq. (1.7) for the Laplace transform. The latter is useful for the time evolution problems when, e.g., an impact brings the system out of equilibrium [49].

Recall, that an applied electric field and the induced electric displacement are constrained by a material relation [47]. The simplest scalar linear relation with the response function  $f(t)$  reads

$$\frac{1}{\epsilon_0}D(t) = E(t) + \int_0^\infty f(t')E(t-t')dt', \quad (1.9)$$

such that, integration over  $t > 0$  naturally appears in electrodynamics.

For instance, a system in question may be excited by a monochromatic field  $E(t)$  with some complex frequency  $\omega$ . The field is *switched on*, i.e.,

$$E(t) = E_\omega e^{-i\omega t} \quad \text{for } t \in (-\infty, t_{\max}) \quad \text{with } \text{Im } \omega > 0,$$

The complex amplitude of the displacement is  $D_\omega = \epsilon_0 \epsilon(\omega) E_\omega$ , where Eq. (1.9) yields an integral representation of the relative permittivity

$$\epsilon(\omega) = 1 + \int_0^\infty f(t')e^{i\omega t'} dt' = 1 + \hat{f}(\omega), \quad \epsilon(-\omega^*) = \epsilon(\omega), \quad (1.10)$$

and  $\omega$  belongs to the upper complex half-plane [47]. The factor  $e^{i\omega t'}$  favors convergence of the integral in (1.10) allowing then exotic response functions. The definition of  $\epsilon(\omega)$  for  $\text{Im } \omega \leq 0$  is a different story and requires an analytic continuation.

▣ The analytic continuation of  $\epsilon(\omega)$  towards  $\omega \in \mathbb{R}$  might work even if the integral in Eq. (1.10) diverges for  $\omega \in \mathbb{R}$ , e.g., for  $f(t) = \text{const}$ .

In the first place, the continuation provides a permittivity for real frequencies. In the second place, the continuation into the domain  $\text{Im } \omega < 0$  can greatly simplify the solution of the initial-value problem for Maxwell equations by means of the Laplace transform [49]. A nonlinear version of Eq. (1.10) is discussed in [50].

It is important for what follows that, except for the simplest cases,  $\hat{f}(\omega)$  has poles in the complex half-plane  $\text{Im}(\omega) \leq 0$  and cannot be approximated by a polynomial. This imposes a restriction on the validity of a generalized envelope equation. The problem and a possible way out are discussed in Chapter 3 following [51].

## 1.6 Space evolution problem

Describing evolution of a physical system, we think first and foremost about the evolution in time. For instance, ODEs of classical mechanics can be equally good solved forward/backward in time starting from the actual system state. For a distributed field-system, the involved PDEs require both initial and boundary conditions. Dissipation makes the backward solution problematic, e.g., the diffusion equation can only be solved forward in time. Furthermore, in electrodynamics we are confronted with convolution integrals, like in Eq. (1.9). To calculate the convolutions, one needs the prehistory of the system, not just the current state. The evolution problems become more and more involved, but in any case, we deal with the evolution in time. It is of interest that:

□ In guided wave systems and especially in fiber optics, it is convenient to consider a *space evolution problem*. Instead of computing the solution from the past to the future, one computes it, e.g., from the left to the right [11, 52].

An abstract time evolution problem can be written as  $\partial_t \Psi = \hat{\mathfrak{L}}(\Psi)$ , where a multicomponent variable  $\Psi$  comprises all fields and characterizes the current system state.  $\hat{\mathfrak{L}}$  is the time evolution operator, it contains spatial derivatives, nonlinear terms, integrals, and whatever else. Speaking about the waves in a spatially homogeneous system, one can choose a real wave-vector  $\mathbf{k}$  and try the substitution  $\Psi \propto e^{i(\mathbf{k}\mathbf{r} - \omega t)}$ . For an infinitely small amplitude, the procedure results in a set of elementary waves, each with its own dispersion relation  $\omega = \omega_t(\mathbf{k})$ .

These waves can be used to construct more general linear and even nonlinear solutions. Dissipation manifests itself in a complex-valued function  $\omega_t(\mathbf{k})$ .

The space evolution problem is a useful alternative for waves in a guided system. Consider pulse propagation in a fiber, assuming that the governing equations are reduced to one spatial variable  $z$ . It is usually possible to transform the equations to the form  $\partial_z \Psi = \hat{\mathcal{G}}(\Psi)$ , where the space evolution operator  $\hat{\mathcal{G}}(\Psi)$  involves time derivatives, time convolutions, and nonlinear terms<sup>1</sup>. The hunt for a monochromatic wave begins with some real frequency  $\omega$ . The substitution  $\Psi \propto e^{i(kz - \omega t)}$  provides the elementary waves with  $k = \beta_t(\omega)$ . Dissipation manifests itself in a complex-valued  $\beta_t(\omega)$ . In optical context, the relation between time and space evolution problems was discussed in [36, 37, 53].

Assume for a moment that the field distribution in a fiber is characterized by a single quantity  $\Psi(z, t)$ , e.g., a complex amplitude of the relevant fiber-mode. A typical (linear) space evolution equation is

$$\partial_z \Psi + (a\partial_t + ib\partial_t^2 + c\partial_t^3)\Psi = 0 \quad \Rightarrow \quad k = a\omega + b\omega^2 - c\omega^3, \quad (1.11)$$

where we assume that  $a, b, c \in \mathbb{R}$ . Equation (1.11) is solved with respect to the space variable, e.g., given the “initial condition”

$$\Psi(z = 0, t) = f(t), \quad (1.12)$$

one calculates  $\Psi(z > 0, t)$ . Here,  $t$  is a kind of “coordinate” and  $z$  is a kind of “time”. One should note that:

- ❶ An attempt to consider Eq. (1.11) as a time evolution problem fails. Even a simple change to the dispersion relation of the form  $\omega = \omega(k)$ , leads to elementary waves that grow without any reason.
- ❷ The initial condition of the form (1.12) violates the causality principle, because the field at  $z = 0$  is known beforehand for all times.

To overcome the difficulty with the causality, one employs a unidirectional approximation. Returning for a moment to the time evolution problem, we note that two time directions are not equivalent (e.g., an isolated macroscopic system irreversibly evolves towards its equilibrium). We now impose an artificial difference between the two possible space directions in a one-dimensional wave system. Being in the lab frame, we assume that all elementary waves propagate from the left to the right.

More precisely, assume that the initial perturbation was created in the domain  $z < 0$ . The backward waves leave the system without imposing any effect on it. The forward waves enter into the fiber. Of course, the backward waves are still permanently generated due to the nonlinearity and possible inhomogeneity within the fiber. Exactly those backward waves are neglected, which at the very least requires a weak nonlinearity. For explicit estimates see [54]. We conclude that:

- ❶ Space evolution models require the unidirectional approximation. If a forward propagating pulse excites a significant amount of backward waves, the function  $f(t)$  in Eq. (1.12) is unknown.

This requirement is almost trivial for quasi-monochromatic waves with slowly varying envelope, but it is essential for ultra-short pulses, as discussed in Chapters 3 and 4. Moreover, the space evolution problem requires reformulation of the Hamiltonian equations, e.g., the very Hamiltonian becomes related to the momentum flux instead of energy. An attempt to apply the unidirectional approximation to the Hamiltonian equations for waves leads to a natural definition of the analytic signal, as discussed in Chapter 2 following [48].

---

<sup>1</sup>In a three-dimensional case, the space evolution operator  $\hat{\mathcal{G}}$  contains also the radial spatial derivatives  $\partial_x$  and  $\partial_y$ , because at any rate only one space variable can serve as the evolution variable.




# Chapter 2

## Methods

Classic envelope equations, which will be discussed in the next Chapter, are complex propagation equations of the first order, as opposed by a real second-order wave equation. There is a deep analogy between this and classical mechanics, where a second-order Newtonian equation is replaced by two first-order Hamiltonian ones. The latter can be combined in a single complex equation. It is well known that complex coordinates are useful in both classical Hamiltonian and quantum mechanics [55]. It is also well known that the Hamiltonian formalism can be applied to (undamped) nonlinear waves [56, 57]. It turns out, that the complex Hamiltonian equations for waves generalize the classic envelope equations. Moreover, the former can be solved by the very same split step approach (Chapter 6), and apply to wave packets of arbitrary duration. Among other things, the complex wave envelope is naturally replaced by a certain combination of the canonical coordinate and momentum, a classical analogue of the annihilation operator from quantum mechanics. If the classic envelope equation applies, the annihilation operation reduces to the analytic signal [48], which “explains” Gabor’s definition (1.2). In this Chapter we first briefly discuss the complex Hamiltonian formalism for particles and waves following [55, 56, 57]. We then explain how the formalism applies to short optical pulses [45, 48].

### 2.1 Hamiltonian framework

On an abstract level, Hamiltonian mechanics deals with a *phase space*  $\Gamma$ , which is a manifold consisting of all possible system states, and *observables*, which map  $\Gamma$  into  $\mathbb{R}$ . In terms of a local coordinate system  $\mathcal{X}_1, \dots, \mathcal{X}_d$  on  $\Gamma$ , an observable  $\mathcal{A}$ , such as energy, is represented by a smooth function  $\mathcal{A}(\mathcal{X}_1, \dots, \mathcal{X}_d)$  with  $d = \dim \Gamma$ . For any two observables  $\mathcal{A}$  and  $\mathcal{B}$ , one can calculate their product and Poisson bracket  $\{\mathcal{A}, \mathcal{B}\}$ , which are further observables.

 Poisson bracket should be bilinear, antisymmetric, and satisfy the Leibniz rule and the Jacobi identity

$$\begin{aligned}\{\mathcal{C}, \mathcal{A}\mathcal{B}\} &= \{\mathcal{C}, \mathcal{A}\}\mathcal{B} + \mathcal{A}\{\mathcal{C}, \mathcal{B}\}, \\ \{\mathcal{C}, \{\mathcal{A}, \mathcal{B}\}\} + \{\mathcal{B}, \{\mathcal{C}, \mathcal{A}\}\} + \{\mathcal{A}, \{\mathcal{B}, \mathcal{C}\}\} &= 0,\end{aligned}$$

respectively. It defines an algebra of observables and turns  $\Gamma$  into a Poisson manifold [58].

Given an observable  $\mathcal{H}$ , we for a moment denote by  $\partial_{\mathcal{H}}$  an operator that maps an arbitrary observable  $\mathcal{A}$  to  $\{\mathcal{H}, \mathcal{A}\}$ . The Leibniz rule and the Jacobi identity can be written as

$$\begin{aligned}\partial_{\mathcal{H}}(\mathcal{A}\mathcal{B}) &= (\partial_{\mathcal{H}}\mathcal{A})\mathcal{B} + \mathcal{A}(\partial_{\mathcal{H}}\mathcal{B}), \\ \partial_{\mathcal{H}}\{\mathcal{A}, \mathcal{B}\} &= \{\partial_{\mathcal{H}}\mathcal{A}, \mathcal{B}\} + \{\mathcal{A}, \partial_{\mathcal{H}}\mathcal{B}\}.\end{aligned}$$

It is clear that Poisson brackets are intrinsically related to derivatives.

▣ A possible Poisson bracket on  $\Gamma = \mathbb{R}^3$  is given by the triple product  $\{f(\mathbf{r}), g(\mathbf{r})\} = \mathbf{r} \cdot (\nabla f \times \nabla g)$ . This is a non-textbook example of a Hamiltonian structure in an odd-dimensional phase space [58].

To define a dynamical system on  $\Gamma$ , we declare some  $\mathcal{H}$  to be a special observable: the Hamiltonian. A system state, which is parameterized by its coordinates  $\mathcal{X}_1, \dots, \mathcal{X}_d$ , shall evolve in time in accord with the law

$$\frac{d\mathcal{X}_\alpha}{dt} = \{\mathcal{H}, \mathcal{X}_\alpha\}, \quad 1 \leq \alpha \leq d. \quad (2.1)$$

Different dynamical systems on a Poisson manifold are labelled by their Hamiltonians.

□ We consider only autonomous systems.

Equation (2.1) implies that any observable  $\mathcal{C}(\mathcal{X}_1, \dots, \mathcal{X}_d)$  may indirectly change with time. Moreover, assume that for two observables  $\mathcal{A}, \mathcal{B}$  it happens that both  $d\mathcal{A}/dt$  and  $d\mathcal{B}/dt$  can be calculated by analogy with Eq. (2.1). Thanks to the Leibniz rule, we have the implication

$$\begin{cases} \frac{d\mathcal{A}}{dt} = \{\mathcal{H}, \mathcal{A}\}, \\ \frac{d\mathcal{B}}{dt} = \{\mathcal{H}, \mathcal{B}\}, \end{cases} \Rightarrow \frac{d(\mathcal{A}\mathcal{B})}{dt} = \{\mathcal{H}, \mathcal{A}\mathcal{B}\}.$$

That is, time evolution of any product of coordinate functions  $\mathcal{X}_\alpha$  (and of any sum of such products) follows the pattern (2.1). Expanding a smooth observable  $\mathcal{C}(\mathcal{X}_1, \dots, \mathcal{X}_d)$  in Taylor series and ignoring convergence issues, we conclude that:

▣ The relation  $d\mathcal{C}/dt = \{\mathcal{H}, \mathcal{C}\}$  holds for any observable  $\mathcal{C}$ . If it happens that  $\{\mathcal{H}, \mathcal{C}\} = 0$ ,  $\mathcal{C}$  is an integral of motion [59].

One can, e.g., change to new coordinates  $\mathcal{Y}_1, \dots, \mathcal{Y}_d$  and Eq. (2.1) preserves its structure

$$\mathcal{Y}_\alpha = \mathcal{Y}_\alpha(\mathcal{X}_1, \dots, \mathcal{X}_d), \quad 1 \leq \alpha \leq d \Rightarrow \frac{d\mathcal{Y}_\alpha}{dt} = \{\mathcal{H}, \mathcal{Y}_\alpha\}.$$

A typical Poisson bracket in the coordinate representation reads

$$\{\mathcal{A}, \mathcal{B}\} = \sum_{\alpha, \beta=1}^d \Lambda_{\alpha\beta} \frac{\partial \mathcal{A}}{\partial \mathcal{X}_\alpha} \frac{\partial \mathcal{B}}{\partial \mathcal{X}_\beta}, \quad \text{e.g., } \{\mathcal{X}_\alpha, \mathcal{X}_\beta\} = \Lambda_{\alpha\beta}, \quad (2.2)$$

and yields a generic (non-canonical) Hamiltonian equation

$$\frac{d\mathcal{X}_\alpha}{dt} = - \sum_{\beta=1}^d \Lambda_{\alpha\beta} \frac{\partial \mathcal{H}}{\partial \mathcal{X}_\beta}, \quad (2.3)$$

where  $\Lambda_{\alpha\beta}(\mathcal{X}_1, \dots, \mathcal{X}_d)$  is an antisymmetric tensor field of second-order.

Jacobi identity imposes an additional restriction on  $\Lambda_{\alpha\beta}$ , see [60]. If  $\det(\Lambda_{\alpha\beta}) \neq 0$ , which among other things requires an even  $d = 2N$ , one can find the so-called *canonical coordinates*  $q_\alpha, p_\alpha$  such that

$$\{q_\alpha, q_\beta\} = \{p_\alpha, p_\beta\} = 0, \quad \{p_\alpha, q_\beta\} = \delta_{\alpha\beta}, \quad 1 \leq \alpha, \beta \leq N, \quad (2.4)$$

$$\{\mathcal{A}, \mathcal{B}\} = \sum_{\alpha=1}^N \left( \frac{\partial \mathcal{A}}{\partial p_\alpha} \frac{\partial \mathcal{B}}{\partial q_\alpha} - \frac{\partial \mathcal{A}}{\partial q_\alpha} \frac{\partial \mathcal{B}}{\partial p_\alpha} \right), \quad (2.5)$$

and therefore

$$\frac{dq_\alpha}{dt} = \frac{\partial \mathcal{H}}{\partial p_\alpha}, \quad \frac{dp_\alpha}{dt} = -\frac{\partial \mathcal{H}}{\partial q_\alpha},$$

which are the canonical Hamiltonian equations.

If one finds a new set of coordinates  $Q_\alpha, P_\alpha$  with the same brackets  $\{Q_\alpha, Q_\beta\} = \{P_\alpha, P_\beta\} = 0$  and  $\{P_\alpha, Q_\beta\} = \delta_{\alpha\beta}$ , the Hamiltonian equations preserve their canonical form. This feature can be used to simplify  $\mathcal{H}$ , see [61, 59]. In the best case scenario of an integrable system, one can find the action-angle variables  $I_\alpha$  and  $\phi_\alpha$  with  $\{I_\alpha, \phi_\beta\} = \delta_{\alpha\beta}$  such that  $\mathcal{H} = \mathcal{H}(I_1, \dots, I_N)$ , which makes it easy to solve the Hamiltonian equations. Each action variable is then an integral of motion.

## 2.2 Complex mechanics

Complex coordinates are helpful in both classical and quantum mechanics [55]. In the classical case,  $2N$  real Hamiltonian equations yield  $N$  complex equations. By, e.g., employing  $z_\alpha = (q_\alpha + ip_\alpha)/\sqrt{2}$ , we derive


$$\{z_\alpha, z_\beta\} = \{z_\alpha^*, z_\beta^*\} = 0, \quad \{z_\alpha, z_\beta^*\} = i\delta_{\alpha\beta}, \quad 1 \leq \alpha, \beta \leq N, \quad (2.6)$$

$$\{\mathcal{A}, \mathcal{B}\} = i \sum_{\alpha=1}^N \left( \frac{\partial \mathcal{A}}{\partial z_\alpha} \frac{\partial \mathcal{B}}{\partial z_\alpha^*} - \frac{\partial \mathcal{A}}{\partial z_\alpha^*} \frac{\partial \mathcal{B}}{\partial z_\alpha} \right), \quad (2.7)$$

such that

$$\frac{dz_\alpha}{dt} = \{\mathcal{H}, z_\alpha\} = -i \frac{\partial \mathcal{H}}{\partial z_\alpha^*}, \quad 1 \leq \alpha \leq N. \quad (2.8)$$

Here  $\partial/\partial z_\alpha$  and  $\partial/\partial z_\alpha^*$  refer to the so-called *Wirtinger derivatives* [62].

 The Wirtinger derivatives are defined such that for any observable  $\mathcal{A}$  the transformation to the complex coordinates has the property

$$\sum_{\alpha=1}^N \left( \frac{\partial \mathcal{A}}{\partial q_\alpha} dq_\alpha + \frac{\partial \mathcal{A}}{\partial p_\alpha} dp_\alpha \right) = \sum_{\alpha=1}^N \left( \frac{\partial \mathcal{A}}{\partial z_\alpha} dz_\alpha + \frac{\partial \mathcal{A}}{\partial z_\alpha^*} dz_\alpha^* \right).$$

In particular, we have  $\partial z_\alpha / \partial z_\beta = \delta_{\alpha\beta}$  and  $\partial z_\alpha / \partial z_\beta^* = 0$ .

Two facts are important for what follows:

- ❶ There are many alternatives to  $z_\alpha = (q_\alpha + ip_\alpha)/\sqrt{2}$ , e.g.,

$$z_\alpha = \frac{1}{\sqrt{2}} \left( C_\alpha q_\alpha + \frac{ip_\alpha}{C_\alpha^*} \right), \quad C_\alpha \in \mathbb{C}, \quad 1 \leq \alpha \leq N, \quad (2.9)$$

where one can check that Eq. (2.6) applies and Eq. (2.8) is valid. The transition from the “old” to “new”  $z_\alpha$  is, of course, a canonical transformation which can be used to simplify  $\mathcal{H}$ . Nonlinear canonical transformations are also helpful. For instance, if the action-angle variables  $I_\alpha$  and  $\phi_\alpha$  are available, one can define  $z_\alpha = \sqrt{I_\alpha} e^{-i\phi_\alpha}$  and check that  $\{z_\alpha, z_\alpha^*\} = i$  whereas the other brackets vanish, such that Eq. (2.6) is satisfied.

- ❷ Complex coordinates give access to the classical analogies of the creation and annihilation operators. Let us consider a set of linear oscillators with a small nonlinear coupling, where

$$\mathcal{H} = \sum_{\alpha=1}^N \left( \frac{p_\alpha^2}{2m_\alpha} + \frac{k_\alpha q_\alpha^2}{2} \right) + \varepsilon \mathcal{H}_{\text{nonl}}, \quad \varepsilon \ll 1.$$

The parameters  $m_\alpha$  and  $k_\alpha$  refer to the individual masses and spring coefficients. We use the freedom in the definition of  $z_\alpha$  to simplify  $\mathcal{H}$ . By setting  $C_\alpha = \sqrt[4]{k_\alpha m_\alpha}$  in Eq. (2.9), one derives

$$\mathcal{H} = \sum_{\alpha=1}^N \omega_\alpha z_\alpha z_\alpha^* + \varepsilon \mathcal{H}_{\text{nonl}}, \quad i \frac{dz_\alpha}{dt} = \omega_\alpha z_\alpha + \varepsilon \frac{\partial \mathcal{H}_{\text{nonl}}}{\partial z_\alpha^*}, \quad (2.10)$$

where  $\omega_\alpha = \sqrt{k_\alpha/m_\alpha}$ .  $\mathcal{H}_{\text{nonl}}$  should be expressed in terms of  $z_\alpha$ ,  $z_\alpha^*$ . The quadratic part of the Hamiltonian comes as close as possible to the quantum-mechanical expression  $\sum_\alpha \hbar \omega_\alpha (a_\alpha^\dagger a_\alpha + \frac{1}{2})$ . As to classical nonlinear mechanics, the first-order Eq. (2.10) is a useful starting point for all sorts of perturbation expansions.

## 2.3 Hamiltonian description of waves

The approach of two previous sections can, with some effort, be adopted for nonlinear waves in a continuous, dissipation-free system. A necessary precondition is that a (possibly hidden) Hamiltonian structure of the respective wave equations can be guessed [56, 57, 60].

Each state of a system is now described by a set of the field components  $u_i(\mathbf{r})$ , where  $i$  enumerates, e.g., six components of the electric and magnetic field. All valid system states compose a phase space  $\Gamma$ , which is an infinite-dimensional functional space. A generic observable  $\mathcal{A}$  is a functional that maps system states into  $\mathbb{R}$ . A small variation  $\delta u_i(\mathbf{r})$  of the actual system state  $u_i(\mathbf{r})$  should lead to a small variation of the observable

$$\delta \mathcal{A} = \sum_i \int \frac{\delta \mathcal{A}}{\delta u_i(\mathbf{r}_1)} \delta u_i(\mathbf{r}_1) d^3 \mathbf{r}_1.$$

Here  $\delta \mathcal{A} / \delta u_i$  refers to the variational derivative, a kind of dummy index  $\mathbf{r}_1$  labels points in space, the sum is over all field components, and the integral is over all possible values of  $\mathbf{r}_1$ .

By analogy with Eq. (2.2), the Poisson bracket of two observables  $\mathcal{A}$  and  $\mathcal{B}$  is defined by

$$\{\mathcal{A}, \mathcal{B}\} = \sum_{i,j} \int \Lambda_{ij}(\mathbf{r}_1, \mathbf{r}_2) \frac{\delta \mathcal{A}}{\delta u_i(\mathbf{r}_1)} \frac{\delta \mathcal{B}}{\delta u_j(\mathbf{r}_2)} d^3 \mathbf{r}_1 d^3 \mathbf{r}_2. \quad (2.11)$$

The sum is over all fields, the integral is over all possible  $\mathbf{r}_{1,2}$ . The structure-function  $\Lambda_{ij}(\mathbf{r}_1, \mathbf{r}_2)$  must be consistent with the properties of the Poisson bracket, among other things we require  $\Lambda_{ij}(\mathbf{r}_1, \mathbf{r}_2) + \Lambda_{ji}(\mathbf{r}_2, \mathbf{r}_1) = 0$ , which yields that  $\{\mathcal{A}, \mathcal{B}\} + \{\mathcal{B}, \mathcal{A}\} = 0$ .

Recall, that a generic Hamiltonian equation (2.3) was formulated in terms of a local coordinate system on a system-states-manifold  $\Gamma$  with  $\dim \Gamma < \infty$ . Now  $\Gamma$  is a functional space. To get a kind of ‘‘coordinates’’ on  $\Gamma$ , we consider an observable  $u_i(\mathbf{r}_a)$  that calculates a chosen field component  $u_i$  at a chosen point  $\mathbf{r}_a$ . By construction we have

$$u_i(\mathbf{r}_a) = \int \delta(\mathbf{r} - \mathbf{r}_a) u_i(\mathbf{r}) d^3 \mathbf{r} \quad \Rightarrow \quad \frac{\delta u_i(\mathbf{r}_a)}{\delta u_j(\mathbf{r})} = \delta_{ij} \delta(\mathbf{r} - \mathbf{r}_a),$$

and the Poisson bracket (2.11) of two such observables reads

$$\{u_i(\mathbf{r}_a), u_j(\mathbf{r}_b)\} = \Lambda_{ij}(\mathbf{r}_a, \mathbf{r}_b),$$

cf. Eq. (2.2). Therefore, Eq. (2.11) gets an invariant formulation

$$\{\mathcal{A}, \mathcal{B}\} = \sum_{i,j} \int \{u_i(\mathbf{r}_1), u_j(\mathbf{r}_2)\} \frac{\delta \mathcal{A}}{\delta u_i(\mathbf{r}_1)} \frac{\delta \mathcal{B}}{\delta u_j(\mathbf{r}_2)} d^3 \mathbf{r}_1 d^3 \mathbf{r}_2.$$

In particular:

- ❶ To make a transformation from  $u_t(\mathbf{r})$  to a new set of the field variables  $w_t(\mathbf{r})$ , one should just calculate their brackets  $\{w_t(\mathbf{r}_1), w_j(\mathbf{r}_2)\}$ .

After the Hamiltonian observable  $\mathcal{H}$  is chosen, each field value  $u_t(\mathbf{r}_a)$  starts to evolve in time in accord with

$$\partial_t u_t(\mathbf{r}_a)(t) = \{\mathcal{H}, u_t(\mathbf{r}_a)\} = - \sum_j \int \Lambda_{tj}(\mathbf{r}_a, \mathbf{r}_1) \frac{\delta \mathcal{H}}{\delta u_j(\mathbf{r}_1)} d^3 \mathbf{r}_1,$$

which defines a Hamiltonian system on  $\Gamma$  in a full analogy with Eq. (2.3).

- ❷ In what follows, we replace, e.g.,  $u_t(\mathbf{r})(t)$  by  $u_t(\mathbf{r}, t)$ , but keep  $\delta / \delta u_t(\mathbf{r})$  for the variational derivative. We then have

$$\partial_t u_t(\mathbf{r}, t) = - \sum_j \int \Lambda_{tj}(\mathbf{r}, \mathbf{r}_1) \frac{\delta \mathcal{H}}{\delta u_j(\mathbf{r}_1)} d^3 \mathbf{r}_1, \quad (2.12)$$

which is the final form of a generic Hamiltonian equation for waves.

The hardest part of the whole thing is to find the canonical variables for Eq. (2.12). These variables depend on the Poisson bracket on  $\Gamma$  and, once found, transform any Hamiltonian system on  $\Gamma$  to its canonical form. In the best case scenario, an even number of fields  $u_t(\mathbf{r})$  with  $1 \leq t \leq 2N$  is replaced by a new set  $q_t(\mathbf{r})$  and  $p_j(\mathbf{r})$  with  $1 \leq t, j \leq N$ , where

$$\begin{aligned} \{q_t(\mathbf{r}_a), q_j(\mathbf{r}_b)\} &= \{p_t(\mathbf{r}_a), p_j(\mathbf{r}_b)\} = 0, & \{p_t(\mathbf{r}_a), q_j(\mathbf{r}_b)\} &= \delta_{tj} \delta(\mathbf{r}_a - \mathbf{r}_b), \\ \{\mathcal{A}, \mathcal{B}\} &= \sum_t \int \left( \frac{\delta \mathcal{A}}{\delta p_t(\mathbf{r})} \frac{\delta \mathcal{B}}{\delta q_t(\mathbf{r})} - \frac{\delta \mathcal{A}}{\delta q_t(\mathbf{r})} \frac{\delta \mathcal{B}}{\delta p_t(\mathbf{r})} \right) d^3 \mathbf{r}, \end{aligned}$$

in analogy with the classical relations (2.4) and (2.5). The Hamiltonian equations (2.12) get their familiar form

$$\partial_t q_t(\mathbf{r}, t) = \frac{\delta \mathcal{H}}{\delta p_t(\mathbf{r})}, \quad \partial_t p_t(\mathbf{r}, t) = - \frac{\delta \mathcal{H}}{\delta q_t(\mathbf{r})}, \quad (2.13)$$

where the variational derivative just replaces the partial derivative.

By analogy with Eq. (2.6) and (2.7),  $2N$  real fields yield  $N$  complex fields  $\psi_t(\mathbf{r}) = [q_t(\mathbf{r}) + ip_t(\mathbf{r})] / \sqrt{2}$ , where

$$\begin{aligned} \{\psi_t(\mathbf{r}_a), \psi_j(\mathbf{r}_b)\} &= \{\psi_t^*(\mathbf{r}_a), \psi_j^*(\mathbf{r}_b)\} = 0, & \{\psi_t(\mathbf{r}_a), \psi_j^*(\mathbf{r}_b)\} &= i \delta_{tj} \delta(\mathbf{r}_a - \mathbf{r}_b), \\ \{\mathcal{A}, \mathcal{B}\} &= \sum_t \int i \left( \frac{\delta \mathcal{A}}{\delta \psi_t(\mathbf{r})} \frac{\delta \mathcal{B}}{\delta \psi_t^*(\mathbf{r})} - \frac{\delta \mathcal{A}}{\delta \psi_t^*(\mathbf{r})} \frac{\delta \mathcal{B}}{\delta \psi_t(\mathbf{r})} \right) d^3 \mathbf{r}, \end{aligned}$$

with  $1 \leq t, j \leq N$ . The complex Hamiltonian equation reads

$$\partial_t \psi_t(\mathbf{r}, t) = -i \frac{\delta \mathcal{H}}{\delta \psi_t^*(\mathbf{r})}, \quad (2.14)$$

which is a continuous analog of Eq. (2.8). A suitable canonical transformation to a new set of the complex fields with the same set of brackets can further be used to simplify  $\mathcal{H}$ .

## 2.4 Examples

### Complex envelope

Consider a wave system that is described by one complex field  $\psi(\mathbf{r}, t)$  with the canonical Poisson bracket

$$\{\mathcal{A}, \mathcal{B}\} = i \int \left( \frac{\delta \mathcal{A}}{\delta \psi(\mathbf{r})} \frac{\delta \mathcal{B}}{\delta \psi^*(\mathbf{r})} - \frac{\delta \mathcal{A}}{\delta \psi^*(\mathbf{r})} \frac{\delta \mathcal{B}}{\delta \psi(\mathbf{r})} \right) d^3 \mathbf{r}. \quad (2.15)$$

Given a quantum-mechanical scalar product  $\langle \psi_1 | \psi_2 \rangle = \int \psi_1^*(\mathbf{r}) \psi_2(\mathbf{r}) d^3\mathbf{r}$  and a self-adjoint operator  $\hat{\mathcal{D}}$ , we define a model

$$\mathcal{H} = \langle \psi | \hat{\mathcal{D}} | \psi \rangle + \varepsilon \mathcal{H}_{\text{nonl}} \quad \Rightarrow \quad i\partial_t \psi(\mathbf{r}, t) = \hat{\mathcal{D}} \psi(\mathbf{r}, t) + \varepsilon \frac{\delta \mathcal{H}_{\text{nonl}}}{\delta \psi^*(\mathbf{r})}. \quad (2.16)$$

The operator  $\hat{\mathcal{D}}$  is, e.g., a space convolution with a real kernel  $K(\mathbf{r})$

$$\hat{\mathcal{D}} \psi(\mathbf{r}) = \int K(\mathbf{r}') \psi(\mathbf{r} - \mathbf{r}') d^3\mathbf{r}'.$$

If the field-relevant spatial scale is considerably larger than the scale introduced by the kernel, one can expand  $\psi(\mathbf{r} - \mathbf{r}')$  and approximate  $\hat{\mathcal{D}}$  by a differential operator with constant coefficients.

For  $\varepsilon = 0$  we have a special solution in the form of a monochromatic linear wave  $\psi \propto e^{i(\mathbf{k}\mathbf{r} - \omega t)}$  subject to the dispersion relation

$$\omega(\mathbf{k}) = \int K(\mathbf{r}) e^{-i\mathbf{k}\mathbf{r}} d^3\mathbf{r}. \quad (2.17)$$

Nonlinear interactions of such waves come into play for  $\varepsilon \neq 0$ . This model covers numerous envelope equations for weakly-nonlinear waves.

### Creation and annihilation fields

In the above example, any valid system-state  $\psi$  is a ‘‘point’’ in the phase space  $\Gamma$ . A set of the field-values  $\psi(\mathbf{r})$  for all possible  $\mathbf{r}$  gives ‘‘coordinates’’ of that point. We now move to a new set of coordinates  $a(\mathbf{k})$ , which are labelled by a new ‘‘index’’  $\mathbf{k}$ , by applying the Fourier transform

$$a(\mathbf{k}) = \frac{1}{(2\pi)^{3/2}} \int \psi(\mathbf{r}) e^{-i\mathbf{k}\mathbf{r}} d^3\mathbf{r}.$$

The Poisson brackets of the new coordinates are calculated from Eq. (2.15)

$$\begin{aligned} \{a(\mathbf{k}_1), a(\mathbf{k}_2)\} &= \{a^*(\mathbf{k}_1), a^*(\mathbf{k}_2)\} = 0, \\ \{a(\mathbf{k}_1), a^*(\mathbf{k}_2)\} &= \frac{i}{(2\pi)^3} \int e^{i(\mathbf{k}_2 - \mathbf{k}_1)\mathbf{r}} d^3\mathbf{r} = i\delta(\mathbf{k}_1 - \mathbf{k}_2). \end{aligned}$$

The brackets retain their standard form, such that:

- ❗ A properly scaled Fourier transform is a canonical transformation.

The quadratic part of the Hamiltonian (2.16) is calculated using the inverse Fourier transform and Eq. (2.17). The transformed Hamiltonian reads

$$\mathcal{H} = \int \omega(\mathbf{k}) a(\mathbf{k}) a^*(\mathbf{k}) d^3\mathbf{k} + \varepsilon \mathcal{H}_{\text{nonl}}, \quad (2.18)$$

and comes as close as possible to the creation and annihilation formalism for quantum fields. The resulting Hamiltonian equation (2.16) is

$$i\partial_t a(\mathbf{k}, t) = \omega(\mathbf{k}) a(\mathbf{k}, t) + \varepsilon \frac{\delta \mathcal{H}_{\text{nonl}}}{\delta a^*(\mathbf{k})}, \quad (2.19)$$

and, in analogy with Eq. (2.10) for nonlinear oscillations, provides a starting point for studies of weakly-nonlinear wave interactions [56, 57].

## Conservation laws

To transform the generic real Eq. (2.12) to the canonical Eq. (2.13) and then to the complex equation, one needs an even number of fields. On the other hand, many wave equations deal with just one real field, such that their canonical reformulation seems to be impossible. For instance, the so-called *Gardner-Zakharov-Faddeev* bracket reads [57, 60]

$$\{u(x_a), u(x_b)\} = \delta'(x_a - x_b) \quad \Rightarrow \quad \{\mathcal{A}, \mathcal{B}\} = \int_{-\infty}^{\infty} \frac{\delta\mathcal{A}}{\delta u(x)} \frac{\partial}{\partial x} \frac{\delta\mathcal{B}}{\delta u(x)} dx,$$

where for simplicity we consider one wave field  $u(x)$  in one-dimensional space. The resulting Hamiltonian equation

$$\partial_t u(x, t) = -\partial_x \frac{\delta\mathcal{H}}{\delta u(x)},$$

represents a conservation law and looks all but canonical.

The canonical variables for the Gardner-Zakharov-Faddeev bracket belong to the Fourier representation of the phase space. They are labelled by wave-vectors  $k > 0$  and defined via [63]

$$q_k = \frac{1}{\sqrt{\pi k}} \int_{-\infty}^{\infty} u(x) \cos(kx) dx, \quad p_k = -\frac{1}{\sqrt{\pi k}} \int_{-\infty}^{\infty} u(x) \sin(kx) dx.$$

One can directly check that

$$\{q_{k_1}, q_{k_2}\} = \{p_{k_1}, p_{k_2}\} = 0, \quad \{p_{k_1}, q_{k_2}\} = \delta(k_1 - k_2).$$

The further transformation to one complex variable is then trivial.

## 2.5 Hamiltonian framework for space evolution

The above-discussed Hamiltonian equations for a continuous wave-system apply to a time evolution problem. As many models in what follows deal with the space evolution, we here discuss the necessary changes following [45, 48]. To begin with, the space version of a complex Hamiltonian equation (2.14) has the opposite sign. Considering, for instance, a wave with the complex envelope  $\psi(z, t)$ , we will have the formulations

$$i\partial_t \psi = \frac{\delta\mathcal{H}^I}{\delta\psi^*} \quad \text{and} \quad i\partial_z \psi = -\frac{\delta\mathcal{H}^{II}}{\delta\psi^*}, \quad (2.20)$$

in time and space respectively, where, e.g.,

$$\begin{aligned} \mathcal{H}^I &= \omega_0 \int |\psi|^2 dz && \text{yields} && \psi \propto e^{-i\omega_0 t}, \\ \mathcal{H}^{II} &= k_0 \int |\psi|^2 dt && \text{yields} && \psi \propto e^{ik_0 z}, \end{aligned}$$

such that either way the wave is proportional to  $e^{i(k_0 z - \omega_0 t)}$ . However, the physical quantities behind  $\mathcal{H}^I$  and  $\mathcal{H}^{II}$  are different. Note, that:

- ❗ The standard Hamiltonian  $\mathcal{H}^I$  and the space Hamiltonian  $\mathcal{H}^{II}$  have different physical dimensions, i.e.,  $\mathcal{H}^{II}$  cannot be energy.

Recall, that energy conservation comes into play if some system is invariant with respect to time shifts [61]. For instance, if  $\mathcal{H}^I$  in Eq. (2.20) does not depend on time explicitly but only through  $\psi$  and  $\psi^*$ , one derives that the total derivative  $\partial_t \mathcal{H}^I = 0$ . The space evolution works in the same way but for systems that are invariant with respect to space shifts. Therefore, the Hamiltonian  $\mathcal{H}^{II}$  must be related to momentum.

- ❶ A direct calculation shows that the space Hamiltonian for pulses propagating in a fiber reduces to a time-averaged momentum flux [48].

Actually, all standard conservation laws for the space evolution problems are related to fluxes. Indeed, consider a continuity equation

$$\partial_t \rho + \partial_z j = 0, \quad (2.21)$$

for a physical quantity with the density  $\rho(z, t)$  and the flux density  $j(z, t)$ . Normally, the conserved integral for Eq. (2.21) is given by a sort of “total charge”  $\int_{-\infty}^{\infty} \rho(z, t) dz$ , which does not depend on time. For the space evolution problem we obtain that  $\int_{-\infty}^{\infty} j(z, t) dt$  does not depend on position.

- ❷ If two observers situated at  $z = z_{1,2}$  measure system’s state for all times and “then” calculate the time-averaged flux, they get the same value. Of course, this formulation implicitly assumes that the perturbation vanishes before and after some characteristic time interval, otherwise there is no “then”.

The conservation law applies if, for instance, one deals with a localized wave packet that propagates forward along a fiber under assumption that all possible backward waves can be neglected. A space propagation problem is then intrinsically related to the unidirectional approximation. This fact is important for derivation of a general envelope equation, as we will discuss in the next Chapter.

It is of interest that in certain exceptional cases a space-propagated conservation law cannot be associated with a continuity equation. In an one-dimensional setting, for instance, one can demonstrate “conservation” of the so-called *electric area* [64]

$$\int_{-\infty}^{\infty} E(z, t) dt = \text{const.} \quad (2.22)$$

despite the fact that a generic electric field  $E(z, t)$  represents neither flux nor density of a physical quantity. Examples of pulses with a non-zero area were first found in [65], such integrals are similar to so-called *Casimir invariants* of degenerated Poisson brackets [58, 59].

We now turn to the space-propagation versions of the equations (2.18) and (2.19), which we recall are perfect starting points for studies on weakly nonlinear wave interactions. The functions  $a(\mathbf{k}, t)$  and  $a^*(\mathbf{k}, t)$ , which are classical versions of the creation and annihilation operators, are replaced by a new complex field  $\mathcal{A}(z, \omega)$  and its conjugate. For a pulse propagating in an optical fiber, the complex field is defined by by [48]

$$E_\omega(z) + \frac{\omega B_\omega(z)}{|\beta(\omega)|} = \sqrt{\frac{2\mu_0\omega^2}{|\beta(\omega)|}} \mathcal{A}(z, \omega), \quad (2.23)$$

where  $E_\omega$  and  $B_\omega$  refer to the Fourier components of the electric and magnetic fields,  $\mu_0$  is the permeability of vacuum. Equation (2.23) directly applies to a single-mode photonic crystal fiber [66].

Of course, the precise form of the full space-propagated Hamiltonian depends on fiber nonlinearity. But anyway, Eq. (2.23) reduces its quadratic part to the form

$$\mathcal{H} = \int |\beta(\omega)| \mathcal{A}(z, \omega) \mathcal{A}^*(z, \omega) d\omega. \quad (2.24)$$

It is a space-propagated analog of the quantity  $\sum_{\mathbf{k}} \omega(\mathbf{k}) a(\mathbf{k}, t) a^*(\mathbf{k}, t)$ .

The Hamiltonian (2.24) is positively defined, because it depends only on the absolute value of the wave-vector. An inverse Fourier transform of  $\mathcal{A}(z, \omega)$  provides a complex field in the space-time domain,  $\mathcal{A}(z, t)$ , which is a kind of generic envelope. In contrast to analytic signal, both real and imaginary parts of  $\mathcal{A}(z, t)$  have a clear physical meaning: they encode electric and magnetic fields.

Equations (2.23) and (2.24) were derived for a bidirectional system. One can demonstrate that positive frequencies in  $\mathcal{A}(z, \omega)$  correspond to the forward waves and negative frequencies to the backward waves. Under



conditions of unidirectional propagation, the negative-frequency components vanish and  $\mathcal{A}(z, t)$  becomes directly related to the analytic signal. The original Gabor's definition (1.2) is then naturally explained by putting it in a general context of Hamiltonian mechanics for waves [45, 48].

## Chapter 3

# Envelope equations

In 1960, Eugene Wigner published a famous paper “The unreasonable effectiveness of mathematics in the natural sciences” [67]. A small part of this amazing general phenomenon is unreasonable effectiveness of the envelope equations in fiber optics. At the end of the day, all classical envelope equations were derived for a wave that is almost monochromatic. However, these models were found to describe, e.g., single-cycle pulses, which are all but monochromatic. In this Chapter, we discuss why it happens and explain how Padé approximants help to avoid the causality-related divergence and to reduce numerical stiffness of the envelope equations [51].

### 3.1 Adiabatic approach

Envelope equations deal with modulated weakly nonlinear waves or oscillations. Consider, for instance, a dissipation-free one-dimensional homogeneous system that admits perturbations in the form of traveling waves. The associated equation for the wave field has then a continuous wave (**CW**) solution

$$\text{field} = A_0 \cos(k_0 z - \omega_0 t + \Phi_0) = \text{Re} \left[ A_0 e^{i(k_0 z - \omega_0 t + \Phi_0)} \right], \quad (3.1)$$

$$\text{with } k_0 = \beta(\omega_0) + \gamma(\omega_0) A_0^2. \quad (3.2)$$

The CW (3.1) is parametrized by its wave angular frequency  $\omega_0$ , phase  $\Phi_0$ , and amplitude  $A_0$ . Furthermore,  $k = \beta(\omega)$  refers to the dispersion relation for linear waves,  $\gamma(\omega_0) A_0^2$  is the nonlinear correction to the wave vector. The wave amplitude  $A_0$  should be small enough to allow for the sine-waves and to separate the nonlinear wave-vector shift from the higher-order nonlinear effects, see, e.g., [68].

A natural extension of the wave shape (3.1) is given by the modulated wave

$$\text{field} = A(z, t) \cos[k_0 z - \omega_0 t + \Phi(z, t)] = \text{Re} \left[ A_0 e^{i(k_0 z - \omega_0 t + \Phi_C)} \right], \quad (3.3)$$

$$\text{with } \Phi_C = \Phi - i \ln(A/A_0), \quad (3.4)$$

where the complex phase  $\Phi_C$  is slow compared to the time and space scales introduced by  $k_0 z - \omega_0 t$ . Parts of the modulated wave (3.3) look like monochromatic waves with the complex local wave vector

$$k_0 + \delta k(z, t), \quad \delta k = \partial_z \Phi_C = \partial_z \Phi - i \partial_z A/A,$$

and frequency

$$\omega_0 + \delta \omega(z, t), \quad \delta \omega = -\partial_t \Phi_C = -\partial_t \Phi + i \partial_t A/A.$$

All the information about the modulation is comprised in the complex envelope

$$\Psi(z, t) = A(z, t) e^{i\Phi(z, t)},$$

where

$$\frac{i \partial_z \Psi}{\Psi} = -\delta k \quad \text{and} \quad \frac{i \partial_t \Psi}{\Psi} = \delta \omega. \quad (3.5)$$

Here, a common simplifying assumption, the slowly varying envelope approximation (**SVEA**), is that  $\delta\omega \ll \omega_0$ . It is convenient to relax the SVEA by assuming that:

- ❶ Being initially small,  $\delta\omega$  may accumulate in the course of wave propagation, but in a slow (adiabatic) way with the vanishing rate  $\partial_t(\delta\omega)$ .

More specifically, we require that

$$|\partial_t \delta\omega| \ll |\delta\omega|^2 \Rightarrow \frac{(i\partial_t)^2 \Psi}{\Psi} = i\partial_t(\delta\omega) + (\delta\omega)^2 \approx (\delta\omega)^2, \quad (3.6)$$

The quasi-CW parts of the modulated wave are subject to the CW dispersion relation (3.2) in the form

$$k_0 + \delta k = \beta(\omega_0 + \delta\omega) + \gamma(\omega_0 + \delta\omega)|\Psi|^2. \quad (3.7)$$

The most famous equation for the complex envelope results from the following assumptions:

- ❶ Dispersion of the nonlinearity is neglected such that  $\gamma(\omega_0 + \delta\omega)$  is replaced by  $\gamma_0 = \gamma(\omega_0)$ .
- ❷ The linear dispersion law  $k = \beta(\omega)$  is approximated by a quadratic polynomial in the vicinity of  $\omega_0$

$$\beta(\omega_0 + \delta\omega) \approx \beta_0 + \beta_1 \delta\omega + \frac{\beta_2}{2} (\delta\omega)^2, \quad (3.8)$$

where the so-called *dispersion coefficients*

$$\beta_j = \left. \frac{d^j \beta(\omega)}{d\omega^j} \right|_{\omega=\omega_0}, \quad j = 0, 1, 2, \dots,$$

are defined by the successive derivatives.

- ❸ The exact relations (3.5) for  $\delta k$  and  $\delta\omega$  are combined with the adiabatic approximation (3.6) for  $(\delta\omega)^2$ .

Using the above assumptions and Eq. (3.2) for  $k_0$ , we reduce Eq. (3.7) to the form

$$-\frac{i\partial_z \Psi}{\Psi} + \gamma_0 A_0^2 = \beta_1 \frac{i\partial_t \Psi}{\Psi} + \frac{\beta_2}{2} \frac{(i\partial_t)^2 \Psi}{\Psi} + \gamma_0 |\Psi|^2. \quad (3.9)$$

Finally, it is convenient to change from the physical time  $t$  to the delay variable

$$\tau = t - \beta_1 z, \quad (3.10)$$

and to introduce

$$\psi(z, \tau) = \Psi(z, t) e^{i\gamma_0 A_0^2 z}. \quad (3.11)$$

The nonlinear wave-vector shift is then “included” in  $\psi$  by construction. The modulated wave (3.3) is now described by the expression  $\text{Re}[\psi e^{i(\beta_0 z - \omega_0 t)}]$ , where  $\beta_0$  results from the dispersion relation for the linear waves, as opposed by the “true”  $k_0$  in Eq. (3.2). The change of variables (3.11) transforms Eq. (3.9) into

$$i\partial_z \psi - \frac{\beta_2}{2} \partial_\tau^2 \psi + \gamma_0 |\psi|^2 \psi = 0, \quad (3.12)$$

which is the famous nonlinear Schrödinger equation (**NLSE**). Note, that to a large extent the NLSE is independent on the seed equation for the wave field. The seed model remains unspecified and it is restricted only by the presence of the CW solution (3.1), which shows that NLSE is a universal model.

Equation (3.12) was derived in many different settings, e.g., for light beams in nonlinear dielectrics [69, 70], for waves in deep water [71, 72], waves in magnetized plasma [73], and pulses in optical fibers [74]. A notable fact is that Eq. (3.12) can be solved by the inverse scattering method [75] and, moreover, gives rise to several hierarchies of solvable equations [52, 76, 77].

We are in a good position to stress, that even a slow accumulation of the frequency shift  $\delta\omega$  may finally violate the quadratic approximation (3.8). The latter is then replaced by the Taylor expansion

$$\beta(\omega_0 + \delta\omega) \approx \beta_0 + \beta_1\delta\omega + \frac{\beta_2}{2}(\delta\omega)^2 + \dots + \frac{\beta_J}{J!}(\delta\omega)^J, \quad (3.13)$$

where the approximation order  $J$  is large enough to cover all relevant values of  $\delta\omega$ . The adiabatic condition (3.6) yields (by induction with respect to  $j$ ) that in the leading order  $(i\partial_t)^j\Psi \approx (\delta\omega)^j\Psi$ . Starting with a proper modification of Eq. (3.9)

$$-\frac{i\partial_z\Psi}{\Psi} + \gamma_0 A_0^2 = \sum_{j=1}^J \frac{\beta_j}{j!} \frac{(i\partial_t)^j\Psi}{\Psi} + \gamma_0 |\Psi|^2,$$

and following the standard NLSE derivation, one obtains the so-called *generalized nonlinear Schrödinger equation (GNLSE)*

$$i\partial_z\psi + \sum_{j=2}^J \frac{\beta_j}{j!} (i\partial_\tau)^j\psi + \gamma_0 |\psi|^2\psi = 0, \quad (3.14)$$

where NLSE (3.12) corresponds to  $J = 2$ .

To derive GNLSE for optical fibers, two radial degrees of freedom are integrated out from the Maxwell equations [11]. An upgrade from the NLSE (3.12) to a more capable GNLSE (3.14) is required for short optical pulses with  $\delta\omega \lesssim \omega_0$ , such that Eq. (3.13) requires a higher-order polynomial (e.g.,  $J = 10$  in [78]).

Equation (3.14) includes higher-order dispersion terms, as compared to Eq. (3.12). This raises a natural question: are there other higher-order terms, which are not captured by the CW solution (3.1)? In the context of optical fibers, an accurate derivation of the GNLSE yields additional dispersive nonlinear terms and should account for losses [12]. The result reads

$$i(\partial_z\psi + \alpha_0\psi) + \sum_{j=2}^J \frac{\beta_j}{j!} (i\partial_\tau)^j\psi + \gamma_0(1 + i\omega_0^{-1}\partial_\tau)(\mathfrak{I}\psi) = 0, \quad (3.15)$$

where the real-valued dispersion law  $k = \beta(\omega)$  was first upgraded to take losses into account

$$k = \beta(\omega) + i\alpha(\omega) = \frac{\omega}{c} \sqrt{\epsilon(\omega)}, \quad (3.16)$$

and then approximated by  $k \approx \beta(\omega) + i\alpha_0$  with the attenuation parameter  $\alpha_0 = \alpha(\omega_0)$ . Here  $\epsilon(\omega)$  refers to the relative permittivity. The term  $i\omega_0^{-1}\partial_\tau$  represents the self-steepening effect. The wave intensity factor  $|\psi|^2$  in the nonlinear term in Eq. (3.14) is replaced by the relation

$$\mathfrak{I} = (1 - f_R)|\psi(z, \tau)|^2 + f_R \int_0^\infty R(s)|\psi(z, \tau - s)|^2 ds. \quad (3.17)$$

The factors  $1 - f_R$  and  $f_R$  relate contributions of the instant and delayed (Raman) nonlinear responses. The Raman term is given by the convolution of the intensity  $|\psi|^2$  and a causal unit-area response function  $R(s)$ , see [12]. If  $|\psi(z, \tau - s)|$  is almost unchanged on the time scale introduced by  $R(s)$ , one can use a local approximation

$$\mathfrak{I} = (1 - \tau_R\partial_\tau)|\psi(z, \tau)|^2, \quad \tau_R = f_R \int_0^\infty sR(s)ds. \quad (3.18)$$

GNLSE (3.15) supplemented by Eq. (3.17) or (3.18) is a standard model for a single-mode nonlinear fiber [11]. The message is that:

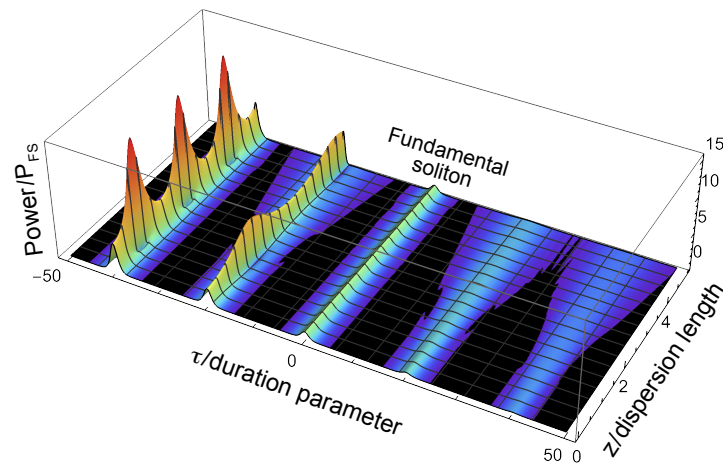


**Figure 3.1:** Solutions of Eq. (3.12) are calculated with the initial condition (3.19) for several pulses with the same duration  $\tau_0$  but different values of  $P_0$ . We put all pulses, which are separated by a “sufficiently large” delay of  $20\tau_0$ , in one simulation box for better visibility. From left to right:  $\sqrt{P_0}$  is 2.0, 1.5, 1.0, 0.6, 0.3 that of the fundamental soliton. As usual, “power” means  $|\psi|^2$ .

- ❗ Neither the precise form of the wave equation nor SVEA are required to derive GNLSE (3.14). This adiabatic equation comes closest to being universal: it describes all common features of all modulated sine-waves, e.g., a generalized Lighthill criterion [79]. However, a more specialized GNLSE (3.15) cannot be guessed from the dispersion relation (3.2), a full derivation is required.

Modulation instability (when a nonlinear wave is subject to growing modulations and finally breaks down in a sequence of pulses), is an example of a common feature [80]. Another example is a sudden, unpredictable appearance of huge short-living waves [81, 15], which nowadays are associated with the so-called *rogue waves*. They are observed in many nonlinear wave systems [82, 16]. These generic phenomena are captured already by Eq. (3.12) and in more details by Eq. (3.14).

An accurate description of a specific wave system requires GNLSE with additional terms, which depend on the system in question. For instance, the additional terms in the optical GNLSE (3.15) differ from those in the GNLSE for the water waves [83].

### 3.2 An exemplary application

Applications of the NLSE/GNLSE and, more general, applications of the SVEA approach for modulated waves is a huge part of nonlinear science. It would be difficult just to cite the most important sources in the field. The purpose of this Section is much more modest, we will discuss how the transition between the “simple” NLSE and “full” GNLSE frameworks affects fundamental solitons following [84].

Description of solitary nonlinear pulses that propagate without changes contrary to dispersive spreading, be it in a water channel or in an optical fiber, has pioneered the field of nonlinear waves [52]. Speaking about solitons in fibers [85], let us consider a family of  $\cosh$  pulses with the initial power parameter  $P_0$  and duration parameter  $\tau_0$ , where

$$\psi(z, \tau)|_{z=0} = \frac{\sqrt{P_0}}{\cosh(\tau/\tau_0)}. \quad (3.19)$$

Regarding the NLSE (3.12), the parameters  $\tau_0$  and  $P_0$  yield the dispersion length  $L_d$  and the nonlinear length  $L_n$ , where by construction

$$\begin{aligned} 1/L_d &= |\beta_2|/\tau_0^2 & \text{on this scale} & \quad \partial_z \psi \simeq \beta_2 \partial_\tau^2 \psi, \\ 1/L_n &= |\gamma_0|P_0 & \text{and on this scale} & \quad \partial_z \psi \simeq \gamma_0 |\psi|^2 \psi, \end{aligned} \quad (3.20)$$

see [11]. Initially, dispersion dominates for pulses with  $L_d \ll L_n$  and nonlinearity for  $L_d \gg L_n$ . Highly nonlinear pulses can be further destroyed or split in sub-pulses with their own scales. Several numerical solutions of the NLSE (3.12) with the initial condition (3.19) are shown in Fig. 3.1, we use fixed  $L_d$  and different values of  $L_n \lesseqgtr L_d$ , i.e., fixed  $\tau_0$  and different  $P_0$ .

Roughly speaking, dispersion leads to spreading, whereas nonlinearity yields oscillations. There is a transitional solution in between for which  $|\psi|^2$  neither oscillates nor spreads. This special solution of Eq. (3.12) describes a *fundamental soliton*, which exists if the signs of  $\beta_2$  and  $\gamma_0$  are opposite.

To get a fundamental soliton solution, one can consider a trial function with four unknown parameters<sup>1</sup>

$$\psi(z, \tau) = \frac{\sqrt{-\beta_2/\gamma_0}}{\sigma} \frac{e^{-i\mathcal{W}(\tau-\mathcal{T})+i\Theta}}{\cosh[(\tau-\mathcal{T})/\sigma]}, \quad \begin{array}{ll} \text{duration} & \sigma(z), \\ \text{frequency} & \mathcal{W}(z), \\ \text{delay} & \mathcal{T}(z), \\ \text{phase} & \Theta(z). \end{array} \quad (3.21)$$

A direct substitution demonstrates that Eq. (3.21) indeed yields an exact solution of the NLSE (3.12), if

$$\frac{d\sigma}{dz} = 0, \quad \frac{d\mathcal{W}}{dz} = 0, \quad \frac{1}{\beta_2} \frac{d\mathcal{T}}{dz} = \mathcal{W}, \quad \frac{1}{\beta_2} \frac{d\Theta}{dz} = -\frac{1}{2\sigma^2} - \frac{\mathcal{W}^2}{2}. \quad (3.22)$$

The simplest representative of this family is given by [11, 86, 87]

$$\psi_s(z, \tau) = \frac{\sqrt{-\beta_2/\gamma_0}}{\tau_0} \frac{e^{-i\beta_2 z/(2\tau_0^2)}}{\cosh(\tau/\tau_0)}, \quad \tau_0 = \text{const}, \quad (3.23)$$

cf. Eq. (3.19). The space scales  $L_d$  and  $L_n$  are now equal.

Equation (3.23) is one of many known analytical solutions to NLSE but, without doubt, the most important one. Fundamental solitons provide building blocks for a class of NLSE solutions consisting of several pulses and a rest term comprising small dispersive waves [75]. We now turn to the solitary solutions of the GNLS. Note, that:

▣ NLSE (3.12) gives birth to hierarchies of integrable models [52, 76, 77]. The most famous representatives within the hierarchies were given by Hirota [88] and Sasa&Satsuma [89].

For instance, Hirota's equation in optical notations is of the form

$$i\partial_z \psi + \frac{\beta_2}{2} (i\partial_\tau)^2 \psi + \frac{\beta_3}{6} (i\partial_\tau)^3 \psi + \gamma_0 |\psi|^2 (\psi + is\partial_\tau \psi) = 0, \quad (3.24)$$

$$\beta_2, \beta_3, \gamma_0, s \in \mathbb{R} \quad \text{and} \quad \beta_3 = s\beta_2.$$

The physical meaning of the restriction to  $\beta_3/\beta_2$  was revealed in [90].

Note, the common approximation (3.18) of the Raman term yields a different nonlinearity, such that the nonlinear term in Eq. (3.24) requires a special fiber design. Given the desired nonlinearity, one still has to adjust the ratio  $\beta_3/\beta_2$ . All further members of the integrable hierarchies follow the same pattern: more and more complicated nonlinear terms come into play together with the more and more involved relations between the coefficients [52, 76, 77].

❶ NLSE is generic: the complex envelope of a typical nonlinear wave is governed by an integrable equation. The extensions of the NLSE are integrable in rare, non-generic cases.

<sup>1</sup>This is not the most obvious approach, we use it for a smooth transition to the soliton perturbation theory in Chapter 5.

For this reason, in what follows we will be interested in the localized solutions of the GNLSE (3.14), be it integrable or not. In general, one can only hope for a numerical solution. We will use a *spectral renormalization method* [91] and assume that  $\beta_2\gamma_0 < 0$ . Motivated by the fundamental soliton (3.23), we use the following substitution

$$\psi_s(z, \tau) = \sqrt{-\frac{\beta_2}{\gamma_0} \frac{e^{-i\beta_2 z / (2\tau_0^2)}}{\tau_0}} f(\xi), \quad \xi = \tau / \tau_0, \quad (3.25)$$

with the yet unknown shape function  $f$  and the desired soliton duration  $\tau_0$ . It is convenient to associate each dispersion parameter  $\beta_j$  with its own (signed) characteristic length scale

$$L_d(j) = \frac{j!}{\beta_j} \tau_0^j \quad \text{on this scale} \quad \partial_z \psi \simeq \frac{\beta_j}{j!} \partial_\tau^j \psi, \quad (3.26)$$

cf., definition (3.20).

- ❗ It is natural to assume that the sequence  $L_d(j)$  increases: the higher the order of a dispersion coefficient, the longer it takes, before the coefficient comes into play. Otherwise the expansion (3.13) is meaningless.

Substitution (3.25) reduces GNLSE (3.14) to the form

$$f'' - f + 2|f|^2 f = \mathcal{F}(i\partial_\xi) f, \quad \mathcal{F}(v) = \sum_{j=3}^J \frac{L_d(2)}{L_d(j)} v^j, \quad (3.27)$$

where prime denotes derivative with respect to  $\xi$ . We change to the Fourier space to get

$$\tilde{f}(v) = \frac{2(|f|^2 f)_v}{1 + v^2 + \mathcal{F}(v)} \quad \text{with} \quad \tilde{f}(v) = \int_{-\infty}^{\infty} f(\xi) e^{iv\xi} d\xi, \quad (3.28)$$

where  $(|f|^2 f)_v$  denotes the Fourier transform of  $|f|^2 f$ .

Using the fundamental soliton (3.23) as the initial guess for the shape function, one calculates the sequence of the approximations  $f_n(\xi)$  and factors  $s_n$  via

$$f_0(\xi) = \frac{1}{\cosh(\xi)}, \quad \tilde{f}_{n+1}(v) = \frac{2s_n (|f_n|^2 f_n)_v}{1 + v^2 + \mathcal{F}(v)}, \quad n = 1, 2, 3, \dots,$$

where the renormalization factors on each step  $s_n$  are chosen such that the norms

$$\|f_1(\xi)\| = \|f_2(\xi)\| = \|f_3(\xi)\| = \dots = 1.$$

In other words, we have a sequence  $f_n(\xi)$  on a unit sphere in the infinite dimensional functional space. The sequence does not have to converge, but if it does converge to some limiting values  $f_\infty(\xi)$  and  $s_\infty$ , the relation

$$\tilde{f}_\infty(v) = \frac{2s_\infty (|f_\infty|^2 f_\infty)_v}{1 + v^2 + \mathcal{F}(v)},$$

indicates that  $\sqrt{s_\infty} f_\infty(\xi)$  solves ODE (3.27) for the solitary solution.

Figure (3.2) demonstrates application of this technique. A soliton containing approximately one-and-half cycle in fused silica is compared to the best-fit fundamental solution (3.23). An interesting observation is that:

- ❗ Whereas spectrum of an ultrashort soliton in Fig. 3.2(b) differs from that of the fundamental soliton, their shapes in space-time are nearly indistinguishable, as shown in Fig. 3.2(a).

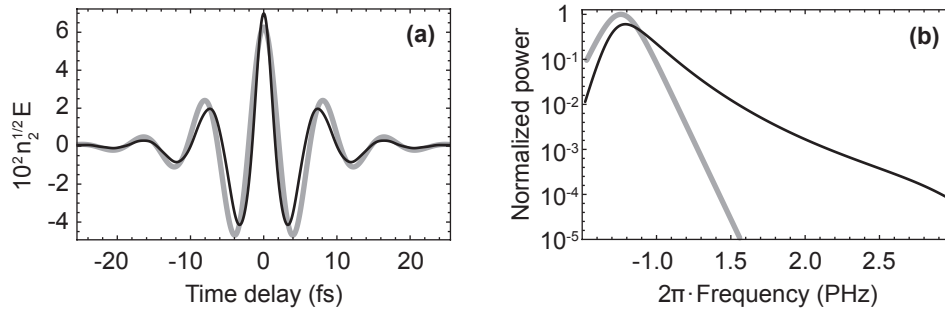


**Figure 3.2:** (a) Shape of an ultrashort soliton in fused silica (at  $\lambda = 2.5 \mu\text{m}$ , grey line) is compared to the fundamental soliton solution (black line). (b) the same pulses are compared in the spectral domain, see [84]

This fact seems to reveal a generic feature of short pulses. Consider, for instance, a rapidly developing field of rogue waves [19], dangerous objects that “come from nowhere and disappear without a trace” [82]. They are often associated with the breather solutions of the NLSE, i.e., Peregrine [81] and Akhmediev breathers [92, 93]. Note, that a single rogue wave seems to be very different from a wave packet with an envelope. Still it can be perfectly fitted by a breather solution.

Last but not least. Equation (3.28) implicitly assumes that the polynomial  $1 + v^2 + \mathcal{F}(v)$  does not have real roots, which lead to divergence. This is indeed so for NLSE, where  $\mathcal{F}(v)$  vanishes, but what about the higher-order polynomials that are used to approximate the dispersion law? There are two possibilities.

- ❶ The denominator  $1 + v^2 + \mathcal{F}(v)$  may vanish within the soliton spectrum. This results in so-called *Cherenkov radiation* [94]. Strictly speaking, the solitary solutions do not exist: they should be considered together with the emitted waves.
- ❷ The denominator  $1 + v^2 + \mathcal{F}(v)$  may vanish outside the soliton spectrum due to the behavior of  $\mathcal{F}(v)$  with the increase of  $v$ . The situation can be improved by a better approximation of the dispersion law, as described in the rest of this Chapter.

### 3.3 What may be wrong with GNLSE?

Equation (3.15) applies to a wide range of phenomena in fiber optics and has useful features, namely:

- ❶ It describes propagation of an isolated few-cycle pulse, which seems to have no envelope. Typically, GNLSE solutions are in excellent agreement with that of Maxwell equations [35, 95, 39].
- ❷ It describes supercontinuum (SC) generation. In some SC scenarios numerous interacting pulses get different carrier frequencies, generate new pulses, and finally fill a wide spectral window. The final state is beyond the scope of SVEA and yet GNLSE (3.15) applies [78, 96].
- ❸ There are SVEA-free derivations of the GNLSE, see [35, 36, 37, 38, 39, 40]. The simplest such derivation was comprised in Section 3.1.
- ❹ Even when GNLSE fails, it can be fixed by adding new terms. E.g., pulses that are initially much longer than a single optical cycle cannot be described by Eq. (3.14) when formation of an optical shock takes place [97]. A more general Eq. (3.15), which contains the self-steepening derivative, was found to be sufficient [98].
- ❺ And if that is not enough, GNLSE can be solved with ease by the split-step method [44]. One alternates between linear and nonlinear steps, which are addressed by the fast Fourier transform and, e.g., by a Runge-Kutta solver respectively. This can be done in parallel, as discussed in Chapter 6



It is no wonder that, whenever possible, GNLSE is the model of choice in fiber optics. The situations in which the most general Eq. (3.15) is unsafe are less known and discussed below.

## Convergence

Let us recall that  $\beta_j = \beta^{(j)}(\omega_0)$ , and take a closer look at the so-called *dispersion operator*

$$\hat{\mathcal{D}} = \sum_{j=2}^J \frac{\beta_j}{j!} (i\partial_\tau)^j, \quad (3.29)$$

which enters GNLSE (3.15). The operator is associated with the Taylor expansion (3.13) of  $\beta(\omega)$  at the carrier frequency  $\omega_0$ . If SVEA applies, operator  $\hat{\mathcal{D}}$  is dominated by the contribution of  $\beta_2$ , the so-called *group velocity dispersion (GVD)* parameter. This is why a relatively simple NLSE (3.12) suffices to address many important problems. The higher-order dispersion coefficients are relevant, e.g., near the zero dispersion frequency (**ZDF**) at which GVD vanishes.

To measure deviation of  $\beta(\omega)$  from a straight line, we introduce the quantity

$$D(\omega) = \beta(\omega) - \beta_0 - \beta_1(\omega - \omega_0), \quad (3.30)$$

where

$$D(\omega) \approx \sum_{j=2}^J \frac{\beta_j}{j!} (\omega - \omega_0)^j. \quad (3.31)$$

The deviation  $D(\omega)$  is strictly zero for a non-dispersive medium with a constant index of refraction. As to dispersive media:

☞ “It is widely believed that the inclusion of just a few additional higher-order terms in the Taylor series approximation of the material dispersion will greatly improve its accuracy” [99].

The reality may be just the opposite. To illustrate the problem, we consider dispersion of the fluoride glass and a carrier wave at  $1.6 \mu\text{m}$ . Taylor approximations of  $D(\omega)$  with the increasing order  $J$  are plotted in Fig. 3.3 by color lines. The black line is for the “exact”  $D(\omega)$ , which is derived from the relation (3.16) which is coupled with the bi-Lorentzian approximation of the relative permittivity

$$\epsilon(\omega) = 1 - \sum_{j=1,2} \frac{b_j^2}{(\omega + i\omega_j'')^2 - (\omega_j')^2}. \quad (3.32)$$

Notations  $\omega_j'$  and  $\omega_j''$  emphasize four poles of  $\epsilon(\omega)$  at  $\omega = \pm\omega_j' - i\omega_j''$  in the complex plane. Two poles are for positive and two for negative  $\text{Re } \omega$ , all four poles belong to the half-plane  $\text{Im } \omega \leq 0$  (Fig. 3.4). For the parameter values in Eq. (3.32) see [99].

It is easy to see that the gray domain in Fig. 3.3 is outside the convergence radius of the Taylor expansion (3.31). Therefore:

❗ Taylor expansion (3.31) calculated at  $\lambda = 1.6 \mu\text{m}$  fails to approximate  $D(\omega)$  for  $\lambda < 0.86 \mu\text{m}$  in fluoride glass. The value of the approximation order  $J$  does not matter.

Figure 3.3 indicates that increase of  $J$  does not improve the approximation in the gray domain ( $\lambda < 0.86 \mu\text{m}$ ). The reason is that all four poles of  $\epsilon(\omega)$ , see Fig. 3.4, are inherited by  $\beta(\omega)$  and limit series convergence in Eq. (3.31). Moreover, such singular points or resonant frequencies are unavoidable for any nontrivial dispersion, being related to the causality [47]. The mathematical reason is that [46]:

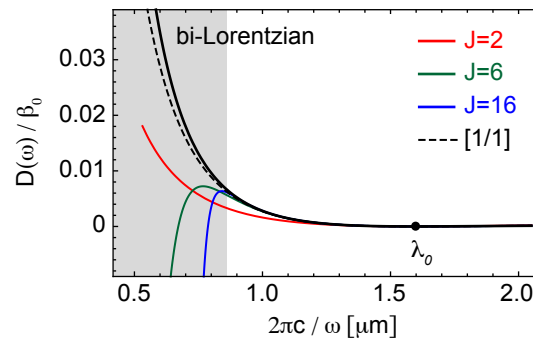


**Figure 3.3:** Deviation  $D(\omega)$  from Eq. (3.30) is plotted for fluoride glass (black line) together with its Taylor expansions of order  $J$  (color lines) with  $\lambda_0 = 1.6 \mu\text{m}$  (black point). The expansions diverge in the dashed domain. The dashed line is obtained by employing the simplest  $[1/1]$  Padé approximant of  $D(\omega)/(\omega - \omega_0)^2$ , it is shown for comparison. Higher-order Padé approximants are not shown, because the resulting curves are indistinguishable from  $D(\omega)$  in the spectral window of interest.

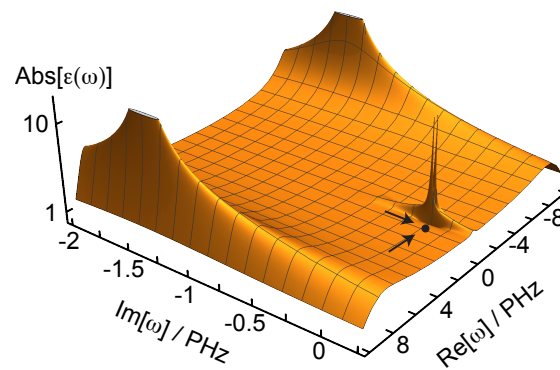


**Figure 3.4:** The absolute value of the permittivity  $\epsilon(\omega)$  in the complex  $\omega$ -plane is plotted for the model Eq. (3.32). The black point, which is indicated by two arrows for better visibility, corresponds to the carrier frequency in Fig. 3.3. The nearest pole in the complex plane limits the convergence of the Taylor series. The fact that  $\epsilon(\omega)$  is smooth for all real frequencies does not matter.

- ❗ The Laplace transform in Eq. (1.10), being bounded and analytic in the upper half-plane, must lose analyticity at some frequencies in the lower half-plane. Either poles or more sophisticated singularities must appear for  $\epsilon(\omega) \neq \text{const.}$

Oughstun and Xiao concluded that:

- 📖 “The inclusion of higher-order terms in the Taylor series approximation of the complex wave number in a dispersive, attenuative medium beyond the quadratic approximation is practically meaningless from both the physical and mathematical points of view” [99].

This statement is an apparent contradiction to the countless successful studies employing the GNLSE (3.15). Let us see how to resolve the contradiction.

### 3.4 Polynomial approximations

The convergence problem, which is raised in the previous section, can be relaxed by accepting the little-known fact that:

- ❗ The right-hand-side of Eq. (3.13) is not necessarily Taylor’s expansion. Any polynomial approximation of  $\beta(\omega)$  will do the job.

At the end of the day, an exact analytic expression for  $\beta(\omega)$ , which can be expanded in a power series, is an exception. One usually deals with either measured or numerically calculated  $\beta(\omega)$  and there is literally nothing to expand.

On the other hand, the GNLSE derivation outlined in Section 3.1 requires only a polynomial representation of  $\beta(\omega_0 + \delta\omega)$ . There is no special reason to use Taylor expansion. The more so, if slow evolution of the carrier frequency  $\omega_0 + \delta\omega$  finally makes it considerably different from  $\omega_0$  and triggers convergence issues.

Polynomial approximations are more flexible than Taylor series. The fundamental Stone-Weierstrass approximation theorem [100] (for the case at hand and in our notations) states that:

☞ For any continuous dispersion relation  $k = \beta(\omega)$ , any finite spectral window, and arbitrarily small  $\delta > 0$  there is a polynomial  $p(\omega)$  such that  $|\beta(\omega) - p(\omega)| < \delta$ . The inequality holds uniformly for all frequencies in the spectral window.

In other words, rather than trying to approximate  $\beta(\omega)$  for  $\omega \rightarrow \omega_0$  as good as possible (Taylor), one uniformly approximates  $\beta(\omega)$  in the whole spectral window of interest (Weierstrass). The GNLSE (3.15) retains its structure, yet the dispersion parameters  $\beta_j$  now refer to the derivatives of the approximation, not to the “true”  $\beta^{(j)}(\omega)$ .

❗ To pull together the mathematically strict results of [99] and countless successful studies, which are based on GNLSE, one should replace *expansion* of the dispersion relation by its *approximation*.

This approach is actually used in all papers operating with several dispersion parameters, even if, without mentioning it. However, it does not resolve all issues.

It is technically easier to discuss the remaining problems for  $\epsilon(\omega)$  and then change to  $\beta(\omega)$ . Note, that the integral representation (1.10) imposes some a priori restrictions on  $\epsilon(\omega)$  [47]. In our context, it is especially important that:

- ❶ Permittivity  $\epsilon(\omega)$  is a holomorphic function in the upper half-plane  $\text{Im } \omega > 0$ . Within this domain, we have  $\epsilon(\omega) \rightarrow 1$  for  $|\omega| \rightarrow \infty$ , which results in the Kramers-Kronig relations.
- ❷ If  $\epsilon(\omega)$  is non-constant, there is a set of complex frequencies (resonances) at which  $\epsilon(\omega)$  is singular. They belong either to the real axis or to the lower half-plane  $\text{Im } \omega < 0$ .

Polynomials are neither bounded nor have they poles or other singularities. They are not subject to the Kramers-Kronig relations, i.e., the dispersion law behind any GNLSE must violate the causality principle. For these reasons, polynomial approximations of  $\epsilon(\omega)$  and  $\beta(\omega)$  may be inappropriate even if they are used for only real frequencies and on a finite  $\omega$ -interval. The following three issues are especially important in the framework of GNLSE.

### Wrong GVD due to interpolation

Assume that a “true”  $\epsilon(\omega)$  is accurately approximated by a higher-order polynomial  $p(\omega)$ . A priori, we have  $\epsilon(\omega) \rightarrow 1$  with the increase of  $\omega$ , which cannot be expected from  $p(\omega)$ . And yet, we have  $|\epsilon(\omega) - p(\omega)| < \delta$  on an arbitrarily chosen  $\omega$ -interval. How a constant value can be approximated by a polynomial?

As  $\delta$  decreases, the difference  $\epsilon(\omega) - p(\omega)$  starts to suffer from small but wild oscillations. Numerical examples imply that this undesired effect occurs when the interpolation interval exceeds the natural convergence domain of the Taylor expansion, as illustrated in Fig. 3.5. So, the curse of the convergence radius is still there.

Returning to  $\beta(\omega)$  approximated by Eq. (3.13), we see that the true group velocity  $1/\beta'(\omega)$  may be very different from that of the approximation, and even more so for the GVD parameter  $\beta''(\omega)$ . Both quantities have a huge impact on behaviour of optical pulses [11] and their wrong values cannot be tolerated.

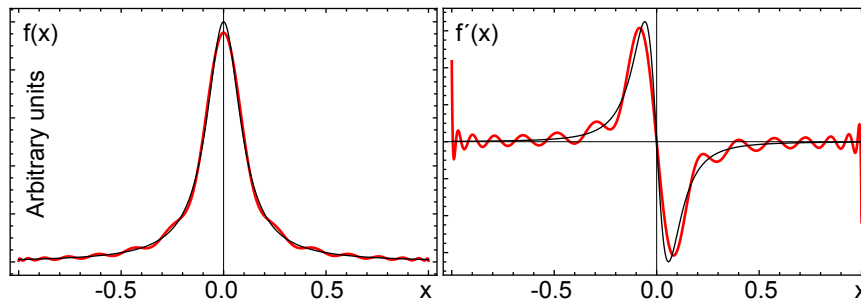


**Figure 3.5:** Left: An exemplary rational function  $f(x) = 1/[1 + (10x)^2]$  is approximated by 30 Chebyshev polynomials far beyond the convergence radius  $R = 0.1$  of the Taylor expansion at  $x = 0$ . Right: approximation of the derivative suffers from oscillations.

### Stiffness due to extrapolation

Material properties, such as fiber dispersion, are in the best case available in the fiber transparency window, say  $[f_1, f_2]$  in the frequency domain. The “optimal” GNLSE is centered at  $(f_1 + f_2)/2$  and covers the whole frequency window. This leaves us with the smallest possible time discretization

$$\left| f - \frac{f_2 + f_1}{2} \right| \leq \frac{f_2 - f_1}{2} \Rightarrow dt = \frac{1}{f_2 - f_1},$$

which is 0.74 fs for the well known Sellmeier model for bulk fused silica [101]. The value of  $dt$  suffers from further increase, if the reference carrier frequency is not in the middle of the interval  $[f_1, f_2]$ . For instance, we have  $dt = 1.7$  fs for the carrier wave at  $0.8 \mu\text{m}$ . As to commercial fibers, the known part of their transparency window is usually much shorter than that of bulk silica, which leads to further increase of  $dt$ .

GNLSE cannot properly resolve field structures with a duration shorter than, say  $5dt$ . Proper description of, e.g., two-cycle 6 fs pulses and even shorter ones [3, 4, 5, 6], which nowadays are generated in optical labs, is then problematic. The more so, when ultrashort structures, such as optical shocks or extreme rogue waves [102], unexpectedly appear in the course of pulse evolution.

A typical workaround is that the GNLSE is solved in a larger spectral window for which purpose the dispersion operator (3.29) is extrapolated beyond  $[f_1, f_2]$ . However, polynomials are not suited for extrapolation: they quickly get extremely large values outside the interpolation interval. These large values of  $\beta(\omega)$  make no sense from the physical point of view. Mathematically, they lead to extremely small spatial steps  $dz$  for the stable numerical solution of Eq. (3.15). In other words, a direct attempt to extrapolate  $\beta(\omega)$  leads to a stiff problem.

### Extrapolation of attenuation

Any attempt to apply polynomials for approximation/extrapolation of the losses term  $\alpha(\omega) = \text{Im}[k(\omega)]$  may result in a huge artificial gain. The latter leads to much worse consequences than “just stiffness” from extrapolation of  $\beta(\omega) = \text{Re}[k(\omega)]$ . Note that, while expansions of  $\alpha(\omega)$  are formally present in the state of art derivations of the GNLSE [35, 95], the final Eq. (3.15) contains only  $\alpha_0$ . The same applies to the complex Ginzburg-Landau equation [103], which accounts for  $\alpha_0$  and  $\alpha_2$ , while ignoring  $\alpha_1$ .

The message is that:

- ❗ A brute force increase of the approximation order in GNLSE is dangerous, especially if pulse spectral broadening takes place due to, e.g., SC generation or shock formation. From the mathematical point of view, polynomials fail to account for resonances: complex frequencies at which  $\epsilon(\omega)$  and  $\beta(\omega)$  take infinite values.

The difficulty may be resolved by changing from polynomial to rational approximations, e.g., to Padé approximants [51], as discussed in the next section.

### 3.5 Padé approximants

Given a smooth function  $f(x)$ , its Taylor approximation, say at  $x = 0$  and of integer order  $p \geq 0$ , is given by a polynomial

$$P(x) = a_0 + a_1x + a_2x^2 + \cdots + a_px^p,$$

where  $p + 1$  parameters  $a_j$  are chosen to keep as many as possible successive derivatives of  $f(x)$  and  $P(x)$ , both calculated at  $x = 0$ , identical. This informal definition requires that

$$\left(\frac{d^j f}{dx^j}\right)_{x=0} = \left(\frac{d^j P}{dx^j}\right)_{x=0} \quad \text{for } 0 \leq j \leq p,$$

which results in an explicit expression for the coefficient  $a_j$ . It is usually assumed that  $f(x)$  has  $p + 1$  derivatives, in which case the local error of the approximation is  $O(x^{p+1})$  for  $x \rightarrow 0$ .

Given two non-negative integers  $p$  and  $q$ , the Padé approximant of  $f(x)$  at  $x = 0$  of order  $[p/q]$  is given by a rational function

$$R(x) = \frac{a_0 + a_1x + a_2x^2 + \cdots + a_px^p}{1 + b_1x + b_2x^2 + \cdots + b_qx^q}, \quad (3.33)$$

with the same requirement of identical successive derivatives, which now reads

$$\left(\frac{d^j f}{dx^j}\right)_{x=0} = \left(\frac{d^j R}{dx^j}\right)_{x=0} \quad \text{for } 0 \leq j \leq p + q. \quad (3.34)$$

The local error of the approximant is  $O(x^{p+q+1})$  for  $x \rightarrow 0$ . For instance, taking exponential function and  $p + q = 2$ , we have three possible  $O(x^3)$  approximations:

exact	$[2/0]$	$[1/1]$	$[0/2]$
$e^x$	$1 + x + \frac{x^2}{2}$	$\frac{1 + \frac{1}{2}x}{1 - \frac{1}{2}x}$	$\frac{1}{1 - x + \frac{1}{2}x^2}$

**Table 3.1:** Examples of the Padé approximants

For  $q = 0$ , Eq. (3.33) reduces to the standard Taylor expansion of  $f(x)$ . For  $p = 0$ , we have Taylor expansion of  $1/f(x)$ . For  $p = q$ , one gets the so-called *diagonal approximant*. Note, that one can face a degenerate situation with, e.g.,  $b_q = 0$ , such that degree of the denominator in Eq. (3.33) is less than expected. Non-degenerate diagonal approximants are bounded for  $x \rightarrow \infty$ , which is welcome for approximations of the material functions like  $\epsilon(\omega)$  and  $n(\omega)$ .

Padé approximants are less flexible than Taylor expansions. Among other things, it should be noted that:

- ❶ As opposed to Taylor series, there is no simple expression for the coefficients  $a_j$  and  $b_j$  in Eq. (3.33). A system of linear equations for the coefficients should be derived from Eq. (3.34) and solved separately for each pair  $[p/q]$ . This makes analytical considerations more involved, but does not really affect applications.
- ❷ The system of equations for the coefficients may happen to be incompatible for some specially chosen functions  $f(x)$  and pairs  $[p/q]$ . For instance,  $[1/1]$  approximant of  $f(x) = x^2$  does not exist. Such degenerate situations do not come into play for approximation of the material relations in optics.

- ⊕ Note, that the  $[1/1]$  approximant of  $e^x$  in the above table is singular for  $x = 2$ . In a similar way, singularities may appear for some pairs  $[p/q]$  when approximating material functions. These singularities may further disappear (move to the complex plane) with the increase of the approximation order. For instance, the next diagonal approximant of the exponential function reads

$$e^x = \frac{1 + \frac{1}{2}x + \frac{1}{12}x^2}{1 - \frac{1}{2}x + \frac{1}{12}x^2} + O(x^5),$$

and it is regular for all real  $x$ . For more information on Padé approximants see [104, 105].

Padé approximants have numerous applications, e.g., they can be used in fiber optics to estimate the response function in Eq. (1.9) for a ring laser, see [106]. We now turn to applications of the Padé approximants for GNLSE, following [51]. Recall, that both GNLSE (3.14) and (3.15) involve the dispersion operator (3.29)

$$\hat{\mathcal{D}}e^{-i\Omega\tau} = \Omega^2 \left( \frac{\beta_2}{2} + \frac{\beta_3}{6}\Omega + \dots + \frac{\beta_J}{J!}\Omega^{J-2} \right), \quad (3.35)$$

which is associated with either Taylor expansion or polynomial approximation of  $\beta(\omega)$  in Eq. (3.13). If the dispersion coefficients  $\beta_{2 \leq j \leq J}$  are available, one can replace the term in brackets in Eq. (3.35) by its Padé approximant.

An example is shown in in Fig. 3.3. We see that even the simplest  $[1/1]$  approximant (dashed line ) works better than all series expansions and does not suffer from divergence for  $\lambda < 0.86 \mu\text{m}$ . The reason is that the approximant goes beyond the convergence radius. Moreover, the stiffness of the resulting equation is much less demanding. With a diagonal approximant GNLSE stiffness is as good as that of NLSE. There is a price to pay:

- ⊕ The denominator in Eq. (3.34) might have zeros in the frequency domain of interest. A rule of thumb is that either these singularities disappear for proper pairs  $[p/q]$  or they are shifted away from the approximation interval.

In both cases the rational approximation works better than the polynomial one. A similar situation arises when a polynomial approximation of the refractive index is available. The index can be reapproximated using a diagonal Padé approximant, to keep  $n(\omega)$  bounded for large frequencies. The message of this section is as follows:

- ⊕ It might be tricky to find a Padé approximant (or a more general rational approximation) of the material function  $\beta(\omega)$  and the induced dispersion operator (3.29). If it works out, the resulting GNLSE is much more friendly to extrapolations of the spectral window and in any case less stiff than the standard GNLSE.

# Chapter 4

## Short pulse equations

The strongest point of GNLSE is without a doubt its *flexibility*. A dispersion law, no matter how complicated, can be approximated by a polynomial. When the spectrum in question becomes too broad, the polynomial is seamlessly integrated with a rational function as described in Chapter 3. Additional effects, like self-steepening or Raman effect, are accounted for by adding new terms to the simplest GNLSE, see the transition from Eq. (3.14) to Eq. (3.15). Other examples are given by inclusion of radial effects [35, 36] and two-photon absorption [107]. All these model equations are loosely referred to as GNLSEs.

The approach of this Chapter is different and leads to the so-called *short pulse equation (SPE)*.

- Model equations that we refer as SPEs, avoid use of the pulse envelope and apply directly to the pulse electric field. Moreover, the pulse is assumed to propagate in a fiber transparency window well between two resonant frequencies.

In analogy with GNLSE, several slightly different SPEs have been derived previously, some of them are integrable like the classic NLSE, others are non-integrable, like a generic GNLSE. In what follows, we will discuss one real and one complex SPE. It is a good point to stress that:

- ❶ Our main point of interest is not the minor differences in derivations and fields of application of different SPEs, but universal properties of short pulses that must be reflected in all such SPEs.

In the first instance we are interested in the shortest possible soliton duration and in mathematical reasons that prevent solitons from being too short. The original results presented in this Chapter are based on [108, 109, 110, 111].

### 4.1 Key concepts

Although there are several slightly different SPEs, all their derivations make use of the following key ideas:

- ❶ An approximated dispersion law for a transparency band between two well-separated resonant frequencies is used

$$\chi(\lambda) = \dots + \frac{c_{-4}}{\lambda^4} + \frac{c_{-2}}{\lambda^2} + c_0 + c_2\lambda^2 + c_4\lambda^4 + \dots, \quad (4.1)$$

where two or three central terms are important for SPEs. The coefficients  $c_0, c_{\pm 2}, c_{\pm 4} \dots$  are just fit parameters.

- ❷ SPEs are derived directly for the electric field. The final equation may be real or complex. It may apply to one field component  $E_x$ , or to its analytic signal, or to a combined quantity like  $E_x + iE_y$ .

- ④ SVEA is replaced by a less restrictive unidirectional approximation. All known SPEs are  $z$ -propagated, as discussed in Chapter 2. They refer to a co-moving frame of reference.

Note, that approximation (4.1) is independent of the pulse carrier frequency. It is associated with a wide transparency band between low- and high-frequency material resonances.

- 📖 Model equations for ultrashort pulses in the vicinity of resonances, which are reviewed e.g. in [112], are out of scope of this work.

Recall, that for real frequencies Eq. (1.10) implies  $\epsilon(\omega) = \epsilon^*(-\omega)$ , such that we assume  $\epsilon(\omega) \approx \epsilon(-\omega)$  for the transparency domain. This is why only even powers with real coefficients appears in Eq. (4.1). The latter looks like a Laurent series but actually is a combination of such series taken for different terms of the full dispersion function, see § 2.3 in [28].

Another important point is that to the best of our knowledge no attempt has been made to improve the SPE by taking more than three terms in Eq. (4.1). This is in apparent contradiction to the numerous dispersion terms that GNLSE inherits from the Taylor expansion (3.13). The improvement is not necessary because:

- ① The main idea behind any SPE is to sacrifice some generality for the sake of simplicity.

In return, SPE provides exact special solutions and useful insights into the fundamental properties of ultrashort pulses. These properties are either not covered by the GNLSE or difficult to extract from it, as discussed in what follows.

## 4.2 Real SPEs

The most popular SPE was derived by Schäfer and Wayne [113].

- 📖 Actually, a more general equation appeared earlier both in a forgotten work [114] and in a sequence of papers that starts with [115].

Schäfer and Wayne studied propagation of light in the infrared range with wavelengths of 1.6–3.0  $\mu\text{m}$ . They have found that  $\chi(\lambda)$  of fused silica is well approximated by a trial function  $c_0 + c_2\lambda^2$  with two fit parameters, see Fig. 4.1(a). This, of course, corresponds to two central terms in Eq. (4.1). Moreover, the specific values  $c_0 = 1.11$  and  $c_2 = -0.011\mu\text{m}^{-2}$  suggest that  $c_0 \gg c_2\lambda^2$ , i.e., in the first approximation all spectral components propagate with the same velocity. One can then introduce a common delay variable

$$\tau = t - \frac{z}{V} \quad \text{with} \quad V = \frac{c}{\sqrt{1 + c_0}}, \quad (4.2)$$

where  $z$  is the propagation length and  $c$  is the speed of light.

Assuming one-dimensional geometry and unidirectional propagation, Schäfer and Wayne derived their SPE for the wave-field  $\mathbf{E} = (E(z, \tau), 0, 0)$

$$\partial_z E + b\partial_\tau^{-1} E + gE^2\partial_\tau E = 0. \quad (4.3)$$

Parameters  $b$  and  $g$  characterize dispersion and nonlinearity and are somewhat similar to  $\beta_2$  and  $\gamma_0$  in NLSE (3.12). Here and in what follows, we use the following definition of the inverse differentiation

$$\partial_\tau^{-1} E(z, \tau) = \int_{-\infty}^{\tau} E(z, \tau') d\tau',$$



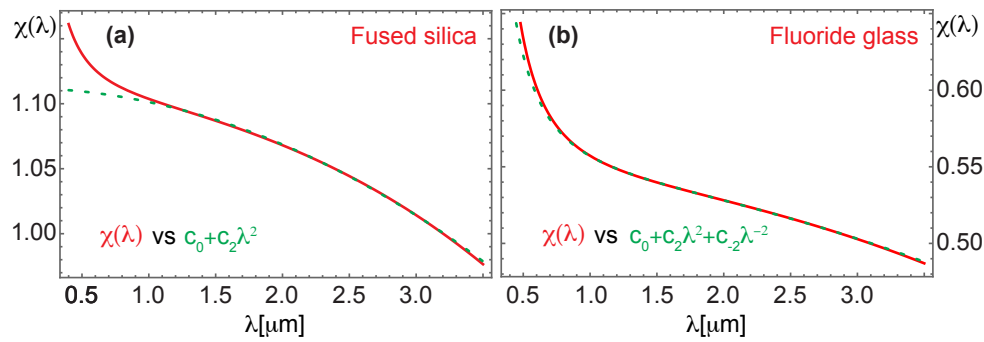


**Figure 4.1:** Approximations, which were used to derive SPEs (green lines, see Table 4.1), are shown versus actual values of  $\chi$  (red lines, see [101]).

where it is natural to assume that  $E(z, \tau)|_{\tau=-\infty} = E(z, \tau)|_{\tau=\infty} = 0$  for the localized pulses of interest.

Equation (4.3) is  $z$ -propagated: it accepts  $E$  at, say,  $z = 0$  for  $\forall \tau$  as the initial condition. Given  $z > 0$ , Eq. (4.3) allows to calculate  $E(z, \tau)$  for  $\forall \tau$ , e.g., the outgoing pulse at the end of the fiber. The possibility to solve the model equation along the fiber comes into play due to the unidirectional nature of the SPE in a full analogy with the GNLS. Among other things, Eq. (4.3) yields

$$\int_{-\infty}^{+\infty} E(z, \tau) d\tau = 0,$$

such that ultrashort pulses in question have only trivial electric area in the sense of Eq. (2.22).

SPE (4.3) is well-posed for sufficiently small initial data [116] and is comparable with no less than the Korteweg-de Vries (**KdV**) equation for shallow water waves

$$\partial_t v + v \partial_x v + \partial_x^3 v = 0, \quad (4.4)$$

where  $v$  is the (normalized) elevation of the water surface above the bottom [117]. The  $t$ -propagated Eq. (4.4) was originally developed to explain appearance of the solitary waves in water channels, the space variable  $x$  points along the channel. Moreover, KdV is an universal model for many nonlinear wave-systems with the dispersion law  $\omega - kV \propto k^3$  and quadratic nonlinearity [68]. It gave rise to the first class of nonlinear PDEs addressed by the inverse scattering method [118] and was recognized as a completely integrable Hamiltonian system [63]. The second such class originated from the NLSE (3.12), see [75].

For some wave-systems with the dispersion law like in KdV but cubic nonlinearity, one derives the so-called *modified KdV* (**mKdV**) equation

$$\partial_t v \pm v^2 \partial_x v + \partial_x^3 v = 0, \quad (4.5)$$

which is integrable as well as KdV. Also the space-propagated versions of KdV and mKdV find their applications, among other things, for pulses in fibers [119].

We now return to the SPE (4.3). Like its better known team-mates, it is an integrable equation and is equivalent to an infinite-dimensional Hamiltonian system with a very special bi-Hamiltonian structure [120]. Integrability of SPE was also proven by its direct reduction to a known integrable equation [121, 122].

The two-term approximation  $c_0 + c_2 \lambda^2$  that is shown in Fig. 4.1(a), covers only the anomalous dispersion domain with  $d\chi/d\lambda < 0$ . Both the normal and anomalous dispersion domains within one transparency window can be covered by three central terms in Eq. (4.1),  $\chi(\lambda) \approx c_0 + c_2 \lambda^2 + c_{-2} \lambda^{-2}$ , as shown in Fig. 4.1(b). The resulting equation for short pulses is derived in a full analogy with Eq. (4.3) and reads [114, 127]

$$\partial_z E + a \partial_\tau^3 E + b \partial_\tau^{-1} E + g E^2 \partial_\tau E = 0. \quad (4.6)$$

Equation (4.6) is also referred to as SPE. It builds a bridge between the simplest SPE (4.3) and mKdV (4.5). As far as we know, SPE (4.6) is non-integrable. For a summary on dispersion approximations see Table 4.1.

Drude model	[115, 123, 113, 124, 21, 125, 126, 108]	[114, 127, 128, 129, 130, 109]
Plasma fr. $\omega_p$	Fit parameters $c_0, c_2$	Fit parameters $c_0, c_{\pm 2}$
$\chi(\omega) = -\frac{\omega_p^2}{\omega^2}$	$\chi(\lambda) \approx c_0 + c_2\lambda^2$	$\chi(\lambda) \approx \frac{c_{-2}}{\lambda^2} + c_0 + c_2\lambda^2$

**Table 4.1:** Dispersion approximations that were used to derive SPEs are shown. Note, that the classical Drude model gives a physically valid  $\chi$  for  $\forall\omega$  with the correct behaviour for  $\omega \rightarrow \pm\infty$  and correct positions of the poles in the complex  $\omega$ -plane. Strictly speaking, this does not apply to  $c_0 + c_2\lambda^2$ , because  $c_0 \neq 0$ . Even more so, this does not apply to the three-term approximation because of the completely wrong behaviour for  $\lambda \rightarrow 0$ . Still, the second column and the SPE (4.3) go as far as possible in providing a simple causal approximation to the dispersion law.

### 4.3 Complex SPEs

Note, that SPE (4.6) with the extra term  $a\partial_t^3 E$ , which “improves” SPE (4.3), is somewhat similar to the special GNLSE (3.14) with just one additional  $\beta_3$  term, which extends NLSE (3.12). In both cases, the extended equation covers both normal and anomalous dispersion domains, cf. Fig. 4.1(a) and (b). On the other hand, Eq. (4.6) is real and GNLSE is complex. However, it is easy to derive a useful complex analogue of a real SPE.

To obtain the complex SPE, we employ Eq. (4.2) to return for a moment to the lab frame in the real SPE (4.6)

$$\partial_t(\partial_z + V^{-1}\partial_t)E + a\partial_t^4 E + bE + \frac{g}{3}\partial_t^2(E^3) = 0, \quad (4.7)$$

and to reconstruct the lab dispersion relation for the linear waves

$$k = \beta(\omega) \quad \text{with} \quad \beta(\omega) = \frac{\omega}{V} - a\omega^3 - \frac{b}{\omega}. \quad (4.8)$$

Note, that the GVD parameter is  $\beta''(\omega) = b\omega^{-2} - 3a\omega^2$ , such that the zero-dispersion frequency indeed appears for  $ab > 0$ .

- ❶ The key idea is to simplify the real SPE by neglecting generation of the third harmonics. The price we have to pay is that the resulting model operates with the analytic signal, i.e., is complex.

Among other things, we have to take care of frequency sign and unidirectional approximation, this is why the lab Eq. (4.8) is required. We now assume that for any triplet of linear waves that belong to pulse spectrum

$$(\omega_i, k_i)_{i=1,2,3} \quad \text{with} \quad \omega_i > 0 \quad \text{and} \quad \underbrace{k_i = \beta(\omega_i) > 0}_{\text{unidirectionality}}$$

the combined wave with  $\omega = \sum \omega_i$  and  $k = \sum k_i$  does not satisfy Eq. (4.8). Such new harmonics, being inevitably generated due to the  $E^3$  term, do not experience resonant growth.

To take advantage of this, we split the positive- and negative-frequency parts in Eq. (4.7) by introducing the analytic signal  $\mathcal{E}$  for the electric field with  $E = \frac{1}{2}(\mathcal{E} + \mathcal{E}^*)$ , as in Eq. (1.2). The lab SPE (4.7) takes the form

$$\partial_t(\partial_z + V^{-1}\partial_t)\mathcal{E} + a\partial_t^4 \mathcal{E} + b\mathcal{E} + \frac{g}{12}\partial_t^2 \underbrace{\left\{(\mathcal{E} + \mathcal{E}^*)^3\right\}}_{\text{positive-freq. part}} = 0,$$

where different terms in  $(\mathcal{E} + \mathcal{E}^*)^3$  correspond to different four-wave mixing processes. As long as the above described resonances are absent, one can neglect both  $\mathcal{E}^3$  and the positive-frequency part of  $|\mathcal{E}|^2\mathcal{E}^*$ , which results in

$$\partial_t(\partial_z + V^{-1}\partial_t)\mathcal{E} + a\partial_t^4 \mathcal{E} + b\mathcal{E} + \frac{g}{4}\partial_t^2(|\mathcal{E}|^2\mathcal{E}) = 0.$$

Strictly speaking, one should take only the positive-frequency part of  $|\mathcal{E}|^2\mathcal{E}$ , but in reality the difference is not significant both in unidirectional and even in bidirectional context, see [110]. Finally, we change back to the co-moving frame and integrate over  $\tau$

$$\partial_z\mathcal{E} + a\partial_\tau^3\mathcal{E} + b\partial_\tau^{-1}\mathcal{E} + \frac{g}{4}\partial_\tau(|\mathcal{E}|^2\mathcal{E}) = 0. \quad (4.9)$$

This model will be referred to as the complex SPE [111]. The complex analog of the simplest SPE (4.3) is, of course, of the form

$$\partial_z\mathcal{E} + b\partial_\tau^{-1}\mathcal{E} + \frac{g}{4}\partial_\tau(|\mathcal{E}|^2\mathcal{E}) = 0. \quad (4.10)$$

and should be considered as a direct analog of the NLSE, but for short pulses.

Another physical situation that directly leads to a complex SPE is propagation of an ultrashort wave packet with circular polarization. Two components of the real electric field are just combined into a single complex field and one obtains a bidirectional complex SPE by combining two real equations [21, 125].

We are now ready to discuss the limiting, shortest solitons. Their properties are universal and to large extent do not depend on the chosen model. However, it is technically easier to derive the solitary solutions for the complex SPE (4.10).

## 4.4 Peaked solitons

As mentioned in the introduction to this Chapter, SPEs provide insights in such properties of ultrashort pulses that are difficult or even impossible to extract from the standard NLSE/GNLSE. The most fascinating example is a quantitative prediction of the shortest soliton duration, which approximately corresponds to one-and-half field cycles (FWHM) [21, 122]. Note, that the fundamental soliton solution (3.23) of the NLSE (3.12) is mathematically valid for any duration  $\tau_0$ .

- ❗ Informally speaking, both NLSE and GNLSE do not care that a valid envelope should cover at least several field cycles and that at any rate a stable sub-cycle soliton is not possible. SPEs are more “clever”.

To begin with, it was found that SPE (4.3) is mathematically equivalent to the integrable sine-Gordon equation [121]. However, certain regular solutions of the latter correspond to the multi-valued solutions of the former, see [122]. Such *loop solitons* may also appear in other contexts [131] and are, of course, nonphysical. What is of interest, is the last valid solitary solution, which serves as the limiting member in a family of the SPE solitons.

More precisely, all solitary solutions with several (ten or more) cycles, be they from SPEs or from NLSE/GNLSE, are similar to each other. As soliton’s duration decreases, the SPE solutions start to develop a certain nonphysical feature and are finally spoiled at the limiting duration. The feature might be a nonlinear steepening, which leads to an infinite slope of the electric field. Another option is formation of a cusp at the top of the soliton, which results in a peaked pulse. The latter is referred to as *peakon* or *cuspon*.

- 📖 Peaked pulses are not uncommon, e.g., prior to short optical pulses they were found by Camassa and Holm for shallow water [132]. Their story arguably begins in 1880, when Stokes demonstrated that gravity waves of the maximum height have a sharp wave crest [133].

In the framework of the Camassa-Holm equation, all solitons have a cusp. In optics, however, the peaked solitons appear as limiting solutions [21]. This phenomenon is universal and has been found for all SPEs. To understand how it works, we consider the complex SPE (4.10).

In the rest of this section it is convenient to change to a normalized Eq. (4.10), which we set to be

$$\partial_\tau\partial_z\mathcal{E} + \frac{1}{2}\mathcal{E} + \partial_\tau^2(|\mathcal{E}|^2\mathcal{E}) = 0, \quad (4.11)$$

for better compatibility with the published solutions. Equation (4.11) yields a normalized dispersion relation for a linear wave with  $\mathcal{E} \propto e^{i(\kappa z - \nu \tau)}$

$$\kappa \nu = -\frac{1}{2} \quad \text{with} \quad v_p = \frac{\nu}{\kappa} = -2\nu^2 \quad \text{and} \quad v_g = \frac{\partial \nu}{\partial \kappa} = 2\nu^2,$$

cf. Eq. (4.8). Note that we have  $v_p + v_g = 0$ .

- The parameter  $\nu \geq 1$  is the normalized frequency,  $\nu = 1$  corresponds to a reference carrier wave. Solitons with the same  $\nu$  but different durations will be labelled by a new parameter  $\eta$  between 1 and  $1\frac{1}{8}$ . The shortest soliton corresponds to the largest  $\eta$ .

Specifically, we set

$$\mathcal{E}(z, \tau) = f \left[ \underbrace{\nu \left( \tau - \frac{z}{\eta v_g} \right)}_{\xi} \right] \exp \left[ -i \nu \left( \tau - \frac{z}{\eta v_p} \right) \right], \quad (4.12)$$

for a solitary solutions of Eq. (4.11). Note, that the nonlinear group and phase velocities,  $\eta v_g$  and  $\eta v_p$ , still have a zero sum.

We will see that for  $\eta \rightarrow 1$ , the soliton gets an infinitely small amplitude and infinitely large duration, the latter is proportional to  $1/\sqrt{\eta - 1}$ . Ansatz (4.12) reduces then to a modulated linear wave. As  $\eta$  increases, the soliton becomes shorter and its peak amplitude increases. For  $\eta \rightarrow 9/8$  one gets the limiting soliton with the FWHM of approximately one-and-half field cycles. Strictly speaking, the solution at  $\eta = 9/8$  cannot be reached because a nonphysical cusp develops on top of the soliton. The above description applies to circular waves [21], to waves with linear polarization after neglecting generation of the third harmonics [111], and even to known bidirectional SPEs [125, 108].

Equation (4.12) and SPE (4.11) yield for  $f(\xi)$

$$\frac{d^2}{d\xi^2} (f - 2\eta\nu^2|f|^2f) - (\eta - 1)f + 2\eta\nu^2|f|^2f + 4i\eta\nu^2 \frac{d}{d\xi} (|f|^2f) = 0. \quad (4.13)$$

Equation (4.13) can be linearized well away from the soliton

$$\frac{d^2 f}{d\xi^2} = (\eta - 1)f,$$

such that localized solutions require  $\eta > 1$  and decay as  $\exp(\mp \xi \sqrt{\eta - 1})$  for  $\xi \rightarrow \pm\infty$ . Soliton duration should be proportional to  $1/\sqrt{\eta - 1}$ .

The fact that for the special case at hand, the PDE (4.11) exactly reduces to the ODE (4.13), speaks in favour of the Ansatz (4.12). We separate amplitude and phase in  $f(\xi)$  by setting

$$\nu \sqrt{\eta} f(\xi) = a(\xi) \exp[i\phi(\xi)],$$

and obtain two second-order ODEs for  $a(\xi)$  and  $\phi(\xi)$ . Both ODEs can be integrated once yielding

$$\frac{d\phi}{d\xi} = -\frac{(3 - 4a^2)a^2}{(1 - 2a^2)^2} \quad \text{and} \quad \left( \frac{da}{d\xi} \right)^2 + U(a) = \text{const}, \quad (4.14)$$

with

$$U(a) = -(\eta - 1) \frac{(1 - 3a^2)a^2}{(1 - 6a^2)^2} + \frac{(1 - 7a^2 + 12a^4)a^4}{(1 - 2a^2)^2(1 - 6a^2)^2}, \quad (4.15)$$

where  $U(a)$  is chosen such that  $U(0) = 0$ .

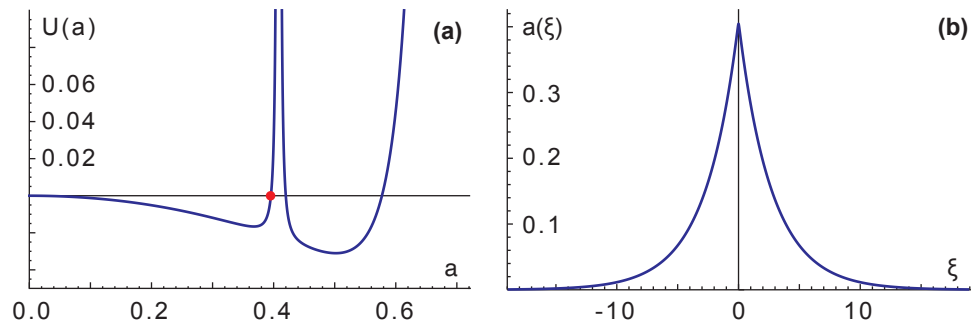


**Figure 4.2:** (a) An exemplary potential  $U(a)$  from Eq. (4.15) for  $\eta = 9/8 - \delta$  with  $\delta = 10^{-3}$ . The red point labels the upper value of  $a(\xi)$ . As  $\delta \rightarrow 0$ , an infinite potential wall is formed at  $a = 1/\sqrt{6}$ , resulting in cusp formation at the top of the soliton. (b) Shape of the shortest soliton calculated from Eq. (4.14).

The second (amplitude) equation in (4.14), as it usually happens with solitary solutions, can be interpreted as the energy conservation law for an imaginary mechanical particle. The particle has mass  $= 2$ , coordinate  $a$ , velocity  $da/d\xi$ , and potential energy  $U(a)$ . Variable  $\xi$  plays the role of time. Solutions of Eq. (4.14) are given by the quadrature. The solitary solution with vanishing  $a(\xi)$  for  $\xi \rightarrow \pm\infty$  corresponds then to the vanishing “total energy”, mathematically speaking, to a homoclinic trajectory [59].

 The same reduction procedure applies to NLSE (3.12). For a proper normalization, it yields

$$U(a) = -(\eta - 1)a^2 + a^4 \quad \Rightarrow \quad a(\xi) = \frac{\sqrt{\eta - 1}}{\cosh(\xi\sqrt{\eta - 1})}. \quad (4.16)$$

This is how the fundamental soliton (3.23) appears.

Note, that Eq. (4.14) requires  $U(a) \leq 0$  for all its solutions. The resulting restrictions on the soliton amplitude are

$$\left| a(\xi) \right| \leq \underbrace{\sqrt{\eta - 1}}_{\text{NLSE}} \quad \text{and} \quad \left| a(\xi) \right| \leq \underbrace{\sqrt{\frac{4\eta - 3 - \sqrt{9 - 8\eta}}{8\eta}}}_{\text{SPE}}.$$

In the first case, unlimited increase in  $\eta$  yields an arbitrarily large peak power and arbitrarily short duration. For the SPE, however, the largest possible value is  $\eta = 9/8$ . The highest peak power correspond to  $a = 1/\sqrt{6}$ . This value cannot be exceeded, because the potential energy (4.15) is singular at  $a^2 = 1/6$ . In terms of the mechanical picture, an infinite force results in an instant change of the particle velocity  $da/d\xi$  yielding a cusp. The limiting solution is illustrated in Fig. 4.2.

## 4.5 Universality

A traditional way to upgrade an envelope equation is to equip it with more and more terms. The resulting GNLSs are, of course, more capable in description of ultrashort pulses. Yet, the upgraded models are more stiff as well and might have nonphysical properties, as discussed in Chapter 3.

Field-level equations for short pulses provide an alternative. Among other things, too short pulses are not allowed, because the corresponding solutions are singular. The conventional point of view is that the singular solutions does not make sense, which is perfectly true for multi-valued loop solitons [131, 122]. Other singular solitons, such as the peaked ones in the Camassa-Holm model [132], can be regularized. Speaking of shallow water waves, one accounts for the surface tension to smooth the cusp.

Peaked SPE solitons are different. Given a family of regular solitons, the peakon appears as its limiting member, which determines the shortest pulse duration. An example is shown in Fig. 4.3. All but the last solitons are

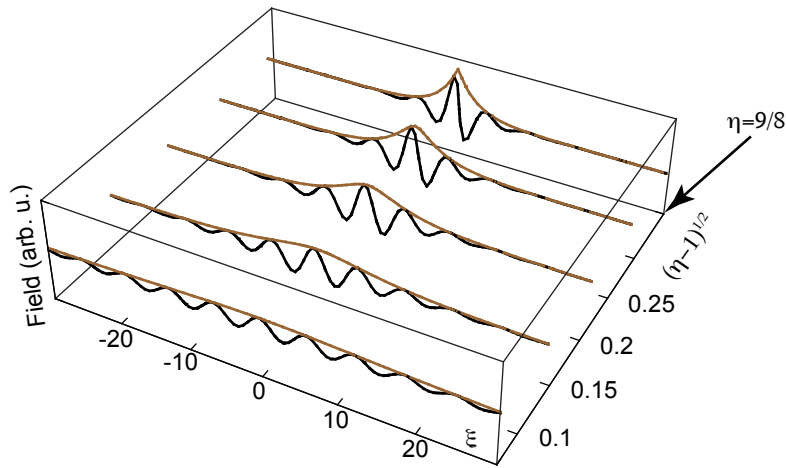


**Figure 4.3:** Normalized electric field and pulse envelope computed from a proper analog of Eq. (4.14) for a bidirectional SPE, as nearly simultaneously reported in [125] and [108].

perfectly valid, the invalid last one constrains the shortest duration. Moreover, such solutions appear in all known SPEs [122, 21, 125, 108, 111]. The example in Fig. 4.3 was actually calculated for a bidirectional second-order (in  $\partial_z$ ) SPE [108], but is nearly identical to that from the first-order unidirectional SPE (4.11). The take home message is:

- ❗ Cusp formation is an universal feature of ultrashort optical pulses. The cusp prevents a regular pulse from becoming too short. The shortest soliton duration is  $\approx 1.5$  cycles (FWHM), as in Fig. 4.3. This applies to all known SPEs.

It is of interest, that at the end of the day a properly modified GNLSE also predicts cusp formation. To this end, dispersion of the nonlinearity should be taken into account. The minimal envelope equation that supports cusp solutions, reads [84]

$$i\partial_z\psi + \frac{1}{2}\partial_t^2\psi + \left(1 + i\sigma\partial_t - \frac{\mu}{2}\partial_t^2\right)|\psi|^2\psi = 0,$$

where cusps appear for  $\mu \neq 0$ . This result once again shows that peaking is a universal feature of optical pulses.

## Chapter 5

# Manipulation of light by light

Interactions of optical pulses in nonlinear fibers is a vast and actively developing field [11, 86, 87, 134, 135]. Typical objects of interest within this Chapter are pulses with the  $\cosh^{-1}$  shape, the fundamental solitons of the NLSE. For a more involved GNLSE, a fundamental soliton yields a robust and long-living pulse, subject to slow changes in amplitude and carrier frequency. And yet, some solitons have a “weakness” and can be manipulated by applying a carefully chosen pump optical pulse. The pump, having a considerably different carrier frequency, should be group velocity matched with the soliton. Such interactions were first discussed in [136, 137], they are related to the so-called *optical event horizons* [138]. The possibility of manipulation was found numerically for a steep GVD profile [139]. A quantitative theory of manipulation, first without the Raman scattering effect, was developed in [140]. The Raman integral (3.17) was accounted for in [141, 142]. The theory of manipulation is discussed in this Chapter.

### 5.1 Relativistic mirrors

Broadly speaking, this Chapter deals with a light beam that is either totally reflected or partly scattered by a relativistic mirror. An interest in this subject goes back to the famous Einstein’s paper [143], where characteristics of the reflected beam were found by applying two successive Lorentz transforms. Here, the problem posing differs from the classical one in the following important aspect:

- ❗ We consider an abstract mirror that moves in a dispersive medium. Moreover, mirror’s velocity is comparable to the group velocity of the scattered light beam. The reasonableness of these assumptions will be demonstrated in the next Section.

For a moment we make a violent assumption that one can speed up a mirror, such that it reaches a relativistic velocity, and observe its non-destructive motion through, e.g., fused silica. Moreover, mirror’s velocity may exceed velocity of the scattered light pulse in question. The mirror may be overtaken by the pulse or it can overtake the pulse, something that never happens in vacuum.

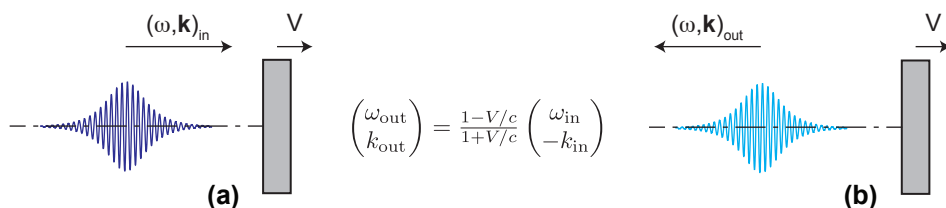
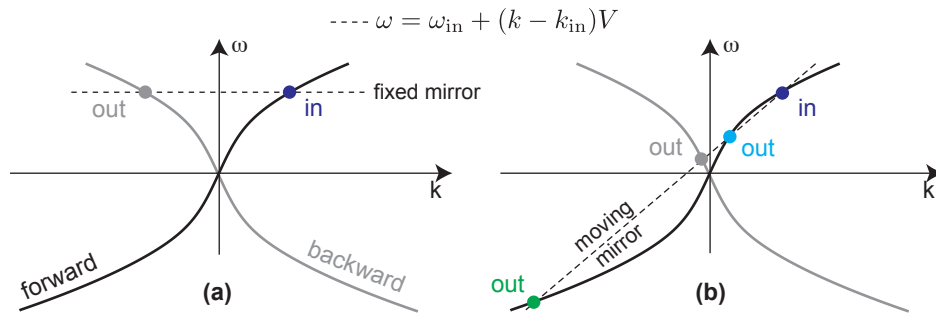
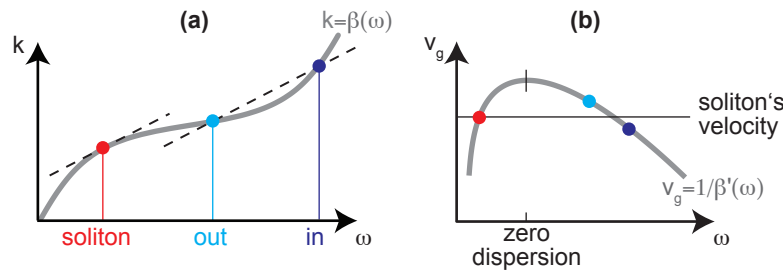


Figure 5.1: Backward (normal) reflection of light by a moving mirror in vacuum [144].



**Figure 5.2:** Graphical illustration of Eq. (5.1). Given  $\omega_{in}$ , it provides frequencies of the reflected waves  $\omega_{out}$  for a moving mirror in a dispersive medium. The slope of the dashed line is determined by mirror's velocity  $V$ . There are up to three outgoing frequencies, although the “green” one (Hawking frequency) might require a special design of the dispersive curve and is difficult to catch [146].



**Figure 5.3:** (a) the same as in Fig. 5.2(b), but the dashed line is now determined by soliton's velocity. Only the positive-frequency forward reflection is shown. (b) for an efficient reflection, soliton's velocity should be close to that of the incoming/outgoing pulses.

We consider only the simplest case, where all waves propagate either forward or backward along one line, which will be later related to an optical fiber. In the classical vacuum formulation, there is only one reflected pulse, which always propagates backward, as summarized in Fig. 5.1. Mirrors in dispersive media are different.

Namely:

- ❶ Reflection of a pulse may yield several new pulses at considerably different frequencies [96].
- ❷ In the lab frame, the reflected pulses may propagate backward as well as forward. The latter case never occurs in vacuum. It is referred to as *forward reflection* [145].
- ❸ For a specially adjusted dispersion law, one of the reflected waves can formally get a negative frequency [146].

Given the incoming wave parameters  $\omega_{in}$  and  $\mathbf{k}_{in}$ , the parameters of the possible outgoing waves are constrained by the relation

$$\omega_{out} - \mathbf{k}_{out} \mathbf{V} = \omega_{in} - \mathbf{k}_{in} \mathbf{V}, \quad (5.1)$$

where  $\mathbf{V}$  denotes mirror's velocity, see Fig. 5.2. Of course, both  $(\omega_{in}, \mathbf{k}_{in})$  and  $(\omega_{out}, \mathbf{k}_{out})$  should belong to a dispersion curve, either forward or backward one. Equation (5.1) simply indicates that in mirror's frame of reference the incoming and the outgoing frequencies (which are given by  $(\omega - \mathbf{k}\mathbf{V}) / \sqrt{1 - V^2/c^2}$ , see [144]) are equal to each other.

Leaving aside the mysterious negative-frequency wave, we see that one wave is reflected forward and another one backward for the situation shown in Fig. 5.2(b). For the forward reflection at hand, it is clear that

$$(d\omega/dk)_{out} > V > (d\omega/dk)_{in},$$

such that the mirror should overtake the input pulse which is reflected and runs away in the same direction but faster. This is shown in Fig. 5.4, where the red pulse replaces the mirror. For another reflection scenario, like



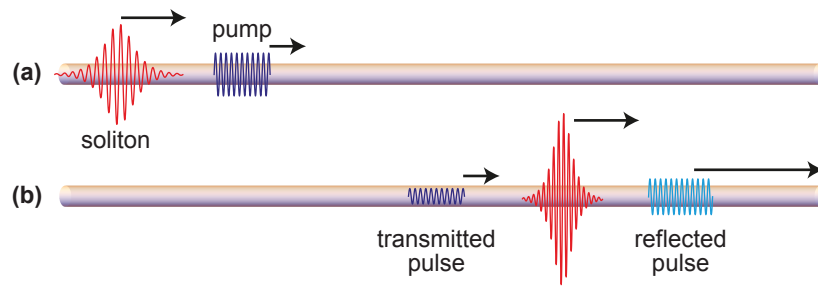


**Figure 5.4:** The pulses before (a) and after (b) scattering at a soliton are schematically shown for the situation of Fig. 5.3. Such a process is not possible for a classical mirror, as in Fig. 5.1.

in Fig. 5.1, one should just exchange the blue and light-blue points in Fig. 5.2. The negative-frequency wave remains unaffected.

## 5.2 Solitons as mirrors

Figure 5.2 makes it clear that the slope of the dashed line must be sufficiently large to get more than one reflected frequency. In other words, mirror's velocity must be relativistic. An obvious disadvantage of the concept is that no real mirror can propagate through glass, not to mention the relativistic velocity. To address this problem we now replace the mirror by another optical pulse.

The idea comes from the so-called *front induced transitions* [147]. A front, which propagates through a transparent medium, can scatter or even perfectly reflect a light beam, i.e., it can replace a moving mirror [148]. True fronts are not common in fibers, however, we can use a soliton instead. An optical pulse that propagates through a Kerr medium, creates a moving localized nonlinear perturbation, which is equivalent to a perturbation of the refractive index [11, 149]. Among other things, the perturbation, say  $\delta n$ , can scatter other optical pulses [96, 136, 137]. This is what we need. The dashed curve in Fig. 5.2 is now determined by the soliton velocity, see Fig. 5.3. Equation (5.1) is replaced by the rule [150, 151]

$$\omega_{\text{in}} \mapsto \omega_{\text{out}} \quad \text{such that} \quad \beta'(\omega_s) = \frac{\beta(\omega_{\text{out}}) - \beta(\omega_{\text{in}})}{\omega_{\text{out}} - \omega_{\text{in}}}, \quad (5.2)$$

where  $k = \beta(\omega)$  refers to the dispersion law and  $\omega_s$  is soliton's frequency. In what follows,  $\omega_s$  will be subject to slow changes, and so then does  $\omega_{\text{out}}$ , whereas  $\omega_{\text{in}}$  will be fixed. This is a good point to stress that:

- ❗ Solitons are very bad mirrors, because even in idealized numerical simulations  $\delta n \lesssim 10^{-4}$ . Such a mirror is almost transparent and most pulses go through the soliton without noticeable changes.

Only the group-velocity matched pulses can be reflected, as illustrated in Fig. 5.5. The reflection was experimentally confirmed in [153, 154, 155, 156]. And yet, given that the scenario depicted in Fig. 5.4 requires a very special set of parameters and is all but generic, the question arises:

- ❓ Why waste time on relativistic mirrors?

One reason is that the scattered waves experience a predictable frequency shift, such that one can generate waves with new frequencies [96, 136, 137, 153, 157, 158, 159, 160, 161, 162]. Another reason is that an optical implementation of event horizons can be used to study at least a classical analog of the Hawking radiation [138, 163, 164, 165, 166, 167, 168, 155, 169, 170]. Our motivation is different.

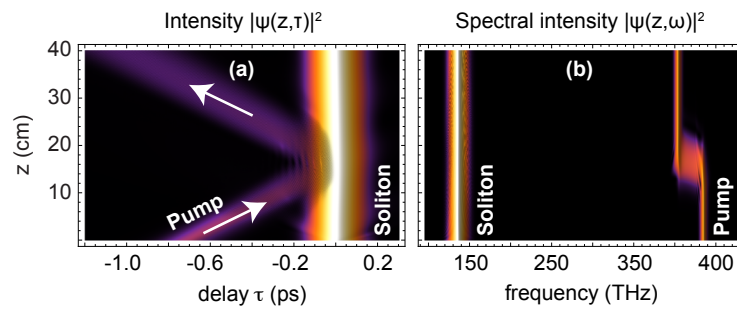


**Figure 5.5:** (a) A nearly perfect reflection of a small-amplitude pump pulse ( $0.67 \mu\text{m}$ ) at an approximately group-velocity matched fundamental soliton ( $2.2 \mu\text{m}$ , FWHM 70 fs) is calculated using GNLSE (3.14). (b) The soliton and the frequency down-shifted pump pulse are shown in the spectral domain. Bulk dispersion of fused silica is used, see [152].

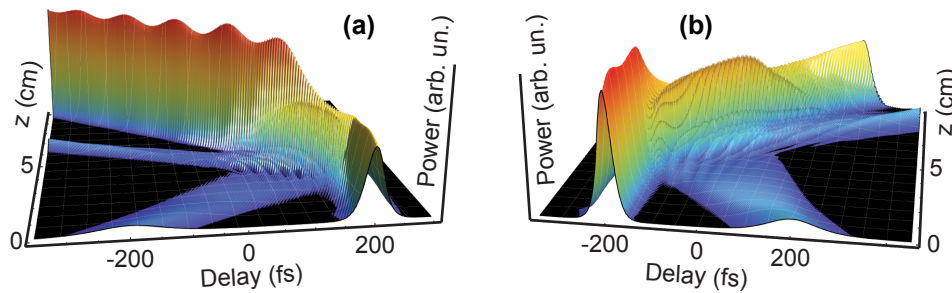


**Figure 5.6:** A small-amplitude pump wave-packet can be effectively scattered by a soliton if the pulses are group velocity matched to a certain level. The scattering leads to a dramatic increase (a) or decrease (b) of soliton's peak power. For simulation parameters and interpretation as an all-optical transistor, see [139, 171].

- ❗ Most papers devoted to scattering at a soliton and artificial event horizons consider the soliton as an object with a fixed behaviour. We will be interested not so much in the evolution of the scattered pump beam, but rather in its effect on the soliton-mirror.

Note that the scattering process depicted in Figs. 5.2 and 5.3 leads to changes in both frequency and wave-vector of the pump. In other words, there is an exchange of energy and momentum between the pump and the mirror. A true mirror, as in Fig. 5.1, is too “heavy” and remains unaffected by the exchange, e.g., its acceleration due to the light pressure is difficult to observe. Solitons are “lightweight” and therefore different. Scattering at a soliton provides an effective way to change it, e.g., to switch the soliton on and off [139], to produce extremely large solitons [172], and even to generate an optical SC state [173]. An example of soliton switching is shown in Fig. 5.6.

Before we proceed, it should be emphasized that:

- ☐ The pump pulse in the “snapshot” Fig. 5.4(a) is physically on the right side of the soliton. The  $z$ -axis is directed from left to right. In accord with the delay definition (3.10), larger  $z$  yields smaller  $\tau$ . This is why the pump pulse in Figs. 5.5(a) and 5.6(a) seems to be on the left side of the soliton.

An opposite situation occurs if the soliton is switched off, see Fig. 5.6(b). Here the pump seems to be on the right, but actually is on the left of the soliton, like in the classical Fig. 5.1(a). Note that:

- ❗ Be it switching on or off, we are always dealing with the forward reflection. Backward reflection from a soliton is too weak and anyway beyond the scope of the unidirectional NLSE and GNLSE.

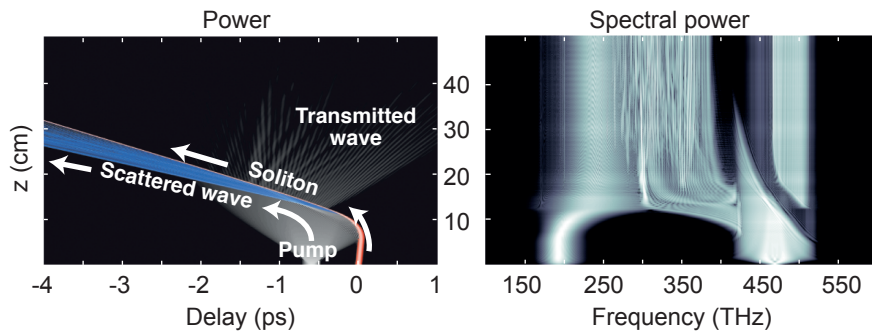


**Figure 5.7:** Scattering of a huge pump pulse at a soliton that leads to the SC generation. For parameters see [173]. This situation is exactly the opposite of the “soft” scattering in Fig. 5.5, where the soliton remains unaffected.

### 5.3 An empirical approach to scattering

Manipulation of the soliton by the pump, as in Fig. 5.6, is effective only if the following empirical rules are met:

- ❶ Carrier frequencies of the soliton and the pump are on either side of the ZDF. The GVD parameter is then negative for the soliton and positive for the pump [139].
- ❷ Group velocities of the soliton and the pump should be reasonably close. If they are too different the pulses go through each other unchanged. If they are too close, the scattering still takes place, but the exchange of energy and momentum is strongly suppressed [139].
- ❸ In a favorable situation, like in Fig. 5.5, the intensity of the transmitted wave is very low as compared to the intensity of the scattered wave [139], [174]. However, the true total reflection, which can be observed for scattering at fronts, never takes place for scattering at solitons.
- ❹ The GVD profile  $\beta''(\omega)$  should be steep for the soliton and slightly sloping for the pump. Otherwise, the group-velocity matched pump is still scattered but the soliton remains nearly unchanged [175, 176, 172].
- ❺ An wide low-amplitude wave-packet pumps the soliton better than a short packet with the same energy [173]. In the latter case the initial delay between the pump pulse and the soliton should be large enough to ensure that the pump spreads naturally, due to medium dispersion, as in Fig. 5.7.

The above empirical rules have been found by trial and error from the numerous numerical investigations of pulse interactions [139, 172, 173, 177, 178, 179, 180, 181]. Later on the rules have been explained and quantified [140, 141], as discussed below.

### 5.4 Relation to quantum mechanics

The simplest approach, which to some extent covers the interaction between the soliton (anomalous dispersion) and the group-velocity matched pump (normal dispersion), is based on two coupled NLSEs [175, 174, 182]. Let us first describe the notations:

- Soliton’s carrier frequency is denoted by  $\omega_s = \omega_s(z)$ , the dependence  $\omega_s(z)$  is not yet known. We denote the initial soliton frequency by  $\omega_a = \omega_s|_{z=0}$ . Parameter  $\omega_b$  denotes the group-velocity matched frequency in the normal dispersion domain. Given  $\omega_a$ , one finds  $\omega_b$  from  $\beta'(\omega_a) = \beta'(\omega_b)$ . The pump frequency will be written as  $\omega_{in} = \omega_b + \Omega$ , where the offset  $\Omega$  is a control parameter, see Fig. 5.8.

The frequency of the scattered wave  $\omega_{out}$  is determined by Eq. (5.2) and changes with  $\omega_s$ . Initially, we have  $\omega_{out} \approx \omega_b - \Omega$ .

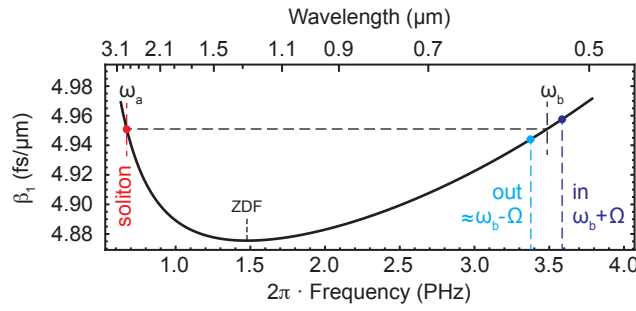


**Figure 5.8:** An example: how the parameters of the soliton and the pump may be chosen for the effective scattering in fused silica, see [140]. Recall that  $\beta_1 = \beta'(\omega)$ . Here,  $\omega_a = \omega_s|_{z=0}$  is the initial soliton frequency,  $\omega_b$  is the reference (group-velocity matched) frequency in the normal dispersion domain,  $\Omega$  is the frequency offset for the incoming pump. The frequency offset for the outgoing scattered wave  $\approx -\Omega$ , as yielded by Eq. (5.2).

- ❗ As the soliton evolves, the same pump yields new and new scattered wave-packets with the different values of  $\omega_{\text{out}}$ . The reflected waves fill some frequency band.

In extreme situations, the initial spectral gap between the soliton and the pump can be completely filled, an example is shown in Fig. 5.7. This is how a SC state can result from a two-pulse collision [173].

- The dispersion coefficients for  $\omega = \omega_a$  and  $\omega = \omega_b$  will be denoted by  $\beta_a, \beta'_a, \beta''_a, \beta'''_a \dots$  and  $\beta_b, \beta'_b, \beta''_b, \beta'''_b \dots$ , cf. Eq. (3.13).

To quantify the scattering of a pump wave at a soliton, it is convenient to use two coupled envelope equations centered at  $\omega_a$  and  $\omega_b$ . The reason is that both frequencies correspond to the same delay variable

$$\tau = t - \beta'_a z = t - \beta'_b z, \quad (5.3)$$

cf. Eq. (3.10). The governing equations, in which only the simplest cross-phase modulation (**XPM**) coupling between the pulses is taken into account, are

$$i\partial_z \psi_a + \frac{\beta''_a}{2} (i\partial_\tau)^2 \psi_a + \gamma_a (|\psi_a|^2 + 2|\psi_b|^2) \psi_a = 0, \quad (5.4)$$

$$i\partial_z \psi_b + \frac{\beta''_b}{2} (i\partial_\tau)^2 \psi_b + \gamma_b (|\psi_b|^2 + 2|\psi_a|^2) \psi_b = 0, \quad (5.5)$$

where  $\psi_a(z, \tau)$  is the complex envelope for the soliton and  $\psi_b(z, \tau)$  is the complex envelope for the pump [175, 174, 182]. Note, that the CW pump corresponds to  $\psi_b \propto e^{i(\kappa z - \Omega \tau)}$ , because the Eq. (5.5) is centered at the reference frequency  $\omega_b$ , not at the pump frequency.

- 📖 Equations (5.4–5.5) are somewhat similar to the classical Manakov equations for the XPM interactions of two waves in a cubic medium [183].

However, in Manakov's case the dispersion parameters for the coupled NLSEs are either identical or close to each other, as one deals with just two polarization states of actually one wave. Equations (5.4–5.5) assume considerably different  $\omega_a$  and  $\omega_b$ . Among other things, we have  $\beta''_a < 0$  for the soliton and  $\beta''_b > 0$  for the pump, see Fig. 5.8. An effective manipulation requires that  $|\beta''_b / \beta''_a| \ll 1$ .

We are in good position to stress that the system (5.4–5.5) perfectly describes the scattering, when (1) the soliton has a sufficient duration to be well described by the NLSE and (2) the soliton remains unchanged because

pump's power is very small. One can then linearize the  $\psi_b$ -equation (5.5), using the soliton Ansatz (3.23) for  $\psi_a$ , and obtain

$$i\partial_z\psi_b + \frac{\beta_b''}{2}(i\partial_\tau)^2\psi_b - \frac{2\beta_a''\gamma_b/\gamma_a}{\tau_0^2 \cosh^2(\tau/\tau_0)}\psi_b = 0. \quad (5.6)$$

Equation (5.6) is of course equivalent to the quantum Schrödinger equation with “time”  $z$ , “coordinate”  $\tau$ , potential well  $\propto 1/\cosh^2$ , and wave function  $\psi_b^*$ .

- ❗ Given a low-power monochromatic continuous pump wave, the pump scattering at a soliton is identical to the scattering problem from quantum mechanics.

A well known analytic solution provides then the reflection and transmission coefficients [184]. This framework is perfectly suited to the situation in Fig. 5.5, see [174]. And yet it fails to describe the energy transfer and soliton manipulation as described in the next Section.

## 5.5 Soliton perturbation theory

What may be wrong with the quasi-Manakov equations (5.4–5.5)? To maximize the reflection coefficient and to maximize the spectral domain of the pump waves that can be reflected, one naturally tries to use shorter and more powerful solitons. A shorter soliton with the higher peak-power appears when one switches on an arbitrary soliton, as in Fig. 5.6(a). Moreover, such switching intrinsically takes place in optical supercontinuum [179, 185]. Either way, the soliton may go beyond the applicability of the NLSE.

Note that the transmission and reflection coefficients in quantum mechanics change exponentially quickly between 0 and 1 [184]. The domain of quick change is extremely sensitive to the potential well and even a small difference between the NLSE and GNLSE solitons becomes important. This is especially true for the extreme solitons. The consequence is that:

- ❗ All predictions of the system (5.4–5.5) enjoy a qualitative agreement with the numerical solutions and help to understand what is going on. For really short pulses, however, these predictions quickly become completely wrong quantitatively.

To improve the model, one needs a full GNLSE for the soliton, whereas the NLSE approximation is still applicable for the temporally extended low-amplitude pump. Equations (5.4–5.5) should then be replaced by the system [140, 141]

$$i\partial_z\psi_a + \hat{\mathfrak{D}}\psi_a + \gamma_a(1 + i\omega_a^{-1}\partial_\tau)(\mathfrak{I}\psi_a) = 0, \quad (5.7)$$

$$i\partial_z\psi_b + \frac{\beta_b''}{2}(i\partial_\tau)^2\psi_b + 2\gamma_b|\psi_a|^2\psi_b = 0, \quad (5.8)$$

where the dispersion operator

$$\hat{\mathfrak{D}} = \frac{\beta_a''}{2!}(i\partial_\tau)^2 + \frac{\beta_a'''}{3!}(i\partial_\tau)^3 + \frac{\beta_a''''}{4!}(i\partial_\tau)^4 + \dots,$$


contains as many terms, as necessary and

$$\mathfrak{I} = (1 - f_R)|\psi_a(z, \tau)|^2 + f_R \int_0^\infty R(s)|\psi_a(z, \tau - s)|^2 ds + 2|\psi_b(z, \tau)|^2, \quad (5.9)$$

is an extended version of Eq. (3.17), which additionally accounts for the XPM interaction with the pump.

- We first ignore the Raman scattering and set  $f_R = 0$ . The results apply, e.g., to Raman-free gas-filled photonic crystal fibers [186]. Effect of the Raman term will be discussed in the next Section.

Of course, one cannot expect a useful analytical solution for the system (5.7–5.8) in a generic case, and approximate methods should be used instead. These methods are provided by the so-called *soliton perturbation theory (SPT)*.

 SPT originates from classical mechanics. Given that some Hamiltonian system is integrable and its action-angle variables are known, consider a small perturbation of that system. It is well known, that the action variables are very resistant to change [61]. On a long run, the solution of the full system may still be close to the solution of the unperturbed one, but with the properly adjusted values of the slowly varying action variables [59].

This approach can be extended to a small perturbation of an integrable nonlinear wave equation [135], where we recall that the full integrability in terms of the inverse scattering method can be treated as a transition to the action-angle variables [63, 60]. The technique includes averaging over the periodic motion, which is captured by the angle variables, and yields numerous approximate methods for nonlinear waves. Many examples can be found in [33, 29].

Moreover, in some non-integrable Hamiltonian systems [187] and in surprisingly many driven nonlinear dissipative systems that are subject to *local activation and global inhibition* [188], the general system state can be seen as a complex of weakly interacting, stable localized structures, which experience slow changes in position, amplitude, and orientation. These localized particle-like objects are referred to as *dissipative solitons* [189, 190, 191, 192]. An essential part of their dynamics is covered by the reduced ODEs for the soliton parameters, which are related to the fundamental symmetries.

For instance, the spatial homogeneity yields that if some stationary field distribution  $u = f(\mathbf{r})$  represents a dissipative soliton localized near the origin, the Ansatz  $u = f(\mathbf{r} - \mathbf{r}_a) + f(\mathbf{r} - \mathbf{r}_b)$  is a zero approximation for a system of two well-separated solitons. Their interaction can be described by a reduced ODEs for two slow variables:  $\mathbf{r}_a(t)$  and  $\mathbf{r}_b(t)$ . A general way to derive such ODEs is discussed in [188].

Let us return to optical solitons. The SPT equations yielded by the optical GNLSE can be found, e.g., in [85, 52]. For a soliton, which is manipulated by a pump wave, these ODEs preserve the general structure (3.22), but have extra-terms on the right-hand side yielded by the pump. The terms were calculated in [140] for an instantaneous response (Eq. (5.9) with  $f_R = 0$ ) and in [141] for the general case.

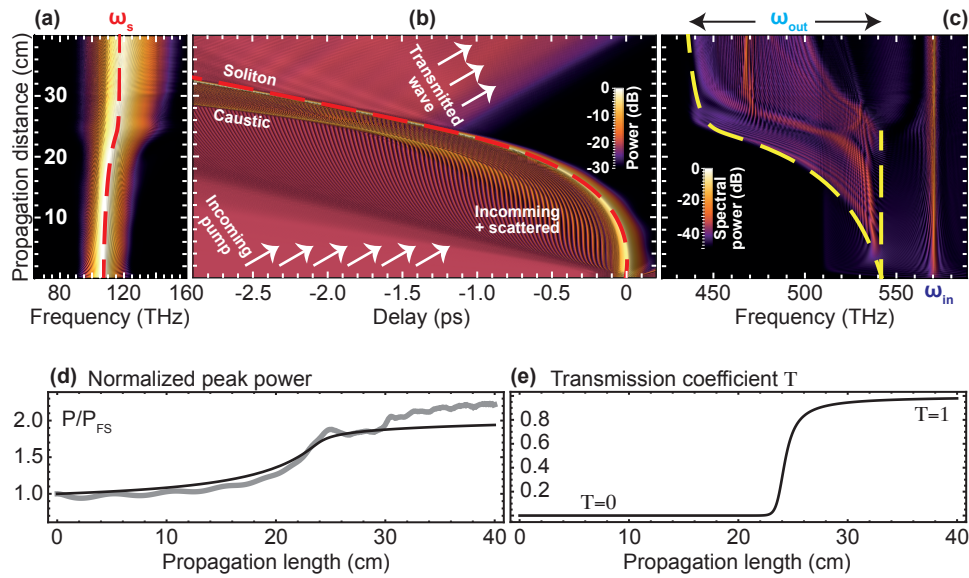
Figure 5.9 shows an example of a scattering problem, with a setup like in Fig. 5.4. The problem was first calculated using the most general “all-in-one” GNLSE that covers the soliton, the pump, and the scattered waves. This calculation is similar to those reported in [139, 172, 173, 177, 178, 179, 181].

Thereafter, the same problem was solved using the SPT equations. The latter look rather complicated and involve numerous hypergeometric functions (not shown, see [140, 141, 193]). Nevertheless, their numerical solution is much faster (e.g.,  $10^4$  times faster), than that of the original GNLSE. Figure 5.9 indicates that the SPT approach captures the most essential features of the soliton manipulation.

## 5.6 Raman scattering

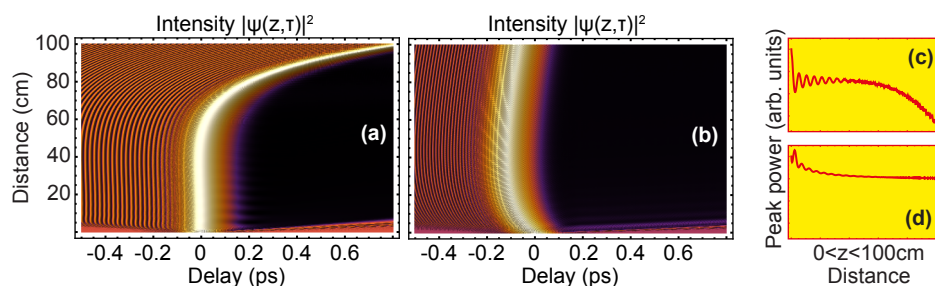
It is well known, that a non-instantaneous nonlinear medium response in Eq. (3.17) leads to a permanent decrease of the soliton frequency, soliton self-frequency shift (**SSFS**), see [194, 195]. Among other things, SSFS is a classical application of the SPT approach [85]. The frequency shift rate was found to be inversely proportional to the fourth power of the soliton duration. Slightly different solitons get different frequency shifts as they propagate. This results in the unwanted jitter effect. SSFS compensation is an important applied problem and many different ways to remove the frequency shift have been studied [196, 197, 198, 199, 200, 200, 201].

Figure 5.9(a) demonstrates that a proper group-velocity matched pump increases the soliton frequency, i.e., the pump can be used to compensate SSFS. Given a “scattering-friendly” offset  $\Omega$  (like one in Fig. 5.8), one can run several GNLSE simulations and adjust pump power to achieve the ideal SSFS compensation. As a



**Figure 5.9:** GNLSE solution for a soliton that scatters a monochromatic pump wave, is compared with the SPT results. Colour labels for  $\omega_s$ ,  $\omega_{in}$ ,  $\omega_{out}$  ensure compatibility with the schematic Figs. 5.3 and 5.4. For more details see [140].

- (a) spectral density in the anomalous dispersion domain (GNLSE, density plot). SPT (dashed line) correctly predicts the increase of the soliton carrier frequency.
- (b) energy density in the space-time domain (GNLSE, density plot). Initially, the soliton perfectly scatters the pump and is compressed. At  $z \approx 24$  cm the compressed soliton loses its opacity. Soliton's trajectory is correctly predicted by the SPT (dashed line).
- (c) spectral density in the normal dispersion domain (GNLSE, density plot). Here, SPT (dashed lines) predicts the frequency band of the outgoing wave packets, but not the features within the band.
- (d) evolution of soliton's peak power from GNLSE (thick line) and SPT (thin line).
- (e) SPT prediction for the soliton's transmission coefficient.



**Figure 5.10:** Two attempts to compensate SSFS by applying a group velocity matched pump. (a,c) the compensation is unstable. SSFS switches on at  $z \approx 60$  cm and soliton's peak power permanently decreases. (b,d) the compensation is stable. For more details see [141].

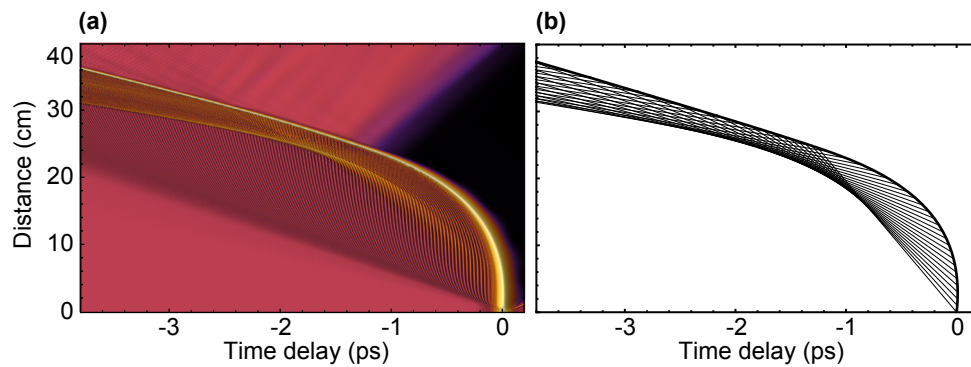


**Figure 5.11:** (a) an example of a soliton that scatters a monochromatic pump wave, like in Fig 5.9. (b) light rays for small portions of the pump as they are reflected by the soliton. The rays are calculated using the SPT, they are responsible for the caustic structure. For more details see [140]

rule, the compensation is unstable and is destroyed as the pulse propagates along the fiber, an example is shown in Fig. 5.10(a). Note, that the averaged mean peak power permanently decreases in the course of pulse propagation, see Fig. 5.10(c).

In principle one can run GNLSSE simulations for all possible parameter combinations (including both soliton and pump parameters) in order to find a domain/domains in the parameter space, where the compensation is stable. This enormous work was never done. Moreover, the compensation might look perfectly stable as long as the propagation length is insufficient. For instance, the calculation shown in Fig. 5.10(a) was first performed for the propagation distance  $z = 20$  cm and soliton's frequency seemed to be stable. Later on it was found that the SSFS compensation is destroyed at  $z \approx 60$  cm. Here is where one can benefit from the SPT approach.

In the SPT framework, one deals with a system of ODEs for the soliton parameters. SSFS compensation corresponds to an equilibrium system state, such that these parameters do not change. Stability of a generic equilibrium state is easy to test by linearization of the ODEs near the equilibrium. For a stable compensation, it was found that pump's frequency offset  $\Omega$  should be chosen such that the resulting soliton's transmission coefficient  $T$  is a little bit smaller than 1, see [141].

- ❶ Given a soliton, the pump should be taken such that only a part – but a considerable part – of the pump beam is reflected. SSFS compensation by that pump is stable. If the pump is nearly perfectly reflected, SSFS compensation is unstable.

An example of the stable compensation is shown in Fig. 5.10(b,d), further examples can be found in [141, 142]. Needless to say, that it never occurred to us to study this regime of scattering, before the SPT analysis has been carried out.

## 5.7 Why to reduce the model?

We are in a good position to conclude by stressing that:

- ❶ SPT is not just about a faster numerical solution. At the end of the day, the split-step GNLSSE solution is fairly quick. However, SPT addresses certain problems that are nearly impossible to address by brute force.

For instance, a mathematically strict formulation of the problem:

- ❷ Is a certain SSFS compensation scheme stable or not?



might be tricky in the all-inclusive GNLSE framework, as we do not deal with an equilibrium state. The SPT framework is much more convenient, moreover, the results derived from the reduced equations nicely agree with the numerical simulations of the full GNLSE [141, 142].

Another example: SPT gives access to the soliton transmission coefficient, as shown in Fig. 5.9(e). The reduced model quantifies a sudden change of “mirror’s opacity” as the soliton becomes too short. Note, that the transmission coefficient is difficult to extract from the full numerical solution, like one in Fig. 5.9(b). One more example is the caustic structure shown in Fig. 5.11(a,b), where SPT gives a direct access to the geometric rays of the scattered pump wave. It turned out that despite of numerous (hundreds) scattering simulations with the full GNLSE [139, 172, 173, 177, 178, 179, 180, 185], the caustic was recognized only after it was predicted by the SPT [140].

## Chapter 6

# Parallel splitting methods

This Chapter is devoted to the split-step approach, a method of choice for numerical solutions of the GNLSE-type equations. We describe a recently found class of additive splittings, which give a promising alternative to, e.g., the standard Strang splitting. The Chapter is based on paper [202].

### 6.1 Split step methods

Splitting methods are widely used for the solution of various linear and nonlinear evolution problems [203, 204, 205, 206, 207]. Consider an abstract initial value problem within a sufficiently short evolution step  $\tau$

$$\frac{d}{dt}u(t) = Hu(t), \quad u(0) = u_0, \quad t \in [0, \tau], \quad H = \sum_{m=1}^M H_m. \quad (6.1)$$

Here  $u(t)$  belongs to a finite or infinite dimensional Banach space and an evolution operator  $H$  should generate a semigroup  $e^{tH}$  at least for  $t \leq \tau$ , such that the formal exact solution of Eq. (6.1) reads

$$u(t) = e^{tH}u_0.$$

The evolution operator is split in  $M$  components  $H_m$  in such a way that the reduced equations  $du/dt = H_m u$  are easily solved and generate individual semigroups  $e^{tH_m}$ . One then constructs a set  $w_0, w_1, \dots, w_M$  via

$$w_0 = u_0 \quad \text{and} \quad w_m = e^{\tau H_m} w_{m-1}, \quad 1 \leq m \leq M.$$

The value  $w_M$  is used as a final numerical approximation of  $u(\tau)$ , i.e.,

$$u(\tau) = e^{\tau H}u_0 \approx e^{\tau H_M} \dots e^{\tau H_2} e^{\tau H_1} u_0. \quad (6.2)$$

Altogether, a splitting method (**SM**) is defined by the ordered sequence of the exponential operators in Eq. (6.2).

The local error of a given SM can be characterised by the operator

$$\ell(\text{SM}) = e^{\tau H_M} \dots e^{\tau H_2} e^{\tau H_1} - e^{\tau H} = O(\tau^2), \quad (6.3)$$

where the error estimate formally follows from the Taylor expansion of the exponential operator. If some of the components  $H_m$  are not bounded, a rigorous proof of the estimate (6.3) may be very complicated. We will always implicitly assume that the use of the Taylor expansions can be justified.

If an applied evolution problem is solved numerically, the interval  $[0, \tau]$  in Eq. (6.1) mimics one time step. Equation (6.3) indicates that any SM produces a first-order integrator when the basic Eq. (6.1) is solved on a fixed time interval  $[0, T]$  by taking  $T/\tau$  time-steps. One can do better than that, and a SM is said to be of order  $p$  if its local error is  $\ell(\text{SM}) = O(\tau^{p+1})$  in which case we write  $\text{deg}(\text{SM}) = p$ .

In what follows, we consider Eq. (6.1) with  $H = A + B$ , where the sub-steps are performed by alternating operators  $A$  and  $B$  and the first sub-step is performed with a multiple of  $A$ . A multiplicative SM  $\mathcal{M}_\tau$  is then defined by two ordered sets of coefficients  $a_{1 \leq m \leq s}$  and  $b_{1 \leq m \leq s}$ , where

$$\mathcal{M}_\tau = e^{b_s \tau B} e^{a_s \tau A} \dots e^{b_2 \tau B} e^{a_2 \tau A} e^{b_1 \tau B} e^{a_1 \tau A}, \quad (6.4)$$

where  $s$  is referred to as the number of stages. By construction, we have

$$\sum_{m=1}^s a_m = \sum_{m=1}^s b_m = 1, \quad a_1 \neq 0.$$

We naturally require that each inner exponential operator  $\neq \mathbb{I}$  (the identity operator). Still it may happen that  $b_s = 0$  in which case the  $\mathcal{M}_\tau$  enjoys the first-same-as-last (**FSAL**) property.

□ We denote SMs by capital calligraphic letters and indicate the time step by the index  $\tau$ , e.g., we write

$$\deg(\mathcal{M}_\tau) = p \Leftrightarrow \ell(\mathcal{M}_\tau) = \mathcal{M}_\tau - e^{\tau(A+B)} = O(\tau^{p+1}).$$

for a multiplicative SM  $\mathcal{M}_\tau$  of order  $p$  and with the local error  $\ell(\mathcal{M}_\tau)$ .

The classical SMs are as follows. The simplest first-order Lie-Trotter SM, which is denoted by  $\mathcal{L}_\tau$ , reads [208]

$$\mathcal{L}_\tau = e^{\tau B} e^{\tau A} \quad \text{with} \quad \ell(\mathcal{L}_\tau) = e^{\tau B} e^{\tau A} - e^{\tau(A+B)} = O(\tau^2). \quad (6.5)$$

A second-order Strang SM, which is denoted by  $\mathcal{S}_\tau$  and has the FSAL property, reads [209]

$$\mathcal{S}_\tau = e^{\frac{1}{2}\tau A} e^{\tau B} e^{\frac{1}{2}\tau A} \quad \text{with} \quad \ell(\mathcal{S}_\tau) = O(\tau^3). \quad (6.6)$$

Another classical example is a second-order SM with a free parameter  $\sigma$

$$\mathcal{S}_{\sigma\tau} \mathcal{S}_{(1-2\sigma)\tau} \mathcal{S}_{\sigma\tau} = e^{\frac{\sigma}{2}\tau A} e^{\sigma\tau B} e^{\frac{1-\sigma}{2}\tau A} e^{(1-2\sigma)\tau B} e^{\frac{1-\sigma}{2}\tau A} e^{\sigma\tau B} e^{\frac{\sigma}{2}\tau A}, \quad (6.7)$$

which is promoted to the fourth-order SM  $\mathcal{Y}_\tau$  (Yoshida) by requiring that

$$2\sigma^3 + (1 - 2\sigma)^3 = 0 \quad \Rightarrow \quad \sigma = \frac{2 + 2^{-1/3} + 2^{1/3}}{3} \quad \Rightarrow \quad \ell(\mathcal{Y}_\tau) = O(\tau^5),$$

see [210, 211, 212], we assume that  $\sigma \in \mathbb{R}$ .

Modern computer-algebra software yields effective methods to construct higher-order SMs, see [213, 214, 215, 216, 217]. A comprehensive list of SMs, including those with  $H = A + B + C$  and those with complex time steps, can be found in [218].

## 6.2 Companions

SMs do not appear alone. In what follows, each SM  $\mathcal{M}_\tau$  will be considered together with its companion SMs:  $\mathcal{M}_\tau^\circ$ ,  $\mathcal{M}_\tau^\bullet$ , and  $\mathcal{M}_\tau^\prime$ . They are derived directly from the definition (6.4), as follows:

❶ To cover SMs that employ  $B$  for the first sub-step, we define a companion SM  $\mathcal{M}_\tau^\circ$ , where

$$\mathcal{M}_\tau^\circ = e^{b_s \tau A} e^{a_s \tau B} \dots e^{b_2 \tau A} e^{a_2 \tau B} e^{b_1 \tau A} e^{a_1 \tau B}. \quad (6.8)$$

The upper index  $\circ$  denotes swapping of  $A$  and  $B$  in the seed SM  $\mathcal{M}_\tau$ .

② Any  $\mathcal{M}_\tau$  generates another companion SM  $\mathcal{M}_\tau^\bullet$  via

$$\mathcal{M}_\tau^\bullet = (\mathcal{M}_{-\tau})^{-1} = e^{a_1\tau A} e^{b_1\tau B} e^{a_2\tau A} e^{b_2\tau B} \dots e^{a_s\tau A} e^{b_s\tau B}. \quad (6.9)$$

Informally:  $\mathcal{M}_\tau^\bullet$  results from reading of  $\mathcal{M}_\tau$  from the right to the left.

③ Sometimes it is useful to apply a SM  $\mathcal{M}_\tau$  in two half-steps, e.g., to utilize Runge's rule. We then define

$$\mathcal{M}'_\tau = \mathcal{M}_{\tau/2} \mathcal{M}_{\tau/2}. \quad (6.10)$$

Note, that  $\mathcal{M}'_\tau$  involves twice as many stages as  $\mathcal{M}_\tau^\circ$  or  $\mathcal{M}_\tau^\bullet$ .

It is easy to demonstrate that the above companion SMs inherit their accuracy order from the seed one, such that

$$\deg(\mathcal{M}_\tau^\circ) = \deg(\mathcal{M}_\tau^\bullet) = \deg(\mathcal{M}'_\tau) = \deg(\mathcal{M}_\tau).$$

Other SMs of the same order are yielded by the combinations like  $\mathcal{M}'_\tau^\bullet$ . Note, that we have the relations

$$\mathcal{M}_\tau^{\circ\circ} = \mathcal{M}_\tau, \quad \mathcal{M}_\tau^{\bullet\bullet} = \mathcal{M}_\tau, \quad \mathcal{M}_\tau^{\circ\bullet} = \mathcal{M}_\tau^{\bullet\circ}, \quad \mathcal{M}'_\tau^\bullet = \mathcal{M}_\tau^{\bullet\prime}, \quad \text{etc.}$$

The number of the companion SMs may be reduced by symmetries, e.g.

□ For the Lie-Trotter SM we have  $\mathcal{L}_\tau^\circ = \mathcal{L}_\tau^\bullet$ . For the Strang SM it happens that  $\mathcal{S}_\tau = \mathcal{S}_\tau^\bullet$ . The latter relation defines the so-called *palindromic* SMs.

On the other hand, all companions of, e.g., the SM  $e^{\frac{1}{5}\tau B} e^{\frac{5}{8}\tau A} e^{\frac{4}{5}\tau B} e^{\frac{3}{8}\tau A}$ , which is referred to as Milne's rational SM [218], are different.

❗ The goal of this Chapter is to explain how to improve accuracy of an arbitrary SM  $\mathcal{M}_\tau$  by using its companions. The proposed method is somewhat similar to Richardson extrapolation and applies when  $\deg(\mathcal{M}_\tau)$  is an odd number.

### 6.3 Main result

A well known advantage of SMs is that a separate treatment of  $e^{\tau A}$  and  $e^{\tau B}$  in Eq. (6.4) may be more efficient than the direct numerical approximation of  $e^{\tau(A+B)}$ . In the context of parallel computing, the SM of choice enables parallel computation of  $e^{\tau A}$ , or  $e^{\tau B}$ , or both [203]. Aside from this, SMs can be run in parallel on standard PCs with multi-core processors even when the sub-steps do not enjoy such a property. Namely, the expression  $\mathcal{M}_\tau u_0$  can simultaneously be calculated by several computer cores starting from the common  $u_0$  but using a different order of the sub-steps [219, 220]. A properly weighted sum of the results may provide a better approximation of  $e^{\tau(A+B)} u_0$  than the individual SMs. This procedure defines a so-called *additive* splitting method (**ASM**), see [203].

A generic ASM  $\mathcal{M}_\tau$  is composed from  $J \geq 2$  multiplicative SMs  $\mathcal{M}_{j,\tau}$  via

$$\mathcal{M}_\tau = \sum_{j=1}^J c_j \mathcal{M}_{j,\tau} \quad \text{with} \quad \sum_{j=1}^J c_j = 1. \quad (6.11)$$

$J$  is referred to as the number of threads to stress that ASMs are tailored to parallel computing [219]. The individual SMs  $\mathcal{M}_{j,\tau}$  in Eq. (6.11) may have different orders, which are controlled by the variables

$$P = \min_{1 \leq j \leq J} \deg(\mathcal{M}_{j,\tau}), \quad \bar{P} = \max_{1 \leq j \leq J} \deg(\mathcal{M}_{j,\tau}).$$

We have  $\deg(\mathcal{M}_\tau) = P$  in the worst case. A useful ASM should be better than the involved SMs and we would like to score  $\deg(\mathcal{M}_\tau) > \bar{P}$  by properly choosing  $c_j$ .

The simplest ASM is given by the swap symmetrization of the Lie-Trotter SM [221]

$$\widetilde{\mathcal{L}}_\tau = \frac{1}{2}\mathcal{L}_\tau + \frac{1}{2}\mathcal{L}_\tau^\circ = \frac{1}{2}\left(e^{\tau B}e^{\tau A} + e^{\tau A}e^{\tau B}\right), \quad P = \bar{P} = 1,$$

where one can demonstrate that  $\deg(\widetilde{\mathcal{L}}_\tau) = 2$ . On the other hand, it is not a good idea to try

$$\widetilde{\mathcal{S}}_\tau = \frac{1}{2}\mathcal{S}_\tau + \frac{1}{2}\mathcal{S}_\tau^\circ, \quad P = \bar{P} = 2,$$

because it turns out that  $\widetilde{\mathcal{S}}_\tau$  is still of the second order. Swap symmetrization does not improve Strang's SM.

Burstein suggested an ASM with four threads [219]

$$\mathcal{B}_\tau = \frac{4}{3}\widetilde{\mathcal{S}}_\tau - \frac{1}{3}\widetilde{\mathcal{L}}_\tau, \quad P = 1, \quad \bar{P} = 2.$$

The local error is expressed in terms of the commutator  $[A, B] = AB - BA$ , where

$$\ell(\mathcal{B}_\tau) = \mathcal{B}_\tau - e^{\tau(A+B)} = -\frac{\tau^4}{24}[A, B]^2 + O(\tau^5), \quad (6.12)$$

such that  $\deg(\mathcal{B}_\tau) = 3$ . Our main result goes further in this direction and establishes when a seed SM of order  $P$  yields an ASM of order  $P + 3$ . It is formulated as follows [202]:

❶ Let  $\mathcal{M}_\tau$  be a SM of the form (6.4) for which  $\deg(\mathcal{M}_\tau)$  is an odd number. Consider an ASM

$$\mathcal{M}_\tau = c_1\mathcal{M}_\tau + c_2\mathcal{M}_\tau^\bullet + c_3\mathcal{M}_\tau' + c_4\mathcal{M}_\tau'^\bullet, \quad (6.13)$$

where by construction  $\sum_{j=1}^4 c_j = 1$  and  $P = \bar{P} = \deg(\mathcal{M}_\tau)$ . We have that  $\deg(\mathcal{M}_\tau) = P$  in a generic case. However, a proper choice of the weight coefficients, namely

$$c_1 = c_2 = -\frac{1}{2(2^{P+1} - 1)}, \quad c_3 = c_4 = \frac{2^P}{2^{P+1} - 1}, \quad (6.14)$$

provides  $\deg(\mathcal{M}_\tau) = P + 3$ .

For instance, the simplest Lie-Trotter SM  $\mathcal{L}_\tau$ , being of the first-order, generates the following ASM

$$\mathcal{N}_\tau = -\frac{1}{6}\left(e^{\tau B}e^{\tau A} + e^{\tau A}e^{\tau B}\right) + \frac{2}{3}\left(e^{\frac{1}{2}\tau B}e^{\frac{1}{2}\tau A}e^{\frac{1}{2}\tau B}e^{\frac{1}{2}\tau A} + e^{\frac{1}{2}\tau A}e^{\frac{1}{2}\tau B}e^{\frac{1}{2}\tau A}e^{\frac{1}{2}\tau B}\right), \quad (6.15)$$

with  $\deg(\mathcal{N}_\tau) = 4$ . After a lengthy calculation, one can demonstrate that

$$\ell(\mathcal{N}_\tau) = \mathcal{N}_\tau - e^{\tau(A+B)} = \mathfrak{c}\tau^5 + O(\tau^6), \quad (6.16)$$

where the coefficient

$$\mathfrak{c}(A, B) = \frac{[A, [A, [A, [A, B]]]] + [[[[A, B], B], B], B]}{2880} - \frac{[[[A, [A, B]], [A, B]]]}{1440} - \frac{[A, [A, [[A, B], B]]] + [A, [[[A, B], B], B]]}{1920} - \frac{[[[A, B], [[A, B], B]]]}{1680},$$

depends on nested commutators.

A relatively simple Eq. (6.12) for the local error of  $\mathcal{B}_\tau$ , implies that Burstein's ASM can be found by trial and error [219]. Equation (6.15) for the local error of  $\mathcal{N}_\tau$  is much more complicated, especially taking into account tenths of terms hidden within the nested commutators.  $\mathcal{N}_\tau$  was found by chance, later on it was realized that ASMs like  $\mathcal{N}_\tau$  appear by virtue of a general principle, as comprised by Eq. (6.13) and (6.14) and as explained in the next Section.

## 6.4 Proof

The ASM  $\mathcal{N}_\tau$  profits from nontrivial relations between the seed multiplicative SM and its companions. Furthermore it takes advantage of the Baker-Campbell-Hausdorff (**BCH**) formula [205]

$$e^{\tau X} e^{\tau Y} = e^{\tau(X+Y) + \frac{\tau^2}{2}[X,Y] + \frac{\tau^3}{12}[X-Y, [X,Y]] - \frac{\tau^4}{24}[X, [Y, [X,Y]]] + \dots}, \quad (6.17)$$

as outlined below.

For a moment we return to a general definition (6.2) of a SM and note that (the continuity condition from [208])

$$\lim_{\tau \rightarrow 0} \left( e^{\tau H_M} \dots e^{\tau H_2} e^{\tau H_1} \right) = \mathbf{I}, \quad (6.18)$$

where  $\mathbf{I}$  denotes the identity operator. One can then employ Taylor expansion of  $\ln(1+x)$  to define the quantity  $\ln(e^{\tau H_M} \dots e^{\tau H_2} e^{\tau H_1})$ . The logarithm is single-valued if all components of  $H$  are bounded operators and  $\tau$  is small enough to guarantee that  $\|e^{\tau H_M} \dots e^{\tau H_2} e^{\tau H_1} - \mathbf{I}\| < 1$ . Let us compare two possibilities to characterize the error of a SM (6.2) for  $\tau \rightarrow 0$

$$\begin{aligned} \ell(\text{SM}) &= e^{\tau H_M} \dots e^{\tau H_2} e^{\tau H_1} - e^{\tau H}, \\ \Delta(\text{SM}) &= \ln \left( e^{\tau H_M} \dots e^{\tau H_2} e^{\tau H_1} \right) - \tau H, \end{aligned}$$

where  $\deg(\text{SM}) = p$  implies that [212]

$$\ell(\text{SM}) = O(\tau^{p+1}) \quad \Leftrightarrow \quad \Delta(\text{SM}) = O(\tau^{p+1}).$$

Calculation of  $\ell(\text{SM})$ , which is the standard local error from Eq. (6.3), requires straightforward but tedious multiplications of the Taylor expansions. The “smart” quantity  $\Delta(\text{SM})$  is calculated by successive application of the BCH formula (6.17) in which we assume that  $\tau$  is small enough to avoid convergence issues. The BCH calculation is more simple and directly provides a more tractable combination of the nested commutators, like one in Eq. (6.16).

Motivated by these observations, we consider a SM  $\mathcal{M}_\tau$  of the form (6.4) and define its discrepancy  $\Delta(\mathcal{M}_\tau)$  by the relation

$$\Delta(\mathcal{M}_\tau) = \ln \left( e^{b_s \tau A} e^{a_s \tau B} \dots e^{b_2 \tau A} e^{a_2 \tau B} e^{b_1 \tau A} e^{a_1 \tau B} \right) - \tau(A+B), \quad (6.19)$$

such that

$$\underbrace{e^{b_s \tau A} e^{a_s \tau B} \dots e^{b_2 \tau A} e^{a_2 \tau B} e^{b_1 \tau A} e^{a_1 \tau B}}_{\mathcal{M}_\tau} = e^{\tau(A+B) + \Delta(\mathcal{M}_\tau)}. \quad (6.20)$$

The BCH formula yields the expression

$$\Delta(\mathcal{M}_\tau) = \sum_{q=2}^{\infty} \frac{[\mathcal{M}]_q}{q!} \tau^q, \quad (6.21)$$

where  $[\mathcal{M}]_q$  denotes a certain linear combination of the basic commutators, e.g.,  $[A, [A, B]]$  and  $[[A, B], B]$  for  $q=3$ . Each basic commutator within  $[\mathcal{M}]_q$  is of length  $q$  and has a numerical factor that does not depend on  $\tau$ , that is why index  $\tau$  is omitted. If we deal with a SM of order  $\deg(\mathcal{M}_\tau) = p$ , the terms  $[\mathcal{M}]_{q \leq p}$  must vanish, such that summation in Eq. (6.21) starts from  $q = p+1$ .

Yoshida [212] found that for a palindromic SM  $\mathcal{P}_\tau$  (the one with the property  $\mathcal{P}_\tau = \mathcal{P}_\tau^\bullet$ ), Eq. (6.21) takes the form

$$\Delta(\mathcal{P}_\tau) = \frac{\tau^3}{3!} [\mathcal{P}]_3 + \frac{\tau^5}{5!} [\mathcal{P}]_5 + \frac{\tau^7}{7!} [\mathcal{P}]_7 + \dots,$$

such that  $\Delta(\mathcal{P}_{-\tau}) = -\Delta(\mathcal{P}_\tau)$ .

Among other things, this is why the second-order SM (6.7) is promoted directly to the fourth-order SM  $\mathcal{Y}_\tau$  after a proper value of  $\sigma$  provides that  $[\mathcal{P}]_3 = 0$ . In our context, the key fact about  $\Delta(\mathcal{M}_\tau)$  is that:

❗ Once calculated for a SM  $\mathcal{M}_\tau$ , Eq. (6.21) constrains expansions for the companion SMs via

$$\Delta(\mathcal{M}_\tau^\bullet) = \sum_{q=2}^{\infty} (-1)^{q-1} \frac{[\mathcal{M}]_q}{q!} \tau^q, \quad \Delta(\mathcal{M}'_\tau) = \sum_{q=2}^{\infty} \frac{[\mathcal{M}]_q}{2^{q-1} q!} \tau^q,$$

whereas  $[\mathcal{M}^\circ]_q$  is obtained by swapping  $A$  and  $B$  in  $[\mathcal{M}]_q$ .

To take advantage of the above relations, we return to the ASM (6.13), in which one expects that  $\deg(\mathcal{M}_\tau) = P$ , and directly calculate  $\ell(\mathcal{M}_\tau)$  in terms of  $\Delta(\mathcal{M}_\tau)$ . The result reads

$$\ell(\mathcal{M}_\tau) = \frac{\tau^{P+1}}{(P+1)!} \left\{ c_1 + (-1)^P c_2 + \frac{c_3 + (-1)^P c_4}{2^P} \right\} [\mathcal{M}]_{P+1} + O(\tau^{P+2}).$$

One can improve ASM's accuracy by choosing the weight coefficients to cancel the term in curly brackets. A priori knowledge of  $[\mathcal{M}]_{P+1}$ , which may contain hundreds of commutators, is not required.

A more elaborated calculation of  $\ell(\mathcal{M}_\tau)$  shows that  $\deg(\mathcal{M}_\tau)$  can at the most be improved from  $P$  to  $P+3$ . It turns out that the resulting system of algebraic equations for the weight coefficients is compatible for odd  $P$  and results in Eq. (6.14). This explains the main result of this Chapter.

## 6.5 Outlook

To gain a better insight into ASM (6.15), assume that parallel evaluation of the operators  $e^{\tau A}$  and  $e^{\tau B}$  scales with the number of computer cores for up to  $N$  cores. Using, e.g., Strang's SM, one employs these  $N$  cores to obtain  $e^{\frac{1}{2}\tau A} e^{\tau B} e^{\frac{1}{2}\tau A} u_0$  with the local accuracy  $O(\tau^3)$ . In our approach three clusters with  $N$  cores can be employed. The first one computes  $e^{\frac{1}{2}\tau B} e^{\frac{1}{2}\tau A} e^{\frac{1}{2}\tau B} e^{\frac{1}{2}\tau A} u_0$ , the second one computes  $e^{\frac{1}{2}\tau A} e^{\frac{1}{2}\tau B} e^{\frac{1}{2}\tau A} e^{\frac{1}{2}\tau B} u_0$ , and the third one performs successive calculation of  $e^{\tau B} e^{\tau A} u_0$  and  $e^{\tau A} e^{\tau B} u_0$ . Altogether, each cluster is involved in calculation of four exponential operators. Finally, the weighted sum of the results can be efficiently evaluated, at least on a shared memory system, and provides the local accuracy of  $O(\tau^5)$ . A direct application of the fourth-order Yoshida's SM  $\mathcal{Y}_\tau$  involves 6 exponential operators (because of FSAL property). Numerical examples for NLSE and GNLSE are given in [202].

# Chapter 7

## Conclusions

This work contributes to Theoretical Physics by considering mathematical and physical problems related to propagation of ultra-short pulses in optical fibers. However the concepts that have been developed to address these problems, seem to go beyond the framework of fiber-optic. It is worth to spend some time and to formulate the ideas that might be of use for a broader community of physicists.

- ❶ Response functions (kernels of the convolution integrals), as they appear in Maxwell equations and in other non-local systems, are usually transformed to the frequency domain and considered in the complex  $\omega$ -plane. They take infinite values at certain complex frequencies being, e.g., meromorphic functions like the famous Lorentzian. On the other hand, these response functions are approximated by polynomials in standard propagation equations like NLSE or GNLSE. Even if the information on a response function is very limited and covers only a small vicinity of the wave carrier frequency, it is worth trying to find a rational approximation to the dispersion relation. At the very least, the approximation leads to a less stiff numerical solution. In fortunate cases, one is left with a completely new model equation; this is how a short-pulse equation comes into play.
- ❷ It seems evident that an optical pulse at carrier frequency  $\omega$  cannot be shorter than  $\pi/\omega$ , but what happens with the corresponding mathematical solution when pulse duration comes to its limit? Seemingly different model equations have a common feature: a cusp is formed at the top of the shortest soliton. This occurs in a full analogy with a sharp water-wave crest of a gravity (Stokes) wave of the maximum height. In fiber optics such a peaked soliton determines the largest peak power and the shortest pulse duration. To the best of our knowledge, the peaked solitons appear in all model equations for ultrashort pulses, but the standard GNLSE. In the latter case the peaked soliton immediately appears after nonlinear dispersion is taken into account. It seems that extreme pulses in different fields of science have the same universal behavior.
- ❸ Many studies try to change one optical pulse by applying another one with something like an “optical transistor” in mind. A soliton and a pump pulse that have considerably different frequencies but nearly identical velocities, provide a possible scenario. In this work we discuss a simplified set of ODEs for the soliton parameters. These ODEs were derived with the evident goal to reduce the computation costs. However, they turned out to be a useful tool in many other ways. For instance, it became possible to treat the soliton as an effective mirror and to optimize parameters of that mirror. Another application is that one can follow the light rays and recognize caustics as well as the rays that are reflected several times providing an additional compression of the soliton. When the pump wave is used to fix the soliton parameters, the ODEs predict whether the resulting system state is stable or not, and so on. All these problems are very difficult to address through the full numerical solution.
- ❹ Numerous scientific calculations are performed in parallel such that different computer cores do the same job but with the different data sets. An alternative is given by a concurrent computation, where the initial problem is divided into independent sub-tasks and the available computer cores just go through these



tasks one by one until a common synchronization point for all tasks is reached. It seems that there is a class of additive split-step methods that are naturally suited for the concurrent computation, the simplest such method was discussed in this work.

Last but not least, this work summarizes a long research period and results from collaborations with many remarkable scientists. It is a great pleasure to note an especially fruitful joint work with:

- ❗ Nail Akhmediev, Uwe Bandelow, Raimondas Čiegis, Ayhan Demircan, Alexander Mielke, Hans-Georg Purwins, Mindaugas Radziunas, Günter Steinmeyer, Andrei Vladimirov,



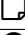

and to acknowledge Uwe Bandelow and Hans-Jürgen Wünsche for careful reading of the manuscript.

Dear friends and colleges, it was a great time and I am extremely grateful to all of you!

# Chapter 8

## Appendices

### 8.1 Acronyms

	take home message	
	quotation or a well known fact	
	notation or agreement	
	rhetorical question	
ASM	additive splitting method	page 58
BCH	Baker-Campbell-Hausdorff	60
CW	continuous wave	24
FSAL	first same as last	57
FWHM	full width at half maximum	57
GNLSE	generalized nonlinear Schrödinger equation	26
GVD	group velocity dispersion	31
KdV	Korteweg-de Vries equation	39
mKdV	modified Korteweg-de Vries equation	39
NLSE	nonlinear Schrödinger equation	25
SC	supercontinuum	30
SM	splitting method	56
SPE	short pulse equation	37
SPT	soliton perturbation theory	52
SSFS	soliton self-frequency shift	52
SVEA	slowly varying envelope approximation	25
XPM	cross-phase modulations	50
ZDF	zero dispersion frequency	31

**Table 8.1:** List of acronyms

## 8.2 Notations

$\beta_j$	dispersion coefficient $\beta^{(j)}(\omega) _{\omega=\omega_0}$	Eq. (3.13)
$\beta_a, \beta'_a, \beta''_a \dots$	special notation for $\beta^{(j)}(\omega) _{\omega=\omega_a}$	page 50
$\beta_b, \beta'_b, \beta''_b \dots$	special notation for $\beta^{(j)}(\omega) _{\omega=\omega_b}$	page 50
$\hat{\mathcal{D}}$	dispersion operator	Eq. (3.29)
D	deviation of $\beta(\omega)$ from a straight line	(3.30)
$\mathcal{E}(t)$	analytic signal of a real-valued $E(t)$	(1.2)
I	identity operator	(6.18)
$\Delta(\mathcal{M}_\tau)$	discrepancy of $\mathcal{M}_\tau$	(6.19)
$L_d, L_d(j), L_n$	characteristic scales for a pulse	(3.20), (3.26)
$\ell(\mathcal{M}_\tau)$	local error of $\mathcal{M}_\tau$	(6.3)
$\mathcal{L}_\tau$	Lie-Trotter splitting	(6.5)
$\mathcal{M}_\tau$	general multiplicative splitting	(6.4)
$\mathcal{M}_\tau^\circ$	swapped splitting	(6.8)
$\mathcal{M}_\tau^\bullet$	inverted splitting	(6.9)
$\mathcal{M}'_\tau$	half-step splitting	(6.10)
$\mathcal{M}_\tau$	general additive splitting method	(6.11)
$\mathcal{N}_\tau$	new additive splitting method	(6.15)
$\tau$	delay for pulses in fibers time step for a split-step solver	(3.10) Chapter 6
$\omega_a, \omega_b, \omega_s, \Omega$	parameters for the scattering problem	page 49, Fig. 5.8
$\tilde{\Phi}_0$	complex phase of a modulated wave	Eq. (3.4)
$\mathcal{S}_\tau$	Strang splitting	(6.6)
$\mathcal{Y}_\tau$	Yoshida splitting	(6.7)

**Table 8.2:** List of notations

# Bibliography

- [1] F.X. Kärtner, E.P. Ippen, and S.T. Cundiff.  
*Femtosecond Laser Development*, chapter 2, pages 54–57.  
Springer, June 2006.
- [2] M. Wegener.  
*Extreme Nonlinear Optics*.  
Springer, 2005.
- [3] J. A. Cox, W. P. Putnam, A. Sell, A. Leitenstorfer, and F. X. Kärtner.  
Pulse synthesis in the single-cycle regime from independent mode-locked lasers using attosecond-precision feedback.  
*Opt. Lett.*, 37(17):3579–3581, September 2012.
- [4] E. Matsubara, K. Yamane, T. Sekikawa, and M. Yamashita.  
Generation of 2.6 fs optical pulses using induced-phase modulation in a gas-filled hollow fiber.  
*J. Opt. Soc. Am. B*, 24(4):985–989, 2007.
- [5] G. Steinmeyer and G. Stibenz.  
Generation of sub-4-fs pulses via compression of a white-light continuum using only chirped mirrors.  
*Appl. Phys. B*, 82(2):175–182, 2006.
- [6] A. L. Cavalieri, E. Goulielmakis, B. Horvath, W. Helml, M. Schultze, M. Fieß, V. Pervak, L. Veisz, V. S. Yakovlev, M. Uiberacker, A. Apolonski, F. Krausz, and R. Kienberger.  
Intense 1.5-cycle near infrared laser waveforms and their use for the generation of ultra-broadband soft-x-ray harmonic continua.  
*New J. Phys.*, 9(7):242, July 2007.
- [7] A. V. Kim, M. Yu. Ryabikin, and A. M. Sergeev.  
From femtosecond to attosecond pulses.  
*Usp. Fiz. Nauk*, 42(1):54–61, 1999.
- [8] M. Hentschel, R. Kienberger, Ch. Spielmann, G. A. Reider, N. Milosevic, T. Brabec, P. Corkum, U. Heinzmann, M. Drescher, and F. Krausz.  
Attosecond metrology.  
*Nature*, 414(6863):509–513, 2001.
- [9] P. M. Paul, E. S. Toma, P. Breger, G. Mullot, F. Augé, Ph. Balcou, H. G. Muller, and P. Agostini.  
Observation of a train of attosecond pulses from high harmonic generation.  
*Science*, 292(5522):1689–1692, 2001.
- [10] M. Drescher, M. Hentschel, R. Kienberger, G. Tempea, Ch. Spielmann, G. A. Reider, P. B. Corkum, and F. Krausz.  
X-ray pulses approaching the attosecond frontier.  
*Science*, 291(5510):1923–1927, 2001.
- [11] G. P. Agrawal.  
*Nonlinear Fiber Optics*.  
Academic, New York, 4 edition, 2007.

- [12] K. J. Blow and D. Wood.  
Theoretical description of transient stimulated Raman scattering in optical fibers.  
*IEEE J. Quantum Electron.*, 25(15):2665–2673, 1989.
- [13] A. V. Husakou and J. Herrmann.  
Supercontinuum generation of higher-order solitons by fission in photonic crystal fibers.  
*Phys. Rev. Lett.*, 87(20):203901, 2001.
- [14] M. Trippenbach, W. Wasilewski, P. Kruk, G. W. Bryant, G. Fibich, and Y. B. Band.  
An improved nonlinear optical pulse propagation equation.  
*Opt. Commun.*, 210(3–6):385–391, 2002.
- [15] N. N. Akhmediev and V. I. Korneev.  
Modulation instability and periodic solutions of the nonlinear Schrödinger equation.  
*Theor. Math. Phys.*, 69(2):1089–1093, 1986.
- [16] B. Kibler, J. Fatome, C. Finot, G. Millot, F. Dias, G. Genty, N. Akhmediev, and J. M. Dudley.  
The peregrine soliton in nonlinear fibre optics.  
*Nature Physics*, 6(10):790–795, August 2010.
- [17] V. E. Zakharov and A. A. Gelash.  
Nonlinear stage of modulation instability.  
*Phys. Rev. Lett.*, 111(5):054101, July 2013.
- [18] A. Tikan, C. Billet, G. El, A. Tovbis, M. Bertola, T. Sylvestre, F. Gustave, S. Randoux, G. Genty, P. Suret, and J. M. Dudley.  
Universality of the Peregrine soliton in the focusing dynamics of the cubic nonlinear Schrödinger equation.  
*Phys. Rev. Lett.*, 119(3):033901, July 2017.
- [19] J. M. Dudley, G. Genty, A. Mussot, A. Chabchoub, and F. Dias.  
Rogue waves and analogies in optics and oceanography.  
*Nature Reviews Physics*, 1(11):675–689, September 2019.
- [20] R. Ramaswami, K. N. Sivarajan, and G. H. Sasaki.  
*Optical Networks A Practical Perspective*.  
Elsevier, 3 edition, 2010.
- [21] S. A. Skobelev, D. V. Kartashov, and A. V. Kim.  
Few-optical-cycle solitons and pulse self-compression in a Kerr medium.  
*Phys. Rev. Lett.*, 99(20):203902, 2007.
- [22] M. A. Nielsen and I. L. Chuang.  
*Quantum Computation and Quantum Information*.  
Cambridge University Press, 2000.
- [23] T. D. Ladd, F. Jelezko, R. Laflamme, Y. Nakamura, C. Monroe, and J. L. O’Brien.  
Quantum computers.  
*Nature*, 464:45–53, March 2010.
- [24] D. A. B. Miller.  
Are optical transistors the logical next step?  
*Nature Photonics*, 4(1):3–5, January 2010.
- [25] S. Wielandy and Alexander L. Gaeta.  
Coherent control of the polarization of an optical field.  
*Phys. Rev. Lett.*, 81(16):3359–3362, October 1998.
- [26] A. M. C. Dawes, L. Illing, S. M. Clark, and D. J. Gauthier.  
All-optical switching in rubidium vapor.  
*Science*, 308(5722):672–674, April 2005.

- [27] X. Hu, P. Jiang, C. Ding, Yang H., and Q. Gong.  
Picosecond and low-power all-optical switching based on an organic photonic-bandgap microcavity.  
*Nature Photonics*, 2(3):185–189, March 2008.
- [28] M. Born and E. Wolf.  
*Principles of Optics*.  
Cambridge University Press, 7 edition, 1999.
- [29] G. B. Whitham.  
*Linear and nonlinear waves*.  
John Wiley & Sons, 1974.
- [30] A. I. Kostrikin and Yu. I. Manin.  
*Linear Algebra and Geometry*, volume 1 of *Algebra, Logic and Applications*.  
Taylor and Francis, 1989.
- [31] B. Van der Pol.  
On “relaxation-oscillations”.  
*Philosophical Magazine Series 7*, 2(11):978–992, 1926.
- [32] D. E. Vakman and L. A. Vainshtein.  
Amplitude, phase, frequency — fundamental concepts of oscillation theory.  
*Usp. Fiz. Nauk*, 20(12):1002–1016, 1977.
- [33] A. H. Nayfeh.  
*Perturbation methods*.  
Wiley, 1973.
- [34] D. Gabor.  
Theory of communication.  
*Journal of the Institute of Electrical Engineers*, 93(3):429–457, 1946.
- [35] T. Brabec and F. Krausz.  
Nonlinear optical pulse propagation in the single-cycle regime.  
*Phys. Rev. Lett.*, 78(17):3282–3285, 1997.
- [36] M. Kolesik, J. V. Moloney, and M. Mlejnek.  
Unidirectional optical pulse propagation equation.  
*Phys. Rev. Lett.*, 89(28):283902, 2002.
- [37] M. Kolesik and J. V. Moloney.  
Nonlinear optical pulse propagation simulation: From Maxwell’s to unidirectional equations.  
*Phys. Rev. E*, 70(3):036604, 2004.
- [38] P. Kinsler, S. B. P. Radnor, and G. H. C. New.  
Theory of directional pulse propagation.  
*Phys. Rev. A*, 72(6):063807, 2005.
- [39] G. Genty, P. Kinsler, B. Kibler, and J. M. Dudley.  
Nonlinear envelope equation modeling of sub-cycle dynamics and harmonic generation in nonlinear waveguides.  
*Opt. Express*, 15(9):5382–5387, 2007.
- [40] P. Kinsler.  
Optical pulse propagation with minimal approximations.  
*Phys. Rev. A*, 81(1):013819, January 2010.
- [41] Sh. Amiranashvili and A. Demircan.  
Ultrashort optical pulse propagation in terms of analytic signal.  
*Advances in Optical Technologies*, 2011:989515, November 2011.

- [42] C. R. Loures, A. Armaroli, and F. Biancalana.  
Contribution of third-harmonic and negative-frequency polarization fields to self-phase modulation in nonlinear media.  
*Opt. Lett.*, 40(4):613–616, February 2015.
- [43] M. Conforti, A. Marini, T. X. Tran, D. Faccio, and F. Biancalana.  
Interaction between optical fields and their conjugates in nonlinear media.  
*Opt. Express*, 21(25):31239–31252, December 2013.
- [44] J. M. Dudley and J. R. Taylor, editors.  
*Supercontinuum generation in optical fibers*.  
Cambridge University Press, 2010.
- [45] Sh. Amiranashvili.  
Hamiltonian framework for short optical pulses.  
In E. Tobish, editor, *New Approaches to Nonlinear Waves*, volume 908 of *Lecture Notes in Physics*, pages 153–196. Springer, 2016.
- [46] T. Needham.  
*Visual Complex Analysis*.  
Oxford University Press, 1997.
- [47] L. D. Landau, E. M. Lifshitz, and L. P. Pitaevskii.  
*Electrodynamics of Continuous Media*.  
Elsevier, New York, 2 edition, 1984.
- [48] Sh. Amiranashvili and A. Demircan.  
Hamiltonian structure of propagation equations for ultrashort optical pulses.  
*Phys. Rev. A*, 82(1):013812, Juli 2010.
- [49] K. E. Oughstun.  
*Electromagnetic and Optical Pulse Propagation*, volume Volume 1: Spectral Representations in Temporally Dispersive Media of *Springer Series in Optical Sciences*.  
Springer, 2019.
- [50] D. C. Hutchings, M. Sheik-Bahae, D. J. Hagan, and E. W. Van Stryland.  
Kramers-Krönig relations in nonlinear optics.  
*Opt. Quantum Electron.*, 24(1):1–30, 1992.
- [51] Sh. Amiranashvili, U. Bandelow, and A. Mielke.  
Padé approximant for refractive index and nonlocal envelope equations.  
*Opt. Commun.*, 283(3):480–485, February 2010.
- [52] J. Yang.  
*Nonlinear Waves in Integrable and Nonintegrable Systems*.  
SIAM, 2010.
- [53] M. Kolesik, P. Jakobsen, and J. V. Moloney.  
Quantifying the limits of unidirectional ultrashort optical pulse propagation.  
*Phys. Rev. A*, 86(3):035801, September 2012.
- [54] Sh. Amiranashvili, M. Radziunas, U. Bandelow, and R. Čiegis.  
Numerical methods for accurate description of ultrashort pulses in optical fibers.  
*Commun Nonlinear Sci Numer Simul*, 67:391–402, February 2019.
- [55] F. Strocchi.  
Complex coordinates and quantum mechanics.  
*Rev. Mod. Phys.*, 38(1):36–40, 1966.
- [56] V. E. Zakharov, S. L. Musher, and A. M. Rubenchik.  
Hamiltonian approach to the description of non-linear plasma phenomena.

- Phys. Rep.*, 129(5):287–366, 1985.
- [57] V. E. Zakharov and E. A. Kuznetsov.  
Hamiltonian formalism for nonlinear waves.  
*Usp. Fiz. Nauk*, 40(11):1087–1116, 1997.
- [58] M. V. Karasev and V. P. Maslov.  
*Nonlinear Poisson Brackets: Geometry and Quantization*, volume 119 of *Translations of Mathematical Monographs*.  
AMS, 1993.
- [59] V. I. Arnold.  
*Mathematical Methods of Classical Mechanics*.  
Springer, Berlin, 2 edition, 1989.
- [60] L. D. Faddeev.  
New life of complete integrability.  
*Usp. Fiz. Nauk*, 56(5):465–472, May 2013.
- [61] L. D. Landau and E. M. Lifshitz.  
*Mechanics*.  
Pergamon, 1969.
- [62] W. Wirtinger.  
Zur formalen Theorie der Funktionen von mehr komplexen Veränderlichen.  
*Mathematische Annalen*, 97(1):357–376, 1927.
- [63] V. E. Zakharov and L. D. Faddeev.  
Korteweg-de Vries equation: A completely integrable Hamiltonian system.  
*Funct. Anal. Appl.*, 5(4):280–287, 1971.
- [64] N. N. Rosanov, R. M. Arkhipov, and M. V. Arkhipov.  
On laws of conservation in the electrodynamics of continuous media.  
*Phys.-Usp.*, 61(12):1227–1233, December 2018.
- [65] E.G. Bessonov.  
On a class of electromagnetic waves.  
*Sov. Phys. JETP*, 53(3):433–436, March 1981.
- [66] T. A. Birks, J. C. Knight, and P. St. J. Russell.  
Endlessly single-mode photonic crystal fiber.  
*Opt. Lett.*, 22(13):961–963, 1997.
- [67] E. P. Wigner.  
The unreasonable effectiveness of mathematics in the natural sciences. Richard Courant lecture in mathematical sciences delivered at New York University, May 11, 1959.  
*Communications on Pure and Applied Mathematics*, 13(1):1–14, February 1960.
- [68] V. I. Karpman.  
*Non-linear waves in dispersive media*.  
Pergamon, 1975.
- [69] P. L. Kelley.  
Self-focusing of optical beams.  
*Phys. Rev. Lett.*, 16(15):384, December 1965.
- [70] V. I. Bespalov and V. I. Talanov.  
Filamentary structure of light beams in nonlinear liquids.  
*JETP Lett.*, 3(12):307–310, June 1966.



- [71] T. B. Benjamin and J. E. Feir.  
The disintegration of wave trains on deep water Part 1. Theory.  
*J. Fluid Mech.*, 27(3):417–430, February 1967.
- [72] V. E. Zakharov.  
Stability of periodic waves of finite amplitude on the surface of a deep fluid.  
*J. Appl. Mech. and Tech. Phys.*, 9(2):190–194, 1968.
- [73] A. Hasegawa.  
Theory and computer experiment on self-trapping instability of plasma cyclotron waves.  
*Phys. Fluids*, 15(5):870–881, 1972.
- [74] Y. Kodama and A. Hasegawa.  
Nonlinear pulse propagation in a monomode dielectric guide.  
*IEEE J. Quantum Electron.*, 23(5):510–524, May 1987.
- [75] V. E. Zakharov and A. B. Shabat.  
Exact theory of two-dimensional self-focusing and one-dimensional self-modulation of waves in nonlinear media.  
*Sov. Phys. JETP*, 34(1):62–69, 1972.
- [76] A. Ankiewicz, D. J. Kedziora, A. Chowdury, U. Bandelow, and N. Akhmediev.  
Infinite hierarchy of nonlinear Schrödinger equations and their solutions.  
*Phys. Rev. E*, 93(1):012206, January 2016.
- [77] U. Bandelow, A. Ankiewicz, Sh. Amiranashvili, and N. Akhmediev.  
Sasa-Satsuma hierarchy of integrable evolution equations.  
*Chaos*, 28(5):053108, May 2018.
- [78] J. M. Dudley, G. Genty, and S. Coen.  
Supercontinuum generation in photonic crystal fiber.  
*Rev. Mod. Phys.*, 78(4):1135–1184, 2006.
- [79] Sh. Amiranashvili and E. Tobisch.  
Extended criterion for the modulation instability.  
*New J. Phys.*, 21(3):033029, March 2019.
- [80] V. E. Zakharov and L. A. Ostrovsky.  
Modulation instability: the beginning.  
*Physica D: Nonlinear Phenomena*, 238(5):540–548, March 2009.
- [81] D. H. Peregrine.  
Water waves, nonlinear Schrödinger equations and their solutions.  
*J. Austral. Math. Soc. Ser. B*, 25(1):16–43, 1983.
- [82] N. Akhmediev, A. Ankiewicz, and M. Taki.  
Waves that appear from nowhere and disappear without a trace.  
*Phys. Lett. A*, 373(2):675–678, February 2009.
- [83] K. B. Dysthe.  
Note on a modification to the nonlinear Schrödinger equation for application to deep water waves.  
*Proc. R. Soc. London, A* 369(1736):105–114, December 1979.
- [84] Sh. Amiranashvili, U. Bandelow, and N. Akhmediev.  
Dispersion of nonlinear group velocity determines shortest envelope solitons.  
*Phys. Rev. A*, 84(4):043834, October 2011.
- [85] A. Hasegawa and M. Matsumoto.  
*Optical Solitons in Fibers*.  
Springer, 2003.

- [86] N. Akhmediev and A. Ankiewicz.  
*Solitons: Nonlinear Pulses and Beams*.  
Chapman and Hall, 1997.
- [87] A. Hasegawa.  
*Optical Solitons in Fibers*.  
Springer, 1989.
- [88] R. Hirota.  
Exact envelope-soliton solutions of a nonlinear wave equation.  
*J. Math. Phys.*, 14(7):805–809, July 1973.
- [89] N. Sasa and J. Satsuma.  
New-type of soliton solutions for a higher-order nonlinear Schrödinger equation.  
*J. Phys. Soc. Jpn.*, 60(2):409–417, February 1991.
- [90] V. E. Zakharov and E. A. Kuznetsov.  
Optical solitons and quasisolitons.  
*JETP*, 86(5):1035–1046, 1998.
- [91] M. J. Ablowitz and T. P. Horikis.  
Solitons and spectral renormalization methods in nonlinear optics.  
*Eur. Phys. J. Special Topics*, 173(1):147–166, June 2009.
- [92] N. N. Akhmediev, V. M. Eleonskii, and N. E. Kulagin.  
Exact first-order solutions of the nonlinear Schrödinger equation.  
*Teoret. Mat. Fiz.*, 72(2):183–196, August 1987.
- [93] N. N. Akhmediev, V. M. Eleonskii, and N. E. Kulagin.  
Generation of periodic trains of picosecond pulses in an optical fiber: exact solutions.  
*Sov. Phys. JETP*, 89(5):1542–1555, November 1985.
- [94] N. Akhmediev and M. Karlsson.  
Cherenkov radiation emitted by solitons in optical fibers.  
*Phys. Rev. A*, 51(3):2602–2607, March 1995.
- [95] P. Kinsler and G. H. C. New.  
Few-cycle pulse propagation.  
*Phys. Rev. A*, 67(2):023813, 2003.
- [96] D. V. Skryabin and A. V. Gorbach.  
Colloquium: Looking at a soliton through the prism of optical supercontinuum.  
*Rev. Mod. Phys.*, 82(2):1287–1299, April 2010.
- [97] J. E. Rothenberg.  
Space-time focusing: breakdown of the slowly varying envelope approximation in the self-focusing of femtosecond pulses.  
*Opt. Lett.*, 17(19):1340–1342, 1992.
- [98] J. K. Ranka and A. L. Gaeta.  
Breakdown of the slowly varying envelope approximation in the self-focusing of ultrashort pulses.  
*Opt. Lett.*, 23(7):534–536, 1998.
- [99] K. E. Oughstun and H. Xiao.  
Failure of the quasimonochromatic approximation for ultrashort pulse propagation in a dispersive, attenuative medium.  
*Phys. Rev. Lett.*, 78(4):642–645, 1997.
- [100] M. H. Stone.  
The generalized Weierstrass approximation theorem.  
*Mathematics Magazine*, 21(4):167–184, 1948.

- [101] M. Bass, E. W. Van Stryland, D. R. Williams, and W. L. Wolfe, editors.  
*Handbook of Optics*, volume 1.  
McGRAW-HILL, 2 edition, 1995.
- [102] N. Akhmediev, B. Kibler, F. Baronio, M. Belić, W.-P. Zhong, Y. Zhang, W. Chang, J. M. Soto-Crespo, P. Vouzas, P. Grelu, C. Lecaplain, K. Hammani, S. Rica, A. Picozzi, M. Tlidi, K. Panajotov, A. Mussot, A. Bendahmane, P. Szriftgiser, G. Genty, J. Dudley, A. Kudlinski, A. Demircan, U. Morgner, Sh. Amiranashvili, C. Brée, G. Steinmeyer, C. Masoller, N. G. R. Broderick, A. F. J. Runge, M. Erkintalo, S. Residori, U. Bortolozzo, F. T. Arecchi, S. Wabnitz, C. G. Tiofack, Coulibaly S., and M. Taki.  
Roadmap on optical rogue waves and extreme events.  
*Journal of Optics*, 18(6):063001, June 2016.
- [103] I. S. Aranson and L. Kramer.  
The world of the complex Ginzburg-Landau equation.  
*Rev. Mod. Phys.*, 74(1):99–143, January 2002.
- [104] G. A. Baker and P. Graves-Morris.  
*Padé approximants. Part I: basic theory*.  
Addison-Wesley, 1981.
- [105] G. A. Baker and P. Graves-Morris.  
*Padé approximants. Part II: extensions and applications*.  
Addison-Wesley, 1981.
- [106] A. Pimenov, Sh. Amiranashvili, and A. G. Vladimirov.  
Temporal cavity solitons in a delayed model of a dispersive cavity ring laser.  
*Math. Model. Nat. Phenom*, 15(47):1–18, September 2020.
- [107] N. Linale, J. Bonetti, A. Sparapani, A.D. Sánchez, and D.F. Grosz.  
Equation for modeling two-photon absorption in nonlinear waveguides.  
*J. Opt. Soc. Am. B*, 37(6):1906–1910, June 2020.
- [108] Sh. Amiranashvili, A. G. Vladimirov, and U. Bandelow.  
Solitary-wave solutions for few-cycle optical pulses.  
*Phys. Rev. A*, 77(6):063821, June 2008.
- [109] Sh. Amiranashvili, A. G. Vladimirov, and U. Bandelow.  
A model equation for ultrashort optical pulses around the zero dispersion frequency.  
*Eur. Phys. J. D*, 58(2):219–226, January 2010.
- [110] Sh. Amiranashvili, U. Bandelow, and N. Akhmediev.  
Few-cycle optical solitary waves in nonlinear dispersive media.  
*Phys. Rev. A*, 87(1):013805, January 2013.
- [111] Sh. Amiranashvili, U. Bandelow, and N. Akhmediev.  
Spectral properties of limiting solitons in optical fibers.  
*Opt. Express*, 22(24):30251–30256, November 2014.
- [112] A. I. Maimistov.  
Some models of propagation of extremely short electromagnetic pulses in a nonlinear medium.  
*Quantum Electron.*, 30(4):287–304, 2000.
- [113] T. Schäfer and C. E. Wayne.  
Propagation of ultra-short optical pulses in cubic nonlinear media.  
*Physica D*, 196(1–2):90–105, 2004.
- [114] S. A. Kozlov and S. V. Sazonov.  
Nonlinear propagation of optical pulses of a few oscillations duration in dielectric media.  
*JETP*, 84(2):221–228, 1997.

- [115] D. V. Kartashov, A. V. Kim, and S. A. Skobelev.  
Soliton structures of a wave field with an arbitrary number of oscillations in nonresonance media.  
*JETP Lett.*, 78(5):276–280, 2003.
- [116] D. Pelinovsky and A. Sakovich.  
Global well-posedness of the Short-Pulse and Sine-Gordon equations in energy space.  
*Commun. Part. Diff. Eq.*, 35(4):613–629, March 2010.
- [117] D. J. Korteweg and G. de Vries.  
On the change of form of long waves advancing in a rectangular channel and a new type of long stationary wave.  
*Phil. Mag.*, 39(5):422–443, 1895.
- [118] C. S. Gardner, J. M. Greene, M. D. Kruskal, and R. M. Miura.  
Method for solving the Korteweg-deVries equation.  
*Phys. Rev. Lett.*, 19(19):1095–1097, 1967.
- [119] E. M. Belenov and A. V. Nazarkin.  
Solutions of nonlinear-optics equations found outside the approximation of slowly varying amplitudes and phases.  
*JETP Lett.*, 51(5):288–292, 1990.
- [120] J. C. Brunelli.  
The bi-Hamiltonian structure of the short pulse equation.  
*Phys. Lett. A*, 353(6):475–478, 2006.
- [121] A. Sakovich and S. Sakovich.  
The short pulse equation is integrable.  
*J. Phys. Soc. Jpn.*, 74(1):239–241, 2005.
- [122] A. Sakovich and S. Sakovich.  
Solitary wave solutions of the short pulse equation.  
*J. Phys. A*, 39(22):L361–L367, 2006.
- [123] S. A. Skobelev and A. V. Kim.  
On the dynamic properties of "elastic" interactions between wave solitons consisting of a few field oscillation cycles.  
*JETP Lett.*, 80(4):623–627, 2004.
- [124] Y. Chung, C. K. R. T. Jones, T. Schäfer, and C. E. Wayne.  
Ultra-short pulses in linear and nonlinear media.  
*Nonlinearity*, 18(3):1351–1374, 2005.
- [125] A. V. Kim, S. A. Skobelev, D. Anderson, T. Hansson, and M. Lisak.  
Extreme nonlinear optics in a Kerr medium: Exact soliton solutions for a few cycles.  
*Phys. Rev. A*, 77(4):043823, 2008.
- [126] M. Pietrzyk, I. Kanattšikov, and U. Bandelow.  
On the propagation of vector ultra-short pulses.  
*J. Nonlinear Math. Phys.*, 15(2):162–170, 2008.
- [127] V. G. Beshpalov, S. A. Kozlov, Yu. A. Shpolyanskiy, and I. A. Walmsley.  
Simplified field wave equations for the nonlinear propagation of extremely short light pulses.  
*Phys. Rev. A*, 66(1):013811, 2002.
- [128] A. A. Balakin, A. G. Litvak, V. A. Mironov, and S. A. Skobelev.  
Self-action of few-cycle pulses in a dispersive medium.  
*Phys. Rev. A*, 80(6):063807, December 2009.
- [129] S. V. Sazonov.  
On the nonlinear optics of few-cycle pulses.

- Bulletin of the Russian Academy of Sciences: Physics*, 75(2):157–160, February 2011.
- [130] A. V. Kim and S. A. Skobelev.  
Few-cycle vector solitons of light.  
*Phys. Rev. A*, 83(6):063832, June 2011.
- [131] V. A. Vakhnenko.  
Solitons in a nonlinear model medium.  
*Journal of Physics A: Mathematical and General*, 25(15):4181–4187, August 1992.
- [132] R. Camassa and D. D. Holm.  
An integrable shallow water equation with peaked solitons.  
*Phys. Rev. Lett.*, 71(11):1661–1664, September 1993.
- [133] George Gabriel Stokes.  
Supplement to a paper on the theory of oscillatory waves.  
In *Mathematical and Physical Papers*, volume 1. Cambridge University Press, 1880.
- [134] H. A. Haus and W. S. Wong.  
Solitons in optical communications.  
*Rev. Mod. Phys.*, 68(2):423–444, April 1996.
- [135] Y. S. Kivshar and B. A. Malomed.  
Dynamics of solitons in nearly integrable systems.  
*Rev. Mod. Phys.*, 61(4):763–915, October 1989.
- [136] A. V. Yulin, D. V. Skryabin, and P. St. J. Russell.  
Four-wave mixing of linear waves and solitons in fibers with higher-order dispersion.  
*Opt. Lett.*, 29(20):2411–2413, Oct 2004.
- [137] D. V. Skryabin and A. V. Yulin.  
Theory of generation of new frequencies by mixing of solitons and dispersive waves in optical fibers.  
*Phys. Rev. E*, 72(1):016619, 2005.
- [138] T. G. Philbin, C. Kuklewicz, S. Robertson, S. Hill, F. König, and U. Leonhardt.  
Fiber-optical analog of the event horizon.  
*Science*, 319(5868):1367–1370, 2008.
- [139] A. Demircan, Sh. Amiranashvili, and G. Steinmeyer.  
Controlling light by light with an optical event horizon.  
*Phys. Rev. Lett.*, 106(16):163901, April 2011.
- [140] S. Pickartz, U. Bandelow, and Sh. Amiranashvili.  
Adiabatic theory of solitons fed by dispersive waves.  
*Phys. Rev. A*, 94(3):033811, September 2016.
- [141] S. Pickartz, U. Bandelow, and Sh. Amiranashvili.  
Asymptotically stable compensation of the soliton self-frequency shift.  
*Opt. Lett.*, 42(7):1416–1419, April 2017.
- [142] S. Pickartz, C. Brée, U. Bandelow, and Sh. Amiranashvili.  
Cancellation of Raman self-frequency shift for compression of optical pulses.  
*Opt. Quantum Electron.*, 49(10):328, October 2017.
- [143] A. Einstein.  
Zur Elektrodynamik bewegter Körper.  
*Annalen der Physik*, 322(10):891–921, 1905.
- [144] L. D. Landau and E. M. Lifshitz.  
*The Classical Theory of Fields*.  
Pergamon, 4 edition, 1975.

- [145] N. N. Rosanov, N. V. Vysotina, and A. N. Shatsev.  
Forward light reflection from a moving inhomogeneity.  
*JETP Lett.*, 93, 2011.
- [146] F. Biancalana.  
Viewpoint: Negative frequencies get real.  
*Physics*, 5(68), June 2012.
- [147] M. A. Gaafar, T. Baba, M. Eich, and A. Yu. Petrov.  
Front-induced transitions.  
*Nature Photonics*, 13(11):737–748, November 2019.
- [148] B. W. Plansinis, W. R. Donaldson, and G. P. Agrawal.  
What is the temporal analog of reflection and refraction of optical beams?  
*Phys. Rev. Lett.*, 115(18):183901, Oct 2015.
- [149] F. Mitschke.  
*Fiber Optics*.  
Springer, 2 edition, 2016.
- [150] N. S. Stepanov.  
Waves in nonstationary media.  
*Radiophys. Quantum Electron.*, 36(7):401–409, July 1993.
- [151] N. N. Rosanov.  
Transformation of electromagnetic radiation at moving inhomogeneities of a medium.  
*JETP Letters*, 88(8):501–504, December 2008.
- [152] U. Bandelow, Sh. Amiranashvili, and S. Pickartz.  
Stabilization of optical pulse transmission by exploiting fiber nonlinearities.  
*J. Lightwave Technol.*, 38(20):5743–5747, October 2020.
- [153] A. Efimov, A. V. Yulin, D. V. Skryabin, J. C. Knight, N. Joly, F. G. Omenetto, A. J. Taylor, and P. Russell.  
Interaction of an optical soliton with a dispersive wave.  
*Phys. Rev. Lett.*, 95(21):213902, 2005.
- [154] L. Tartara.  
Frequency shifting of femtosecond pulses by reflection at solitons.  
*IEEE J. Quantum Electron.*, 48(11):1439–1442, Aug 2012.
- [155] K. E. Webb, M. Erkintalo, Y. Xu, N. G. R. Broderick, J. M. Dudley, G. Genty, and S. G. Murdoch.  
Nonlinear optics of fibre event horizons.  
*Nature Comm.*, 5(4969):1–7, September 2014.
- [156] L. Tartara.  
Soliton control by a weak dispersive pulse.  
*JOSA B*, 32(3):395–399, Mar 2015.
- [157] A. V. Gorbach and D. V. Skryabin.  
Bouncing of a dispersive pulse on an accelerating soliton and stepwise frequency conversion in optical fibers.  
*Opt. Express*, 15(22):14560, Oct 2007.
- [158] A. V. Gorbach and D. V. Skryabin.  
Light trapping in gravity-like potentials and expansion of supercontinuum spectra in photonic-crystal fibres.  
*Nature Photonics*, 1(11):653–657, 2007.
- [159] A. V. Gorbach and D. V. Skryabin.  
Theory of radiation trapping by the accelerating solitons in optical fibers.  
*Phys. Rev. A*, 76(5):053803, 2007.

- [160] R. Driben, F. Mitschke, and N. Zhavoronkov.  
Cascaded interactions between Raman induced solitons and dispersive waves in photonic crystal fibers at the advanced stage of supercontinuum generation.  
*Opt. Express*, 18(25):25993–25998, Dec 2010.
- [161] A. V. Yulin, R. Driben, B. A. Malomed, and D. V. Skryabin.  
Soliton interaction mediated by cascaded four wave mixing with dispersive waves.  
*Opt. Express*, 21(12):14481–14486, Jun 2013.
- [162] I. Oreshnikov, R. Driben, and A. V. Yulin.  
Weak and strong interactions between dark solitons and dispersive waves.  
*Opt. Lett.*, 40(21):4871–4874, Nov 2015.
- [163] S. Robertson and U. Leonhardt.  
Frequency shifting at fiber-optical event horizons: The effect of Raman deceleration.  
*Phys. Rev. A*, 81(6):063835, June 2010.
- [164] J. M. Dudley and D. Skryabin.  
Viewpoint: New horizons for Hawking radiation.  
*Physics*, 3(95), November 2010.
- [165] E. Rubino, F. Belgiorno, S. L. Cacciatori, M. Clerici, V. Gorini, G. Ortenzi, L. Rizzi, V. G. Sala, M. Kolesik, and D. Faccio.  
Experimental evidence of analogue hawking radiation from ultrashort laser pulse filaments.  
*New Journal of Physics*, 13(8):085005, August 2011.
- [166] D. Faccio.  
Laser pulse analogues for gravity and analogue hawking radiation.  
*Contemporary Physics*, 53(2):97–112, March-April 2012.
- [167] E. Rubino, J. McLenaghan, S. C. Kehr, F. Belgiorno, D. Townsend, S. Rohr, C. E. Kuklewicz, U. Leonhardt, F. König, and D. Faccio.  
Negative-frequency resonant radiation.  
*Phys. Rev. Lett.*, 108(25):253901, June 2012.
- [168] D. Faccio, T. Arane, M. Lamperti, and U. Leonhardt.  
Optical black hole lasers.  
*Classical and Quantum Gravity*, 29(22):224009, October 2012.
- [169] D. Bermudez and U. Leonhardt.  
Hawking spectrum for a fiber-optical analog of the event horizon.  
*Phys. Rev. A*, 93(5):053820, May 2016.
- [170] C. Ciret, F. Leo, B. Kuyken, G. Roelkens, and S.-P. Gorza.  
Observation of an optical event horizon in a silicon-on-insulator photonic wire waveguide.  
*Opt. Express*, 24(1):114–124, January 2016.
- [171] G. Steinmeyer, Sh. Amiranashvili, and A. Demircan.  
SPIE Newsroom Article: Optical switching in the event horizon.  
<http://spie.org/x57285.xml?pf=true&ArticleID=x57285>, September 2011.
- [172] A. Demircan, Sh. Amiranashvili, C. Brée, Ch. Mahnke, F. Mitschke, and G. Steinmeyer.  
Rogue events in the group velocity horizon.  
*Sci. Rep.*, 2(850):1–6, November 2012.
- [173] A. Demircan, Sh. Amiranashvili, C. Brée, and G. Steinmeyer.  
Compressible octave spanning supercontinuum generation by two-pulse collisions.  
*Phys. Rev. Lett.*, 110(23):233901, June 2013.
- [174] A. Choudhary and F. König.  
Efficient frequency shifting of dispersive waves at solitons.

- Opt. Express*, 20(5):5538–5546, Feb 2012.
- [175] V. E. Lobanov and A. P. Sukhorukov.  
Total reflection, frequency, and velocity tuning in optical pulse collision in nonlinear dispersive media.  
*Phys. Rev. A*, 82(3):033809, September 2010.
- [176] J. Gu, H. Guo, S. Wang, and X. Zeng.  
Probe-controlled soliton frequency shift in the regime of optical event horizon.  
*Opt. Express*, 23(17):22285–22290, August 2015.
- [177] A. Demircan, Sh. Amiranashvili, C. Brée, U. Morgner, and G. Steinmeyer.  
Adjustable pulse compression scheme for generation of few-cycle pulses in the midinfrared.  
*Opt. Lett.*, 39(9):2735–2738, May 2014.
- [178] A. Demircan, Sh. Amiranashvili, C. Brée, U. Morgner, and G. Steinmeyer.  
Supercontinuum generation by multiple scatterings at a group velocity horizon.  
*Opt. Express*, 22(4):3866–3879, February 2014.
- [179] A. Demircan, Sh. Amiranashvili, C. Brée, Ch. Mahnke, F. Mitschke, and G. Steinmeyer.  
Rogue wave formation by accelerated solitons at an optical event horizon.  
*Appl. Phys. B*, 115(3):343–354, August 2014.
- [180] I. Babushkin, Sh. Amiranashvili, C. Brée, U. Morgner, G. Steinmeyer, and A. Demircan.  
The effect of chirp on pulse compression at a group velocity horizon.  
*IEEE Photonics Journal*, 8(3):7803113, June 2016.
- [181] C. Brée, G. Steinmeyer, I. Babushkin, U. Morgner, and A. Demircan.  
Controlling formation and suppression of fiber-optical rogue waves.  
*Opt. Lett.*, 41(15):3515–3518, August 2016.
- [182] B. W. Plansinis, W. R. Donaldson, and G. P. Agrawal.  
Cross-phase-modulation-induced temporal reflection and waveguiding of optical pulses.  
*J. Opt. Soc. Am. B*, 35(2):436–445, February 2018.
- [183] S. V. Manakov.  
On the theory of two-dimensional stationary self-focusing of electromagnetic waves.  
*Sov. Phys. JETP*, 38(2):248–253, February 1974.
- [184] L. D. Landau and E. M. Lifshitz.  
*Quantum Mechanics*.  
Pergamon, 2 edition, 1965.
- [185] A. Demircan, Sh. Amiranashvili, C. Brée, F. Mitschke, and G. Steinmeyer.  
From optical rogue waves to optical transistors.  
*Nonlinear Phenomena in Complex Systems*, 16(1):24–32, April 2013.
- [186] T. Balciunas, C. Fourcade-Dutin, G. Fan, T. Witting, A. A. Voronin, A. M. Zheltikov, F. Gerome, G. G. Paulus, A. Baltuska, and F. Benabid.  
A strong-field driver in the single-cycle regime based on self-compression in a kagome fibre.  
*Nature Comm.*, 6(6117):6117, Jan 2015.
- [187] V. E. Zakharov, A. N. Pushkarev, V. F. Shvets, and V. V. Yan'kov.  
Soliton turbulence.  
*JETP Lett.*, 48(2):83–87, July 1988.
- [188] H.-G. Purwins, H. U. Bödeker, and Sh. Amiranashvili.  
Dissipative solitons.  
*Adv. Phys.*, 59(5):485–701, September 2010.
- [189] N. N. Rozanov.  
Dissipative optical solitons.  
*Usp. Fiz. Nauk*, 43(4):421–424, 2000.



- [190] M. Bode, A. W. Liehr, C. P. Schenk, and H.-G. Purwins.  
Interaction of dissipative solitons: particle-like behaviour of localized structures in a three-component reaction-diffusion system.  
*Physica D*, 161(1–2):45–66, 2002.
- [191] E. Knobloch.  
Spatially localized structures in dissipative systems: open problems.  
*Nonlinearity*, 21(4):T45–T60, 2008.
- [192] T. Ackemann, W. J. Firth, and G.-L. Oppo.  
Fundamentals and applications of spatial dissipative solitons in photonic devices.  
In P. R. Berman, E. Arimondo, and C. C. Lin, editors, *Advances in Atomic, Molecular, and Optical Physics*, volume 57, pages 323–421. Academic, 2009.
- [193] S. Pickartz, U. Bandelow, and S. Amiranashvili.  
Efficient all-optical control of solitons.  
*Opt. Quant. Elect.*, 48(11):503:1–7, November 2016.
- [194] J. P. Gordon.  
Theory of the soliton self-frequency shift.  
*Opt. Lett.*, 11(10):662–664, October 1986.
- [195] F. M. Mitschke and L. F. Mollenauer.  
Discovery of the soliton self-frequency shift.  
*Opt. Lett.*, 11(10):569–661, 1986.
- [196] D. Schadt and B. Jaskorzynska.  
Suppression of the Raman self-frequency shift by cross-phase modulation.  
*J. Opt. Soc. Am. B*, 5(11):2374–2378, November 1988.
- [197] K. J. Blow, N. J. Doran, and D. Wood.  
Suppression of the soliton self-frequency shift by bandwidth-limited amplification.  
*JOSA B*, 5(6):1301–1304, June 1988.
- [198] D. V. Skryabin, F. Luan, J. C. Knight, and P. St. J. Russell.  
Soliton self-frequency shift cancellation in photonic crystal fibers.  
*Science*, 301(5640):1705–1706, September 2003.
- [199] F. Biancalana, D. V. Skryabin, and A. V. Yulin.  
Theory of the soliton self-frequency shift compensation by the resonant radiation in photonic crystal fibers.  
*Phys. Rev. E*, 70(1):016615, 2004.
- [200] T. P. Goldsmith, S. Coen, J. D. Harvey, and F. Vanholsbeeck.  
Cancellation of Raman soliton self-frequency shift by cross-phase modulation.  
In *Conference on Lasers and Electro-Optics Europe*, pages 231–231. IEEE, 2005.
- [201] I. M. Uzunov and T. N. Arabadzhev.  
Suppression of the soliton self-frequency shift and compression in the presence of bandwidth-limited amplification.  
*Phys. Rev. E*, 84(2):026607, August 2011.
- [202] Sh. Amiranashvili, M. Radziunas, U. Bandelow, K. Busch, and R. Čiegis.  
Additive splitting methods for parallel solutions of evolution problems.  
*Journal of Computational Physics*, 436(110320):1–14, July 2021.
- [203] W. Hundsdorfer and J. Verwer.  
*Numerical solution of time-dependent advection-diffusion-reaction equations*.  
Springer, 2003.
- [204] H. Holden, K. Karlsen, K.-A. Lie, and H. Risebro.  
*Splitting methods for partial differential equations with rough solutions. Analysis and Matlab programs*.

- European Mathematical Society, Zürich, 2010.
- [205] E. Hairer, C. Lubich, and G. Wanner.  
*Geometric Numerical Integration. Structure-Preserving Algorithms for Ordinary Differential Equations*,  
volume 31 of *Springer Series in Computational Mathematics*.  
Springer, Berlin, 2 edition, 2006.
- [206] R. Glowinski, S. J. Osher, and W. Yin, editors.  
*Splitting Methods in Communication, Imaging, Science, and Engineering*.  
Scientific Computation. Springer, 2017.
- [207] Sh. Amiranashvili, R. Čiegis, and M. Radziunas.  
Numerical methods for a class of generalized nonlinear Schrödinger equations.  
*Kinetic and Related Models*, 8(2):215–234, June 2015.
- [208] H. F. Trotter.  
On the product of semi-groups of operators.  
*Proceedings of the American Mathematical Society*, 10(4):545–551, August 1959.
- [209] G. Strang.  
Accurate partial difference methods I: Linear Cauchy problems.  
*Arch. Rat. Mech. Anal.*, 12(1):392–402, January 1963.
- [210] E. Forest and R. D. Ruth.  
Fourth-order symplectic integration.  
*Physica D*, 43(1):105–117, May 1990.
- [211] M. Suzuki.  
Fractal decomposition of exponential operators with applications to many-body theories and Monte Carlo  
simulations.  
*Phys. Lett. A*, 146(6):319–323, June 1990.
- [212] H. Yoshida.  
Construction of higher order symplectic integrators.  
*Phys. Lett. A*, 150(5-7):262–268, November 1990.
- [213] S. Blanes and P. C. Moan.  
Practical symplectic partitioned Runge-Kutta and Runge-Kutta-Nyström methods.  
*Journal of Computational and Applied Mathematics*, 142(2):313–330, May 2002.
- [214] E. Hansen and A. Ostermann.  
High order splitting methods for analytic semigroups exist.  
*BIT Numerical Mathematics*, 49(3):527–542, September 2009.
- [215] S. Blanes, F. Casas, P. Chartier, and A. Murua.  
Optimized high-order splitting methods for some classes of parabolic equations.  
*Journal: Math. Comp.*, 82(283):1559–1576, July 2013.
- [216] W. Auzinger, H. Hofstätter, D. Ketcheson, and O. Koch.  
Practical splitting methods for the adaptive integration of nonlinear evolution equations. Part I: Construc-  
tion of optimized schemes and pairs of schemes.  
*BIT Numerical Mathematics*, 57(1):55–74, March 2017.
- [217] W. Auzinger, I. Březinová, H. Hofstätter, O. Koch, and M. Quell.  
Practical splitting methods for the adaptive integration of nonlinear evolution equations. Part II: Com-  
parisons of local error estimation and step-selection strategies for nonlinear Schrödinger and wave  
equations.  
*Computer Physics Communications*, 234:55–71, January 2019.
- [218] W. Auzinger, H. Hofstätter, and O. Koch.  
Coefficients of various splitting methods.

<https://www.asc.tuwien.ac.at/winfried/splitting/>, August 2017.

- [219] S. Z. Burstein and A. A. Mirin.  
Third order difference methods for hyperbolic equations.  
*J. Comput. Phys.*, 5(3):547–571, June 1970.
- [220] A. Čiegis, A. Mirinavičius, and M. Radziunas.  
Comparison of split step solvers for multidimensional Schrödinger problems.  
*Computational Methods in Applied Mathematics*, 13(2):237–250, April 2013.
- [221] G. Strang.  
On the construction and comparison of difference schemes.  
*SIAM J. Numer. Anal.*, 5(3):506–517, September 1968.